University of Massachusetts Amherst

The physical properties of polyurethanes and ionomers.

Item Type	dissertation
Authors	Kajiyama, Tisato
DOI	10.7275/sdjf-tf89
Download date	2024-10-12 02:24:45
Link to Item	https://hdl.handle.net/20.500.14394/16261

THE PHYSICAL PROPERTIES OF POLYURETHANES AND IONOMERS

A Dissertation Presented

By

Tisato Kajiyama

Submitted to the Graduate School of the
University of Massachusetts in
partial fulfillment of the requirements for the degree of

DOCTOR OF PHILOSOPHY

May 1969

Major Subject: Polymer Science and Engineering

THE PHYSICAL PROPERTIES OF POLYURETHANES AND IONOMERS

A Dissertation Presented

By

Tisato Kajiyama

Approved as to style and content by:

(Chairman of Committee)

(Head of Department)

(Member)

(Member

May 1969

A C K N O W L E D G M E N T

The author wishes to express appreciation and thanks to all members of the Polymer Science and Engineering Program for their assistance and cooperation during the course of the work.

The inspiration, patience and thoughtfulness of the student advisor, Professor William J. MacKnight, is graciously acknowledged.

Professor Richard S. Stein who gave the kind opportunity to study at the University of Massachusetts and also helpful advice for the course of the work to the author is sincerely acknowledged.

Acknowledgment and thanks to to the Thesis Committee which consisted of Dr. William J. MacKnight, Dr. Richard S. Stein and Dr. Robert W. Lenz. Their constructive comments in reviewing the thesis are appreciated.

Professor Motowo Takayanagi (Kyushu University) gave his kind help in order to make it possible for the author to study under the direction of Dr. William J. MacKnight and Dr. Richard S. Stein.

The assistance of Professor Yoichi Ishida (Osaka University) is gratefully acknowledged.

Thanks are also extended to Mrs. Sophia Kinney for providing secretarial work during the course of the research and for typing the thesis.

Mr. Michael Yang was most helpful in the work on the differential scanning calorimetry measurement.

Mr. Lawrence W. McKenna kindly discussed the experimental works with the author.

The author wishes to thank the National Science Foundation and the Petroleum Research Fund of the American Chemical Society for support of this research.

TABLE OF CONTENTS

CHAPTER I

INTRODUCTION AND POLYMERIZATION METHOD 1

Introduction 1

Sample Preparation 6

A. Polymerization Method 7

B. Notes for Polymerization 8

C. Sample Identification 9

Experimental 10

A. Sample Preparation 10

B. Measurements 11

CHAPTER II

THE LOW TEMPERATURE RELAXATION (γ RELAXATION) IN POLYURETHANES 14

Results 14

A. The Effect of Thermal History on the γ Relaxation 16

B. The δ Relaxation 17

C. The Dielectric γ Relaxation 18

Discussion 19

A. The δ Relaxation 19

B. The γ Relaxation 20

C. Conclusions 31

CHAPTER III

THE EFFECT OF WATER ON THE MECHANICAL PROPERTIES 33

The Effect of Water on the γ Relaxation 33

The New Sharp Peak 36

The Effect of Water on the β Relaxation 39

The Effect of Water on the α Relaxation 42

CHAPTER IV

HIGH TEMPERATURE RELAXATIONS (α RELAXATION) IN POLYURETHANES 43

The β_ϕ Relaxation 43

The α and α_t Relaxations 44

The α_c Relaxation 52

CHAPTER V

THERMAL PROPERTIES OF POLYURETHANES 54

Experimental 54

A. Thermal Analysis 54

B. Heat of Fusion 54

C. Degree of Crystallinity 55

Melting Points and Glass Transition 55

A. Melting Points 55

B. The Glass Transitions 63

Cold Crystallization and Solid-Solid Transition 68

Heat of Fusion and Entropy of Fusion 69

CHAPTER VI

STRUCTURE-MECHANICAL PROPERTY RELATIONSHIPS IN ETHYLENE METHACRYLIC ACID COPOLYMERS AND THEIR SALTS 74

Introduction 74

Experimental 76

Results and Discussion 78

A. The β' Relaxation 80

B. The β Relaxation 81

C. The γ Relaxation 83

TABLE I-I 91

TABLE I-II 92

TABLE I-III 93

TABLE I-IV 94

TABLE I-V 95

TABLE IV-I 96

TABLE IV-II 97

TABLE IV-III 98

TABLE V-I 99

TABLE V-II 100

TABLE V-III (1) 101

TABLE V-III (2) 102

CAPTIONS FOR FIGURES 103

BIBLIOGRAPHY 109

CHAPTER I

INTRODUCTION AND POLYMERIZATION METHOD

Introduction

The field of polyurethanes is rapidly growing in commercial importance, especially in foam and elastomer applications. This group of polymers includes a very broad range of chemical structures and molecular weights. In many cases polyurethanes are synthesized from α, ω polyester glycols or α, ω polyether glycols and diisocyanates so that the urethane groups are fewer in number than other functional groups (ester groups or ether groups). This method of synthesis leads to a very wide range of polymer properties, adding interest to the studies of the relationship between structure and properties.

Though a considerable number of publications dealing primarily with the properties of urethane polymers have appeared, few of them have contributed to a fundamental understanding of the relationship between those properties and the corresponding polymer structure.

Within the last few years reliable data have become available, and Saunders[1] has established semi-quantitative relationships by the use of those data. He discussed in his reports general considerations concerning structure-property relationships.

The term "polyurethane" is more one of convenience than of accuracy since these polymers are not derived by polymerizing a monomeric urethane molecule. They include those polymers which contain a significant number of urethane groups, regardless of what the rest of the molecule may be. Usually these polymers are obtained by a combination of a polyisocyanate

1 Rubber Chem & Tech 33 1259 (1960).

with reactants which have at least some hydroxyl groups, e.g., polyethers and simple glycols. Thus, a typical "polyurethane" may contain, in addition to urethane groups, aliphatic and aromatic hydrocarbon, ester, ether, amide and urea groups.

Polyurethane materials are being used in many ways, for example as plastics, fibers, flexible foams, elastomers, coating materials and so on. By varying the nature of the polyester and the isocyanate component as well as the NCO/OH ratio, a wide range of properties is obtained ranging from very flexible elastomers to hard brittle films.

Instead of the polymerization method mentioned above, using the prepolymer and diisocyanate to obtain elastomer, another method was developed to obtain hard polyurethane materials of high molecular weight. In 1937, Bayer[2] indicated the preparation of high molecular weight polyurethanes. These polymers, made by reacting a diisocyanate with a glycol, were later the basis for the preparation of urethane fibers. The simplest high molecular weight urethane polymer is a linear chain with urethane linkages periodically situated in the skeleton, arising from the polycondensation reaction of a difunctional hydroxy-containing molecule and a difunctional isocyanate monomer. The linear urethane polymer is soluble in suitable solvents and may be molded by the application of heat and pressure.

Polymerization techniques and physical properties of "soft" polyurethane materials were summarized in the textbook written by Saunders[3]. Also, synthetic methods and physical properties of "hard" type of polyurethanes have been reported in detail by Lyman[4]. Though many reports

have been published on polymerization techniques, fundamental studies of polyurethane chemistry, especially of homopolymers, lagged behind these developmental studies largely because of the commercial development and success of other synthetic plastics and fibers such as the polyamides, the polyesters and polyacrylonitriles. Lack of a good versatile technique for preparing polyurethanes having a wide variety of structure also contributed heavily to their slow development. It became apparent, however, to some researchers from their growing knowledge of relationships between molecular structure and polymer properties that linear polyurethanes had a large, unrealized potential for giving polymers with a new and unique combination of properties.

Studies of physical properties and structural analysis of polyurethane materials have been developed in parallel with the developments of synthetic methods as follows.

Studies of x-ray analysis of samples prepared by polymerizing hexamethylene diisocyanate and 1,4-butanediol were first reported by Zahn, et.al.[5] They calculated the unit cell constants of the polymer and concluded that the backbone chain is in the planar zigzag conformation. The results of the x-ray analysis for the urethane polymer having an odd number of methylene sequences in the diol part which was prepared from hexamethylene diisocyanate and 1,5-pentanediol were reported by Saito, et.al.[6] They proposed a crystal structure which indicated deviation from the planar zigzag conformation with twisting in the left and right hand sides to form complete hydrogen bonding similar to the γ-form of nylon materials. Also, two modifications similar to the α- and γ-forms

found in polyamides have been observed by Lyman, et.al.[7] using polyurethane materials prepared from nonamethylene diisocyanate and ethaneglycol. They mentioned that the relative amount of each form present appeared to depend on temperature and degree of draw.

As discussed above, the "hard" polyurethane materials prepared from diisocyanates and diols show crystalline regions as detected by x-ray diffraction. The next problem is to define the crystal morphology. There are many types of morphological entities observed in bulk polymeric materials, e.g., spherulites, hedrites, dendrites and extended chain structures. Eppe, et.al.[8], indicated that the material crystallized from the glassy state of polyurethane materials by annealing had a fibrillar structure. These workers found that polyurethanes can be quenched to a glassy state with spherulites developing during subsequent annealing similar to the case of poly(ethylene terephthalate). Also, they have shown that the discrete small angle x-ray diffraction maxima develops during the annealing of glassy polyurethanes coincidentally with development of crystallinity. From these results they concluded that the spherulites of polyurethanes found during annealing might be composed of fibrous or ribbonlike structures.

Kern, et.al.[9], has investigated the internal structure of the crystalline regions using oligomers of polyurethanes crystallized from solution. They found that the small angle x-ray diffraction long period at first increases with increasing molecular weight and then remains constant. The results were interpreted as indicating that molecules greater than a certain critical length form chain folded structures.

It is well known that interchain interaction forces, including hydrogen bonding, affect many physical properties of urethane elastomers to a considerable extent[3]. The polyethers and esters from which urethane elastomers can be obtained vary in structure and consequently they can contain different proton-acceptor groups. Also, the hydrogen bonding formation plays a very important role in the determination of the chain allignment as shown for the α- and γ- forms in polyamides. Boyarchunk, et.al.[10], studied the mechanism of hydrogen bonding formation in urethane elastomers based on polyesters and polyethers and suggested the conclusion that in polyester-urethanes the main type of hydrogen bonding is the bond between the NH group and the C=O of the ester group and in poly(ether urethanes) it is the bond between the NH and C=O groups of the urethane unit.

Studies of the viscoelastic properties of polyurethanes have been more extensive than other investigations. Results of dielectric studies of the samples prepared from hexamethylene diisocyanate and 1,4-butanediol have been reported by Hirata, et.al.[11] They observed two loss peaks which located around 1 Hz and 10^5 Hz at 64°C and suggested that the high frequency dielectric loss is related to the mechanical loss which is the α relaxation process due to the segmental motion in the amorphous region and also the low frequency loss peak would be a manifestation of a certain kind of molecular motion in the crystalline regions.

Polyurethanes prepared from hexamethylene diisocyanate and 1,4-butanediol have been studied mechanically by Becker, et.al.[12], Illers, et.al.[13] and Jacobs, et.al.[14] Jacobs and Jenckel found three relaxation

regions labeled α, β and γ respectively for four polyurethanes prepared from hexamethylene diisocyanate and 1,4-butane, 2,5-hexane, 1,6-hexane and 1,10-decanediol. They interpreted the results of the mechanical property studies as follows: the α relaxation is probably related to the amorphous glass transition, the β relaxation involves absorbed water molecules, and the γ relaxation is probably associated largely with motions of the $(CH_2)_n$ sequences in the diols.

The literature discussed above summarizes earlier work concerning the studies of thermal, dielectric and mechanical properties and x-ray analysis of "hard" polyurethane materials. In order to further elucidate the relationships between these properties and the chemical structures of "hard" polyurethanes, some samples of "hard" polyurethanes were chosen for investigation in this thesis. Several techniques have been used in this study. These are the dynamic mechanical, dielectric, x-ray, differential thermal scanning calorimetry, infrared, electron microscope and dilatometry techniques.

Sample Preparation

Three different diisocyanates (hexamethylene-, 4,4'-methylene-diphenyl- and 4-methyl meta-phenylene diisocyanates) were reacted with the various diols which have numbers of methylene units from n=2 to n=10. The diisocyanates and diols were polymerized by the method of step-growth polymerization described by Lyman[4] in a mixed solvent of methyl isobutyl ketone (MIBK) and dimethyl sulfoxide (DMSO).

The structures of the repeat units of the polyurethanes are:

H Series

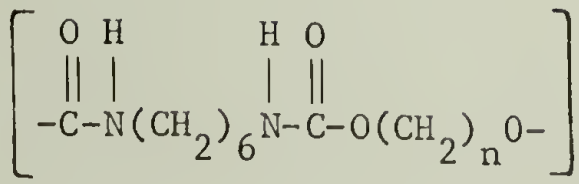

n=2-10

DP Series

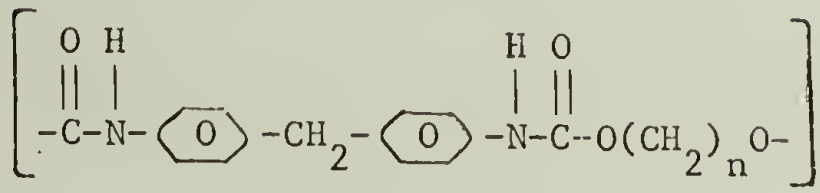

n=2-10

4M Series

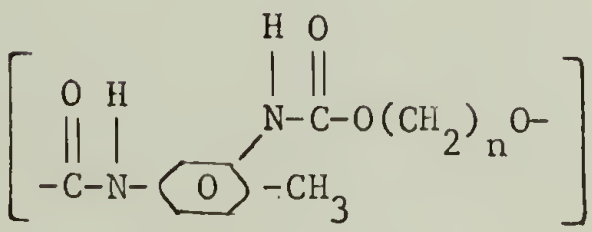

n=2-10

The polymerization processes are described in detail in the following section.

A. Polymerization Method.

Diisocyanate (0.1021 mole) was mixed with 40 ml of MIBK in the vessel in which the air was displaced by nitrogen. The reactor was a three-necked, round-bottomed flask with ground glass joints, equipped with a thermometer, an agitator sealed to prevent access of air, a Friedrich condensor with a drying tube on the outlet and a heating mantle. Forty ml of DMSO were added to the mixture of MIBK and diisocyanate and gentle agitation was started and the mixture heated to about 20°C below reflux temperature as listed in Table I-I. Diol was added to the

mixture volumetrically from a hypodermic syringe calibrated in 0.1 cc divisions.

The mixture was heated to the reflux temperature and maintained for the time listed in Table I-I after the diol was added. After the time listed in Table I-I, the solution became cloudy, indicating separation of polymer. Heating was continued for 10 to 60 min at the reflux temperature after the cloudiness first appeared. During this time the polymer precipitated. One or two drops of methyl alcohol was added to the slurry to terminate the reaction. The slurry was poured into water to precipitate the polymer while it was at a temperature above 70°C. The polymer precipitated in the water was filtered using a Bucher funnel. It was then washed twice with water and methyl alcohol to flush out most of the remaining solvent and monomer. The slurry was agitated to prevent bumping and foaming, and the reactor was heated at 100°C for 1 hr to remove the remaining solvents and monomers by steam distillation. The polymer was dried under a pressure of about 30 mm Hg at 75°C for 24 hrs.

B. Notes for Polymerization.

1. Diisocyanates and solvents were purified by distillation under the following conditions.

	Boiling Point
hexamethylene diisocyanate	113 ~ 114°C/5 mm Hg
4,4'-methylene diphenyl diisocyanate	110°C/4.3 mm Hg
4-methyl meta-phenylene diisocyanate	70.3°C/0.6 mm Hg
MIBK	113.1 ~ 113.4°C/760 mm Hg
DMSO	60 ~ 61°C/55 mm Hg

A slight excess, corresponding to NCO/OH=1.02, was used to make up for slight but inevitable losses of diisocyanate functions by reaction with moisture. The stoichiometric amount produces a polymer with lower melting point.

2. The reactor components were dried at 110°C for at least 1 hr, then quickly assembled while hot and flushed with dry nitrogen to displace the air in the system.

3. Monomers were stored in the refrigerator under vacuum.

4. The solvent was dried by distillation just before use.

5. The diol must be anhydrous. The diols from 1,2-ethanediol to 1,7 heptanediol and the three diisocyanates were purified by vacuum distillation. 1,8-octanediol to 1,10-decanediol were purified by recrystallization from hexane. The conditions for purification of diols are listed in Table I-II, including the weights corresponding to 0.1021 mole.

6. The solubilities of polyurethanes are tabulated in Table I-III.

C. Sample Identification.

An elemental analysis for carbon, hydrogen and nitrogen was carried out and theoretical values for these elements calculated on the assumption that the repeat units are exactly as depicted in the Introduction and that no chain branching occurred due to allophanate formation or the presence of impurities. The results are given in Table I-IV and it may be seen that the agreement is good. The deviations noted for hydrogen in the case of the 4M series probably arise from the presence of absorbed water as this series is extremely hydrophilic.

The viscosity average molecular weights, $\overline{M}_V$, are listed in Table I-V[15] using the following relationships.

$$[\eta] = K\,\overline{M}_V^{\,a}$$

where

$$K = 5.52 \times 10^{-4}$$

$$a = 0.66$$

The values of K and "a" used were calculated on a polymer containing polycaprolactam and dissolved in DMF at 25°C[16].

Experimental

A. Sample Preparation.

1. The H and DP series samples were compression molded into films suitable for mechanical testing at 10°C above their melting point. The films were allowed to cool in air to room temperature or they were quenched to various temperatures by plunging them into liquid nitrogen.

2. The 4M series samples were compression molded into films at temperatures approximately 50°C in excess of their T_g's.

3. Annealing was carried out in an oil bath with the samples enclosed in a sealed tube under dry nitrogen.

4. The solution grown samples in the H series were prepared by crystallization in cyclohexanone at 65°C for 24 hrs.

B. Measurements.

1. X-Ray. A continuous radial scanning technique was used with a molybdenum source. The degree of crystallinity was calculated from the ratio of the area of the crystalline peaks to the area of the amorphous peak. Only the H and DP series showed evidence of crystallinity by the x-ray method. In the case of the DP series, it was possible to obtain completely amorphous material by quenching into a dry ice-alcohol mixture. In the H series, completely amorphous polymers were not obtainable in this way and so the measurement of the area of the amorphous peak had to be carried out by heating the polymers above their melting points.

2. Dynamic Mechanical Measurements. All measurements were carried out using a Vibron Dynamic Viscoelastometer (Toyo Measuring Instrument Company), Model DDV II. The temperature range was from -190°C to 200°C and the samples were heated at 1 to 2 degrees per minute under dry nitrogen. The frequencies of measurement were 3.5, 11 and 110 Hz.

3. Dielectric Relaxation. Measurements were carried out with a mutual inductance bridge similar to the Cole-Gross bridge. The apparatus was constructed with three terminal electrodes in order to avoid edge and surface effects as well as the stray capacity effect. Samples were sputtered with silver on both surfaces and were kept sealed under dry nitrogen to avoid absorption of water. The temperature range used was from -190°C to -20°C and all measurements were carried out at 100 Hz.

4. Thermal Analysis. Measurements were carried out by Differential Scanning Calorimetry (DSC, Perkin Elmer Model IB). The scanning speed was 10°C per minute in all cases.

5. Infrared Analysis. Measurements were carried out on a Grating Infrared Spectrophotometer (Perkin Elmer 257). The characteristic frequencies lie in the infrared frequency range between 4000 cm^{-1} and 200 cm^{-1}. The sample thickness used for this purpose ranged between 20 to 40μ.

6. Volumetric Measurements. The dilatometric technique was used for this measurement. The sample was sealed under vacuum in the sample chamber and after 2 hrs under vacuum, mercury was poured into the chamber. The heating rate was 0.5°C per minute and the relative volume increase was read as the height of mercury using cathetometer.

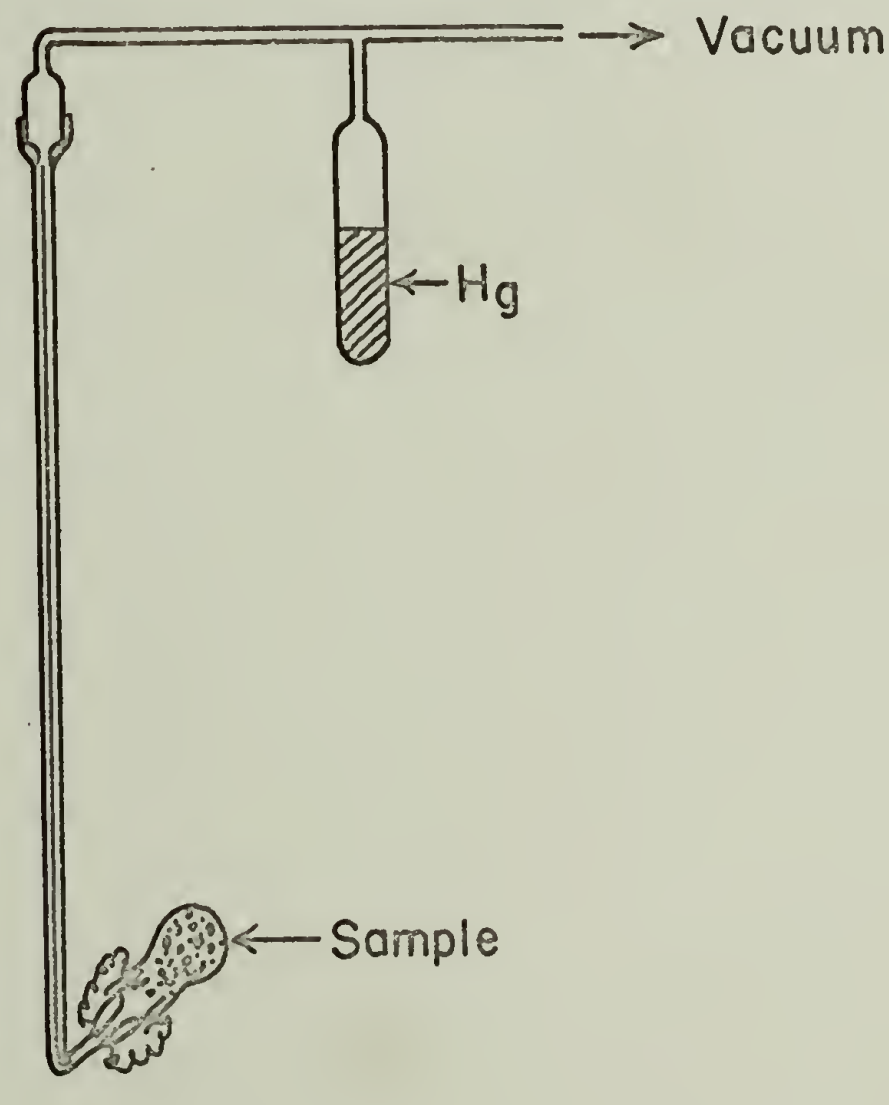

7. Electron Microscope. The surface replica technique was adopted for this purpose using cellulose acetate to take the replica. The cellulose acetate was coated by carbon vapor to remove the mirror image on the carbon-coated substrates. The electron microscope pictures of the replica were taken by a Hitachi HU-11 electron microscope at 78kv and at the beam current of 10 to 20μA.

CHAPTER II

THE LOW TEMPERATURE RELAXATION (γ RELAXATION) IN POLYURETHANES

Results

The temperature region investigated encompasses the so-called γ relaxation region for all three series of polyurethanes. Figure 1 gives the temperature dependence of the mechanical loss tangent, $\tan\delta$, for the 4M series. It is seen that for 4M-1,2 and 1,3, there is a small, very low temperature relaxation peak (to be discussed later), but the main γ peak is absent at 110 Hz. There is some evidence for a small γ peak in 4M-1,3 at 11 Hz. It is at once apparent from inspection of Figure 1 that the magnitude and temperature location of the γ relaxation is sensitive to n, the number of methylene units in the diol part of the repeat unit. This behavior is general for all three series and forms the basis for the molecular interpretation of the γ relaxation in the polyurethanes investigated.

Figure 2 shows the dependence of the temperature of the γ peak maximum on n. The temperatures of the E" and $\tan\delta$ maxima are both plotted and both show the same trends. With the exception of 4M-1,2, both the 4M and DP series show the same behavior which is a gradual decrease in peak temperature as n increases. 4M-1,2 displays a peak with a maximum at the anomalously low value of -160°C, much lower than that observed for any of the other polymers in any series. The H series exhibits a small increase in temperature in going from H-1,2 to H-1,4 and then the same general trend as the DP and 4M series for the higher values of n.

For the sake of comparison are also plotted temperatures of the peak maxima for the polyethers[17] poly(ethylene-oxide), $[-OCH_2CH_2O-]_n$, and poly-(tetramethylene oxide), $[-OCH_2CH_2CH_2CH_2O-]_n$[17], as well as the temperature of the peak maxima of a series of poly(methylene terephthalates),

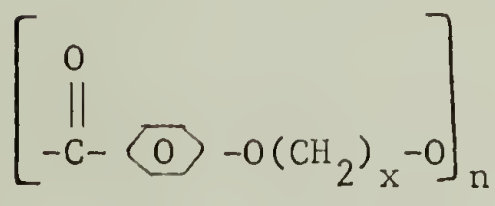

for x=5-10[18]. The comparisons are somewhat suspect in that the frequencies at which the measurements on these polymers were made were somewhat different from those used in the present work. However, the assumption was made that the γ peak had an activation energy comparable to that observed for the polyurethanes and the peak temperatures were thus adjusted to 110 Hz on this basis. It can be seen that the polyether data corresponds quite closely to the DP and 4M series while the poly(methylene terephthalates) show peak temperatures higher than those observed in the polyurethanes. The poly(methylene terephthalates) show tendencies for the peak temperatures to decrease with increasing n in a similar manner to the behavior of the DP, H and 4M series.

The activation energy of the γ process for the three series is plotted as a function of n in Figure 3. These values are obtained in the usual manner, i.e., from the slope of the line resulting from a plot of the logarithm of frequency versus the reciprocal of the absolute temperature of the peak maximum at the corresponding frequency as given by the next equation

$$\Delta H^{\ddagger} = 2.303\ R \frac{d \log f_{max}}{d\left(\frac{1}{T}\right)}$$

Although the points are somewhat scattered, it can be seen that the activation energy shows a general increase with increasing n for the DP and 4M series. There is no apparent regular trend in the case of the H series. As the basis for comparison may be cited the dielectric studies of Michailov[19] who investigated the activation energy of the γ process for a series of poly(n-alkyl acrylates) of varying side chain lengths. It was found that the activation energy remained constant at a value of 9 kcal $mole^{-1}$, independent of the length of the side chain. The γ process in the polyacrylates is thought to arise from local motions of three or more methylene units in the side chain. It would thus appear that the main chain γ process in the polyurethanes differs in its mechanism from the side chain relaxation in the poly(alkyl acrylates).

Figures 4 and 5 show the dependence of the magnitude of the tanδ peaks and the E" peaks on n for the various series at 110 Hz. The γ peak is essentially absent for values of n less than 4 at 110 Hz for both the DP and 4M series while it is present for all values of n in the case of the H series. (For the moment, the peak occurring at -160°C for 4M-1,2 and 4M-1,3 is not included in the discussion.) In all series, the magnitude of the peaks show a tendency to increase with increasing n, although this is much less marked in the H series than in the 4M and DP series.

A. <u>The Effect of Thermal History on the γ Relaxation</u>.

Figures 6 and 7 show the temperature dependence of tanδ and E" in the γ region for H-1,2 and H-1,5 respectively as well as the effect of various thermal treatments on the shapes of these peaks. It can be

seen from Figures 6 and 7 that the γ relaxation for the H series consists of three different overlapping peaks. These are labeled γ_1, γ_2 and γ_3 in order of decreasing temperature and are most clearly evident in the case of the E" plots for the annealed samples. Figure 8 shows the behavior of DP-1,5 under the same conditions, and it can be seen that there now appear to be only two overlapping peaks, labeled γ_1 and γ_2 in the figure. In this case the two peaks are most clearly evident in the quenched tanδ plot. The 4M series behaves in a similar manner to the DP series as shown in Figure 9, except that, for 4M-1,5, which is chosen for purposes of illustration, the two overlapping peaks are best distinguished in the annealed E" plot.

As a general rule, inspection of Figures 6 - 9 reveals that the overall magnitude of the γ relaxation peak is decreased by annealing. Also, the γ_1 process becomes relatively less prominent on annealing. Annealing has two effects: it increases the degree of crystallinity as measured by the x-ray method in the case of the H and DP series, and it increases the amount of hydrogen bonding for all three series. (The 4M series remains completely amorphous as determined by x-rays regardless of the thermal history.) The decrease in the magnitude of the overall γ process with annealing is thus indicative of an amorphous phase origin for the process and/or an association with hydrogen bonded groups.

B. The δ Relaxation.

Figure 10 shows the temperature dependence of E" in the region of -180°C to -100°C for several members of the 4M series. It is readily seen that 4M-1,2 does not exhibit any well defined peak in the γ region

of the -140°C to -120°C. Rather, a small peak with a maximum at -160°C is noted. This is labeled δ and is seen to persist for the higher members of the 4M series in the form of a shoulder on the γ relaxation peak. The anomalous temperature of the peak maximum of the δ peak relative to the "normal" γ peak temperature of the other members of the 4M series has already been noted, as well as the absence of this peak in the DP and H series. It is thus proposed that the δ relaxation arises from a separate and distinct molecular mechanism that is different from the γ relaxations observed for all three series.

C. The Dielectric γ Relaxation.

Figures 11 and 12 show the temperature dependence of the dielectric loss, ε", for two members of the 4M series and two members of the H series, respectively. The higher temperature peak located in the -40°C to -60°C range is apparently connected with absorbed water and is the subject of a subsequent publication. It will not be discussed further at this time except to note the fact that this peak overlaps the dielectric γ relaxation quite severely in all three series. In the case of the 4M series, Figure 11 shows that the dielectric γ relaxation behaves in a similar manner to the mechanical γ relaxation insofar as an increase in magnitude occurs with increasing n. However, the dielectric γ relaxation is not completely absent for 4M-1,2 as it is in the mechanical case, but rather a small peak is discernible at -110°C, although precise location is difficult because of the overlap of the water peak. In contrast to the mechanical results, the dielectric data shows no trace of the δ relaxation peak. Turning to the H series, Figure 12 shows that the dielectric γ relaxation for H-1,2 is much smaller in magnitude than the mechanical

γ relaxation for the same polymer. H-1,5 exhibits an asymmetric dielectric γ peak which appears to consist of two overlapping peaks in contrast to the three overlapping peaks of the mechanical γ relaxation.

Discussion

In the light of the results presented above, it is possible to propose molecular mechanisms responsible for the loss peaks observed in the low temperature region. Each relaxation will be discussed in turn starting at the low temperature end.

A. The δ Relaxation.

It has already been suggested in the results section that the δ relaxation arises from a mechanism distinct from that of the γ relaxation. Inasmuch as this relaxation occurs only in the 4M series, it is reasonable to suspect it to be associated with a structural feature occurring in the 4M series but absent in the DP and H series. The 4M series possesses the unique structural characteristics of having a methyl group attached to the 4 position of the benzene ring (see the structure of the repeat unit given in the Introduction). In the case of poly(methyl methacrylate) a loss peak assigned to the rotation of the α methyl group has been observed by mechanical measurements[20,21] and by NMR line width studies[22]. This loss peak occurs at a temperature of -173°C at 1 Hz. Allowing for the frequency difference of the measurement, this value is quite close to the temperature of the δ relaxation observed in the present work. It thus seems reasonable to assign the δ relaxation to the rotation of the methyl group attached to the 4 position of the benzene ring.

It has been pointed out[23] that the rotation of a methyl group cannot give rise to mechanical loss if the potential energy as a function of rotation angle is given by three energetically equivalent minima each separated by 120° as has generally been supposed. It thus appears that the potential energy must be some more complex function of the rotation angle of the methyl group than would be expected on the basis of the simple rotational isomer model. In the case of the 4M series, it seems reasonable to expect this behavior in view of the possibility of the volume change originated by the rotation of the methyl group attached to the benzene ring.

The absence of a dielectric δ relaxation also lends support to the assignment of the mechanical δ relaxation to methyl group rotations. Since such motions do not involve any dipole reorientations, they would not be expected to give rise to a dielectric loss peak.

B. <u>The γ Relaxation</u>.

Since the γ relaxation in the polyamides has been extensively investigated, the findings will be used as a basis for the discussion of the γ relaxation in the polyurethanes studied here. The polyamides differ structurally from the polyurethanes only in that the

$-\overset{\overset{\displaystyle H}{|}}{N}-\overset{\overset{\displaystyle O}{\|}}{C}-O-$ group in the polyurethanes is replaced by the $-\overset{\overset{\displaystyle H}{|}}{N}-\overset{\overset{\displaystyle O}{\|}}{C}-$ group in the polyamides. The following facts have been established concerning the γ relaxation in the polyamides[23].

(1) The γ relaxation in polyamides arises in part from the motion of $(CH_2)_n$ units between amide groups with $n \geq 3$.

(2) The polar amide groups are partially responsible for the γ relaxation.

(3) The activation energy of the γ relaxation is 9 - 10 kcal $mole^{-1}$.

Low temperature relaxations of the γ type have been observed for a great many polymers of different structural characteristics. It has been proposed, notably by Schatzki[24], that the mechanism of the γ relaxation consists of the hindered rotation of a few methylene groups as a unit. These groups may be located either in the main chain or in side chains. The essential features of the model of Schatzki are that the end bonds of the rotating unit of methylene sequences are colinear and remain fixed. In order for this condition to be met, assuming tetrahedral bond valence angles, equal bond lengths and the rotational isomer conformation model, it must be that in the sequence $-CH_2\{CH_2-(CH_2)_n-CH_2\}CH_2$, n=4 or greater. Parenthetically, it should be noted that such a mechanism must be operative in the amorphous phase since, in the crystal phase, all the CH_2 groups are in the trans conformation (0° rotational angle) and this does not allow for the colinearity of the end bonds required by Schatzki's mechanism. However, it has been shown, at least for the cases of polyethylene[25], an ethylene-methacrylic acid copolymer[26] and polychlorotrifluoroethylene[27] that the γ transition arises partially from the crystalline phase. Thus, a crystalline contribution to the γ relaxation in the case of the polyurethanes cannot be entirely ruled out. Restricting attention to the amorphous phase for the moment, and adopting Schatzki type mechanisms for the γ relaxation in the polyurethanes, the

following sequential structures may be examined in addition to methylene sequences alone

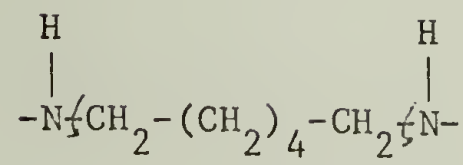

(1)

Here the N-C bonds act as the rotation axis for the methylene sequence and it is presumed that the NH groups are fixed by intermolecular hydrogen bonds. This case is thus really identical to the Schatzki model and would be expected to be active in the H series only. Inasmuch as the γ_3 relaxation occurs only in the H series, it may reasonably be assigned to the above type of motion.

The strict application of the above mechanism to the γ_3 process would indicate the absence of a dielectric γ_3 peak since, as in the δ process, no dipole reorientation is involved. As will be discussed shortly, the conclusion may also be reached that no dielectric γ relaxation of any kind should be present for H-1,2. While it is true that the dielectric γ relaxation in H-1,2 is much smaller in magnitude than the mechanical γ relaxation in H-1,2, Figure 12 nevertheless reveals traces of a γ peak. A plausible explanation for this is that the γ_3 process causes a certain amount of motion of the polar groups to take place. This need not involve rotations but may only consist of vibrations or torsional oscillations. The requirement of dipole reorientation would obviously be satisfied by many types of motion of the polar groups.

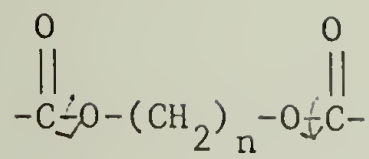

(2)

In this case, which is common to all three series, the carbonyl groups are considered fixed once again by intermolecular hydrogen bonds and the C-O bonds define the rotation axis. If we enforce the condition of colinearity of the C-O bonds, then rotation of the methylene groups and oxygens as a unit can occur for $n \geq 4$. The essential absence of a γ peak in the DP and 4M series for the polymers containing 2 or 3 methylene units in the diol part is in accord with the proposal that n must be 4 or greater. In addition, the good agreement between the temperatures of the low temperature relaxation in the polyethers and the γ relaxation of the 4M and DP series indicates identical molecular mechanisms in the two cases.

It has been shown by Wetton and Williams[28] that the low temperature dielectric loss peak in poly(tetramethylene oxide) is located at a comparable position to the low temperature mechanical loss peak of this polymer, namely, -110°C at 100 Hz. (It should be pointed out that the best comparison between dielectric and mechanical results is obtained using the mechanical tanδ and the dielectric ε''.) It can be seen from Figures 11 and 12 that the main dielectric γ peak for both the 4M and H series is also located in this vicinity. It would thus appear that the main dielectric γ peak in the polyurethanes is identical to the γ_2 mechanical relaxation in the polyurethanes and arises from the same molecular mechanism responsible for the low temperature dielectric and mechanical loss peaks

in poly(tetramethylene oxide), that is, motions of type (2). Figure 12 shows that there is a small shoulder on the low temperature side of the main dielectric γ loss peak in H-1,5. Inasmuch as this occurs at approximately the same temperature as the γ relaxation in H-1,2, it seems reasonable to assume that this peak is the result of motions of the polar groups induced by the γ_3 mechanism. The presence of but a single γ peak between -180°C and -110°C in 4M-1,5 (Figure 11), also tends to confirm this assignment.

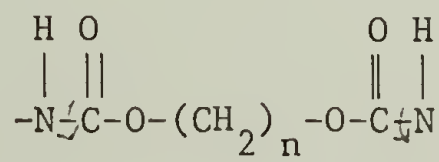

(3)

This case is again common to all three series and it is assumed that the N-H groups are fixed by hydrogen bonding, but the C=O groups are not hydrogen bonded. Once again, enforcing the colinearity of the N-C bonds, free rotation of the unit composed of the methylene groups and the ester groups can occur if $n \geq 5$. There are two major pieces of evidence indicating that motions of type (3) are responsible for the γ_1 relaxation. The first is that annealing, which is known to increase the degree of hydrogen bonding, decreases the magnitude of the γ_1 relaxation relatively more than either the γ_2 or γ_3 relaxation. The second is that the low temperature relaxation in polyesters, which may reasonably be assumed to arise from type (3) motions, occurs at a slightly higher temperature than the low temperature relaxations in polyethylene and the polyethers. (See the Results section.) Type (3) motions should obviously

be dielectrically active. However, the overlap of the very strong dielectric water peak prevents the γ_1 dielectric relaxation from being resolved. Resolution might be obtained at lower frequencies and experiments are currently underway to investigate this point.

The mechanisms proposed here for the γ relaxation require that there be no mechanical γ relaxation peak for 4M-1,2, 4M-1,3, DP-1,2 and DP-1,3 and this is borne out by the experimental facts. However, H-1,2 should show a single γ relaxation peak which would be identified as γ_3 and should be dielectrically inactive. Figure 6 shows the presence of all three mechanical γ peaks in H-1,2 and the presence of a small dielectric γ peak has already been commented on. The probable explanation for this behavior is that the γ_3 type motion, the motion of six CH_2 sequences, induces the motion of the polar groups and thus causes both dielectric activity and the presence of a mechanical γ_2 and γ_1 in H-1,2.

The question of a partial crystalline origin for the γ relaxation in the polyurethanes cannot be settled at the present time. It is certain that the γ relaxation in the polyurethanes arises largely in the amorphous phase as shown by its presence in the 4M series and by the decrease in magnitude observed on annealing. It is realized that the mechanisms proposed here are but first approximations to the true behavior but it is hoped that they will serve as a basis for further refinements concerning the elucidation of low temperature relaxations in polar polymers.

According to the phenomenological theory, we may obtain the dynamic storage modulus, E', and the dynamic loss modulus, E", respectively, using the decay function.

$$E'(\omega) = E_r + (E_u - E_r) \int_{-\infty}^{\infty} \frac{\phi_E (\ln \tau)\, \omega^2 \tau^2}{1 + \omega^2 \tau^2} \, d \ln \tau$$

$$E''(\omega) = (E_u - E_r) \int_{-\infty}^{\infty} \frac{\phi_E (\ln \tau)\, \omega \tau}{1 + \omega^2 \tau^2} \, d \ln \tau$$

where E_u is the unrelaxed modulus which corresponds to the modulus at $\omega \to \infty$ and E_r is the relaxed modulus which corresponds to the modulus at $\omega \to 0$. The quantity $\phi_E (\ln \tau)\, d \ln \tau$ can be regarded as the fraction of relaxation processes with relaxation times between $\ln \tau$ and $(\ln \tau + d \ln \tau)$ and $\phi_E (\ln \tau)$ satisfies the condition

$$\int_{-\infty}^{\infty} \phi_E (\ln \tau)\, d \ln \tau = 1$$

The relative magnitude, $E_u - E_r$, during relaxation process is obtained assuming a single relaxation time as follows

$$\tau = \tau_o \exp (\Delta H^{\ddagger}/RT)$$

where $\Delta H^{\ddagger}$ is the activation energy, R the gas constant and T, absolute temperature.

$$\int_{o}^{\infty} E''d\left(\frac{1}{T}\right) = (E_u - E_r) \int_{o}^{\infty} \frac{\omega\ \tau}{1 + \omega^2\ \tau^2}\ d\left(\frac{1}{T}\right)$$

$$= (E_u - E_r) \int_{1}^{\infty} \frac{\omega\ \tau_o\ \chi}{1 + \omega^2\ \tau_o^{\ 2}\ \chi^2}\ d\chi$$

here

$$\chi = \exp\ (\Delta H^{\ddagger}/RT)$$

Therefore

$$\int_{o}^{\infty} E''d\left(\frac{1}{T}\right) = (E_u - E_r)\ \frac{R}{\Delta H^{\ddagger}} \left(\frac{\pi}{2} - \tan^{-1}\ \omega\ \tau_o\right)$$

If $\omega\ \tau_o \simeq 0$ because τ_o is the relaxation time at $\Delta H^{\ddagger}/RT \simeq 0$.

$$\int_{o}^{\infty} E''d\left(\frac{1}{T}\right) = (E_u - E_r)\ \frac{\pi}{2}\ \frac{R}{\Delta H^{\ddagger}}$$

Then we can derive the equation for the relative magnitude during the relaxation process.

Figure 13 shows a plot of E" versus 1/T for H-1,5. We can calculate $E_u - E_r$ using the area under the E" versus 1/T plot and the $\Delta H^{\ddagger}$'s given in Figure 3 for all three series.

Figure 14(a) shows T_{max} (E") of the γ relaxation of the H series including the peak temperatures of the γ_1 and γ_3 relaxations obtained in the following manner. The peak temperature of the γ_3 relaxation was assumed independent of n and to be located at the same temperature as the γ_3 peak of H-1,2. The γ_1 relaxation temperatures for the various members of the H series were assumed to be identical to those of the corresponding polyesters[18]. In addition, it was assumed that there were no relaxation mechanisms on the higher temperature side of the γ_1 relaxation and the lower temperature side of the γ_3 relaxation. In the calculation of $E_u - E_r$ for the γ_1 and γ_3 relaxation, the contribution from the γ_2 mechanisms was neglected for convenience. Figure 14(b) plots $E_u - E_r$ values for the γ_1 and γ_3 relaxation versus n. If the γ_3 relaxation arises only from motions of methylene sequences in the diisocyanate part of the repeat unit $E_u - E_r$ for the γ_3 relaxation should be independent of n. However, $E_u - E_r$ gradually increase with n for $n>4$. This indicates the γ_3 relaxation is also influenced by the methylene sequences in the diol part as might be expected.

Figures 4 and 5 show plots of the magnitude of the tanδ and E" versus n at 110 Hz. At least four methylene sequences are required for the γ relaxation to be mechanically active. Therefore, the relative ratio of the magnitude of E" for two successive n's may be calculated using $n/(n-1)$ $(n\geq 2)$ for the H series and $(n-3)/(n-4)$ $(n\geq 5)$ for the DP

and 4M series. The calculated values using the magnitudes of E" in Figure 5 are

n	n/(n-1)	H Series	(n-3)/(n-4)	DP Series	4M Series
2	2.00				
3	1.50	1.11			
4	1.33	1.08			
5	1.25	1.07	2.00	1.32	1.27
6	1.20	1.07	1.50	1.19	1.18
7	1.16	1.05	1.33	1.25	1.15
8	1.14	1.05	1.25	1.24	1.12
9	1.12	1.02	1.20	1.24	1.09
10	1.11	1.06	1.16	1.14	1.06

Even though the effect of internal energy changes on the chain conformation is neglected in the calculation, good coincidence between the calculated and experimental values result, especially at high values of n. This is probably because the internal energy effects are averaged out at high values of n. The results discussed above indicate that the γ relaxation mechanism is composed of the independent motion of each four methylene units.

The contribution of the mode with relaxation time τ_i to the relaxation spectrum, $H(\ln \tau)$, is given by its frequency (f_i) times the value proportional to the probability (p_i) for changing conformation between two states.

f_i = n for the H series

f_i = n-3 for the DP and 4M series

$p_i = Ce^{-\Delta E_i/RT}$

C = constant

ΔE_i = internal energy difference between two states

$$H(\ln \tau) = \sum_{\substack{i=3 \\ n \geq 4}}^{n-1} C \ (n-i) \ e^{-\Delta E_i/RT} \ E_i^{\ o} + C_o$$

$$C_o = \sum_{i=3}^{5} C' \ (6-i) \ e^{-\Delta E_i/RT} \ E_i^{\ o} \qquad \text{for the H series}$$

$$C_o = 0 \qquad \text{for the DP and 4M series}$$

where C' is the constant and $E_i^{\ o}$ is the modulus of mechanisms having relaxation time, τ_i.

Suppose that $E_i^{\ o} = E^o$ for all i and ΔE_i is proportional $1/(i+1)$ because chain flexibility increases with n and i (chain flexibility is proportional to $1/\Delta E_i$).

If we adopt the zeroth order of approximation for the relaxation spectrum, the following relationship is obtained

$$H(\ln \tau) = \frac{2}{\pi} E''(\omega)$$

$$E''(\omega) = \frac{\pi}{2} H(\ln \tau)$$

$$= \frac{\pi}{2} \left[CE^{o} \sum_{\substack{i=3 \\ n \geq 4}}^{n-1} (n-i)\ e^{-K/i+1} + C_{o} \right]$$

where

$$K = 1/RT$$

If the contribution arising from the motion of four methylene units (i=3) may be assumed to be larger than that of i>4, we can finally obtain the following equation

$$E''(\omega) = \frac{\pi}{2} \left[CE^{o}\ (n-3)\ e^{-K/4} + C_{o} \right]$$

This equation indicates that E" should increase in magnitude with increasing n. Though the equation is derived on qualitative grounds, it serves to explain the general trend of the experimental results.

C. Conclusions.

The low temperature relaxations in the polyurethanes investigated in this study consist of several overlapping peaks which arise largely from motions in the amorphous phase.

The δ relaxation (-160°C at 110 Hz) is due to rotation of the methyl group attached to the four position of the benzene ring in the diisocyanate part of the repeat unit of the 4M series.

The γ_3 relaxation (-150°C, 110 Hz) arises from motions of methylene sequences in the diisocyanate part of the repeat unit of the H series.

The γ_2 relaxation (-140°C, 110 Hz) arises from motions of methylene sequences including oxygen in the diol part of the repeat unit of all three series.

The γ_1 relaxation (-120°C, 110 Hz) arises from motions of methylene sequences including ester groups with non-hydrogen bonded carbonyl groups in all three series.

CHAPTER III

THE EFFECT OF WATER ON THE MECHANICAL PROPERTIES

The 4M series polymers are very hygroscopic materials while the H and DP series absorb only a very slight amount of water. The samples were prepared by immersing in water for a certain period. The initially clear and transparent films changed to nontransparent and cloudly materials after this treatment. The percentage of absorbed water was defined as the ratio of the weight of the sample with water to the weight of the original sample.

The effect of water on the dynamic mechanical properties of polyurethane materials has been observed by Jacobs and Jenckel[14] using polymers prepared from hexamethylene diisocyanate and 1,4-butanediol (H-1,4 in our notation) in which the amount of absorbed water ranged from 0 to 28%. The magnitude of the peak located around -70°C increased with increasing amounts of water and the peak shifted to lower temperatures, from -70°C to -90°C.

Figure 15 shows the temperature dependence of E' and E" and illustrates the effect of water on several of the relaxation peaks of 4M-1,10, showing the effect of both water and D_2O on the relaxation peaks.

The Effect of Water on the γ Relaxation

Figures 15 and 16 show that the magnitudes of both the tanδ and E" γ peaks decrease with increasing amounts of water and D_2O and that the peak temperatures increase. This behavior is more marked with D_2O than with water. As already discussed in Chapter II, the γ peak consists

principally of three overlapping mechanisms, that is, the γ_1 relaxation arising from the vibrational and rotational motions of the methylene units including non-hydrogen bonded ester group, the γ_2 relaxation arising from motions of methylene sequences including oxygen in the diol part of the repeat units, and the γ_3 arising from the motions of methylene sequences in the diisocyanates part of the repeat unit. The non-hydrogen bonded carbonyl groups may associate with added water molecules as indicated in the following schematic.

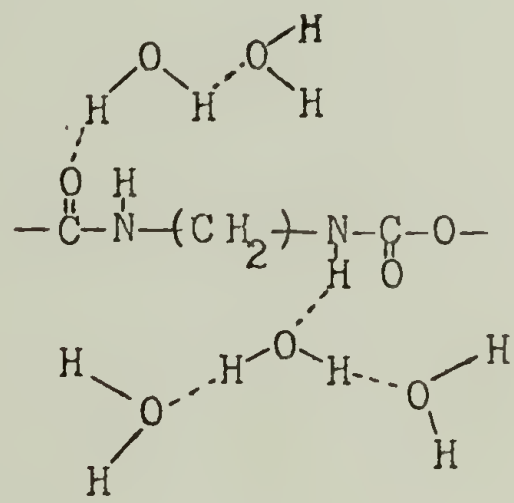

In addition to hydrogen bonding to the carbonyl groups, water molecules may form clusters[29] in the polymer as discussed later in detail. This cluster formation may lead to additional restriction on the rotation of methylene sequences in the diol or the ester part of the repeat unit. This mechanism is in agreement with the experimental results cited above concerning the decrease in magnitude of the γ peak and its increase in temperature with increasing amounts of absorbed water. The γ relaxation of H-1,4 exhibited somewhat different behavior in that the γ peak temperature as well as the magnitude of the γ relaxation decreased with increasing amounts of absorbed water[14]. The peak

temperature shift, however, was very slight (only 3-4°C shift with 28.8 mole percent water) and this is almost negligible in comparison with results of the 4M series.

If hydrogen bond formation between carbonyl groups and water molecules, as well as the formation of cluster of water molecules, is indeed the molecular mechanism responsible for the observed changes in the γ relaxation on absorption of water, alcohols should give rise to a different effect. When alcohols are added as diluents, they can hydrogen bond to carbonyls but they cannot form clusters because only one -OH group in alcohol molecules is available for hydrogen bonding in contrast to the two -OH groups in water molecules. If alcohol molecules act as "pure" diluents without formation of hydrogen bonded clusters, γ relaxation peaks can be expected to shift to lower temperatures with increasing addition of alcohol. This postulated idea is completely consistent with the results in Figure 17 where hexanol was used as diluent. The sample with 79 weight percent hexanol showed a decrease of 15° in the γ peak temperature.

Also, Shen, et.al.[30], have reported that the γ relaxation arising from the motion of side chains of polymethacrylates, was elevated on account of the hindering effect of the immobilized diluent molecule (water).

Since heavy water (D_2O) molecules are larger in radius and more massive than water, the γ relaxation mode involving the rotation of methylene sequences may be expected to be more restricted by heavy water than by water. This is shown in Figure 16, that is, the relaxation shows a

greater decrease in magnitude and a greater temperature shift with heavy water.

Figure 18 shows the temperature dependences of E' and E" of the 4M-1,5 and 4M-1,10 polymers containing water and heavy water. Both polymers exhibit comparable shifts in both peak magnitude and temperature. This shows that the effects are independent of the particular polymer used.

The results are consistent with the idea that absorbed water in polyurethanes associates with carbonyl groups by hydrogen bonding and that water molecules also hydrogen bond to each other to form clusters.

The New Sharp Peak

Additional very sharp peaks appear in both E" and tanδ curves exactly at -120°C with water and -117°C with heavy water as shown in Figures 15, 16 and 18. The temperature location of these peaks is independent of the amount of water and of the polymer sample. The magnitudes of these sharp peaks seem to decrease with increasing absorbed water or heavy water content as shown in Figures 15 and 16. However, since these sharp peaks are overlapped with the γ peak and the γ peak magnitude is itself affected by added water, it is impossible to separate the magnitude effect of water on the sharp peak.

According to the phenomenological theory of mechanical relaxation, the following equations may be written in the case of single relaxation

$$E'' = \frac{(E_u - E_r)\,\omega\,\tau}{1 + \omega^2\,\tau^2}$$

$$\tan\delta = \frac{(E_u - E_r)\ \omega\ \tau}{E_r + E_u\ \omega^2\ \tau^2}$$

where E_u is the unrelaxed modulus which corresponds to E' at the beginning of the relaxation and E_r is the relaxed modulus which corresponds to E' at the end of the relaxation mechanism. $E_u - E_r$ shows the relative magnitude of the relaxation and τ is the relaxation time. In the case of the sharp peak T_{max} (E") is equal to T_{max} ($\tan\delta$) within the experimental error as shown in Figures 15 and 16. This means τ (E") derived from $\partial E''/\partial\omega\tau = 0$ is equal to τ ($\tan\delta$) derived from $\partial\tan\delta/\partial\omega\tau = 0$.

$$\omega_{max}\ \tau\ (E'') = 1$$

$$\omega_{max}\ \tau\ (\tan\delta) = (E_r/E_u)^{1/2}$$

The result $E_u - E_r$ leads to the conclusion that the modulus does not change during the relaxation process and that the magnitude of E" should be zero. The experimental results are obviously at variance with this conclusion. Thus, it may be concluded that the phenomenological theory is not applicable to this type of relaxation mechanism. From this consideration it would appear that the sharp peak does not originate from the polymeric material but is rather associated with low molecular weight substances present in the polymer.

There are many possibilities to explain the origin of the sharp peak, e.g., water by itself, the combination of water and diol monomers,

the combination of water and diisocyanate monomer (4 methyl-methaphenylene diisocyanate) and the stretched part of the chain reported by Matsuoka[31].

The phase transition of ice from the hexagonal form to the cubic form which is located about -110°C has been reported by Shimaoka, et.al.[32,33] If this is the origin for the sharp peak, the decrease of the magnitude with increasing the absorbed water cannot be explained and also the fully swollen material of polyvinyl alcohol (107 wt %) did not show any comparable sharp peak.

Figure 19 shows the temperature dependence of E' and E" for a decanol-water and a diisocyanate-water mixture sandwiched between thin polystyrene film and also the stretched 4M-1,10 (drawn ratio 300%). It is clear that no sharp peak resulted from these experiments.

When the 4M-1,10 polymer has purified by precipitation by pouring its acetone solution into water, samples with absorbed water and heavy water also did not show any sharp peaks as shown in Figure 20. The behavior of E' and E" are almost identical to the results observed for the regular 4M-1,10 except for the disappearance of the sharp peak. Though the regular 4M-1,10 was purified by boiling in hot water and washing with alcohol, low molecular weight impurities or cyclic compounds may have still remained in the sample. The existence of these materials may be one reason for the deviation of the values of the elemental analysis from the calculated theoretical values in the 4M series.

Thus, the sharp peak may arise from motions involving a combination of low molecular weight impurities or cyclic compounds with water or heavy water. At present the mechanism of the sharp peak is not completely clear.

The Effect of Water on the β Relaxation

Small peaks appear around -60°C to -80°C for the samples both rapidly cooled at room temperature and annealed at 60°C as shown in Figures 15, 16 and 21. All these three series showed these peaks in this temperature range. We label this peak β. Similar peaks have been observed for other hydrogen bonded polymers, for example, nylon[34,35], polyurethane[36] and poly(vinyl alcohol)[37,38]. Illers proposed that this peak is due to the motion of carbonyl groups of the polymer to which water molecules are attached by hydrogen bonding. Curtis[35] suggested that this relaxation involves the motion of a water-polymer complex. On the other hand, another idea has been proposed by Rushton and Russell[39]. They were unable to eliminate the β peak of nylon 66 by exhaustive drying and thus concluded that this relaxation results from the motion of $-NH_2$ and -OH chain end groups. In the case of the polyurethanes used in the present investigation, a similar explanation that the β relaxation arises from the motion of chain end groups of -NCO and -OH may be possible but no correlation was found between the peak height of the relaxation and the molecular weight listed in Table I-V as shown in Figure 22. This suggests that relaxation arising from the polar chain ends are negligible in the case of the present experiments. Since the 4M series is very hygroscopic, it is possible that the annealed sample absorbs water on cooling even if the sample chamber is carefully sealed with dry N_2 gas and also the annealing temperature may not be sufficient to completely remove water.

The H and DP series which are very slightly hygroscopic are easier to use for comparisons of the β relaxation. Figure 21 is the temperature

dependence of tanδ of the H and DP series in the γ and β region. This shows the peak height of tanδ around -60°C is remarkably decreased by annealing but the peak is never eliminated completely. Depression of the magnitude may be caused by reduction of water content as a result of annealing process. Since annealing was carried out in sealed glass tubes, the water molecules absorbed in the sample could not be removed absolutely due to the presence of water vapor.

As shown in Figures 15 and 16, the peak temperature of the β relaxation located originally around -60°C shifts first to lower temperatures and then back to higher temperatures at higher concentrations of water. In addition, a new peak occurs at large amount of absorbed water. The shift of the peak temperature is clearly shown in Figure 23(a). Poly(vinyl alcohol) fully swollen with water (10 wt %) shows a peak associated with pure water molecules around -90°C. Plate 1 is an electron micrograph of a surface replica of 4M-1,10 sample containing 32 wt % water. It can be seen that many voids on holes are present.

Nemethy, et.al.[40], have reported that the cooperative character of hydrogen bonding in water leads to the formation and dissociation of clusters of hydrogen bonded molecules. The formation of the holes revealed in the electron microscope picture may be attributed to clusters of embedded water molecules.

The rapid depression of the peak temperature at small amounts of absorbed water may be attributed to the formation of clusters of water molecules inasmuch as the peak temperature is very close to that of pure water as in poly(vinyl alcohol).

Water molecules may play a part in breaking the original NH---O=C hydrogen bonding and reforming a new hydrogen bonded network[38] as well as in the formation of hydrogen bonding between originally non-hydrogen bonded carbonyl groups and water molecules. The magnitude of the relaxation associated with hydrogen bonding between the carbonyl groups of the backbone chain and water molecules may be expected to increase with increasing amounts of water. The schematic explanation of the two overlapping peaks which arise from motions associated with water molecules and hydrogen bonded parts shown in Figure 23(b) is very consistent with the results of the peak temperature locations observed in the E" and tanδ curves. Therefore we can summarize the contribution of absorbed water to the β relaxation as follows.

At the lower amounts of water (<20 wt %), water molecules form clusters which give rise to the water relaxation peak located around -80°C. At water content greater than 20 wt %, as shown in Figure 23(a), water molecules hydrogen bond to non-hydrogen bonded carbonyl groups or break the original carbonyl NH hydrogen bonds and replace them with water-carbonyl hydrogen bonds.

The peak around -80°C, labeled β_w, arises from motions associated with clusters of water molecules and the peak around -60°C, labeled β, arises from motions associated with water hydrogen bonded to the polymer through the carbonyl groups.

The comparisons between water and heavy water are shown in Figures 16 and 18. Also saturated poly(vinyl alcohol) with heavy water shows a heavy water peak at -70°C (10° higher than that of water). Since the β_w

peak is located very close to the β peak, it is very difficult to distinguish between the β_w and β relaxations due to overlapping. The peak temperature has a tendency to increase with increasing heavy water content. This may indicate that the relaxation shifts to higher temperatures with increasing heavy water to a greater degree than with increasing water because of the larger size or greater weight of the heavy water molecule compared to the water molecules.

The Effect of Water on the α Relaxation

4M-1,10 shows the very peculiar result that the peak temperature of the α peak increases with increasing water and heavy water content as shown in Figure 15. This indicates that these materials act as anti-plasticizers in contrast to the plasticizing effect of water in polymers of similar structure such as the polyamides. A possible explanation of this strange behavior is that the glass transition temperature increases due to decreasing free volume resulting from cluster formation which compresses the amorphous region.

CHAPTER IV

HIGH TEMPERATURE RELAXATIONS (α RELAXATION) IN POLYURETHANES

Figure 24 shows the overall dynamic mechanical behavior of typical samples from each series, namely H-1,5, DP-1,5 and 4M-1,5. The γ and β loss peaks in E" will not be discussed further and attention is directed to the β_ϕ, α, α_t and α_c loss peaks. Before these are discussed in detail, it may be noted that E' shows small changes in the temperature regions of the secondary loss peaks but the catastrophic decrease in E' is associated with the α peak in each case. This decrease occurs at increasing temperatures in the order H-1,5 < 4M-1,5 < DP-1,5. Such a large decrease in E' has been traditionally associated with the main glass transition temperature of the material and the behavior of E' in the α loss peak region thus lends support to the assignment of the α peak to motions associated with the glass transition.

The β_ϕ Relaxation

Both the DP and 4M series exhibit broad shoulders below the α relaxation in the temperature region from 0 to 60°C at 110 Hz as shown in Figure 24 for DP-1,5 and 4M-1,5. At 3.5 Hz, the DP series shows an especially well resolved β_ϕ peak at 20°C as shown in Figure 25. This is in contrast to the behavior of the 4M series which still only exhibits a shoulder at about 30°C at 3.5 Hz. Similar behavior has been observed for polystyrene by Takayanagi[37] and Illers and Breuer[41] noted the same phenomenon in the case of a polycarbonate (poly 1,5 naphthalenedi-β-oxyethyl ether). All of these polymers share the structural feature of

possessing phenyl groups in either the main chain or the side chain (in the case of polystyrene). Thus it is reasonable to assign this relaxation mechanism to torsional motions of the benzene ring. Support for this assignment may be derived from the absence of the β_ϕ relaxation in the H series which, of course, does not contain phenyl groups. The lower temperature of the β_ϕ relaxation in the DP series as compared to the 4M series probably reflects the greater mobility of the phenyl groups in the DP series relative to the 4M series.

The α and α_t Relaxations

The glass transition temperatures, (T_g's), of the three series were previously measured by DSC[46]. At that time it was found that, for the DP series, T_g is a monotonically decreasing function of n and a similar effect was noted for the H series, although the decrease in T_g with increasing n is much less marked in this case. The 4M series, on the other hand, was found to possess an irregular dependence of T_g on n, with no clear trends emerging.

Figure 26 provides a comparison between the T_g's measured by DSC and the temperatures of the E" α loss peak at 110 Hz. Only the DP and 4M series are included in Figure 26 inasmuch as the relaxation behavior of these series is less complex than that of the H series. It may be seen that there is a very good correlation between the α loss peak and the DSC T_g in all cases. The α loss peak occurs at a higher temperature than the DSC T_g because of the difference in the time scale of the measurements. The behavior of the α relaxation of the DP series is very similar to that of the α relaxation in a series of polymethylene terephthalates,

$\left[\overset{O}{\overset{\|}{C}} - O - O - (CH_2)_x - O \right]_n$ reported by Ward[18], who observed a temperature decrease in the α peak with increasing x in a manner roughly parallel to the decrease in the crystal melting points of these polymers with increasing n. The reason for the irregular behavior of the T_g's of the 4M series is unknown at present. It was suggested[46] that differences in water content or degree of hydrogen bonding among the various members of the 4M series might account for the data. Considerable care was taken to insure sample dryness and measurements by the DSC and dynamic mechanical techniques were made some months apart. Thus it seems unlikely that water is responsible for the differences noted. Variations in hydrogen bonding as a function of n are currently being investigated using infrared spectroscopy and further interpretation must await these results. It is perhaps worth noting, however, that if the T_g of 4M-1,8 is disregarded, a zigzag pattern emerges with the odd members of the series showing higher T_g's than the even numbers.

The activation energies in the α region were calculated using the following equation

$$\frac{1}{k} \propto \tau = \frac{1}{2\pi f} = \frac{h}{kT} \quad e^{-\Delta F^{\ddagger}/RT}$$

where K is the rate constant, h the Planck constant, k the Boltzmann constant and $\Delta F^{\ddagger}$ the free energy.

$$f_{max} = C \frac{kT}{h} e^{-\Delta H^{\ddagger}/RT}$$

$$\Delta H^{\ddagger} = 2.303R \frac{d \log (f_{max}/T)}{d\left(\frac{1}{T}\right)}$$

The activation energies in the α region ranged from 80 to 150 kcal/mole as listed in Table IV-I and these values are much higher than the activation energies in the α region of most other polymers (40 kcal/mole). The polymers having hydrogen bonding, e.g., polyamides and polyvinyl alcohol also show high values of the activation energy. Therefore, this phenomenon appears to be associated with motional restrictions in the amorphous region imposed by the presence of the hydrogen bonds.

The H series is unique in its behavior in the glass transition region inasmuch as there are two loss peaks in this region, labeled α and α_t in Figure 24. Figure 27 is a plot of the peak temperatures for the α and α_t peaks vs. n for the H series together with the corresponding DSC data. The α peak correlates very well with the DSC T_g and is thus identified as arising from the segmental motions associated with the main glass transition. The points in the figure labeled T_t (DSC) are the maxima in small endothermic DSC peaks. The temperature locations of these peaks are almost independent of n are those of the α_t loss peaks. In addition, the T_t (DSC) peaks are very sensitive to the thermal history of the sample. Figure 28 indicates the shapes of DSC curves for H-1,2 subjected to various thermal histories. In the first run, the samples were quenched

from the melt to -78°C and then heated at 10°C per minute. The notation T_c refers to the exothermic peak observed for quenched samples above T_g which arises from crystallization. The absence of a T_t peak in the quenched samples as well as its endothermic nature indicates that it does not originate from the crystallization of amorphous material. In the second run, the samples after the first run were quenched from 120°C to -78°C and then heated at 10°C per minute. Now the endothermic T_t peak is evident. It thus becomes clear that the T_t peak is due to a solid-solid phase transition (a first order thermodynamic transition) involving a change from one crystal habit to another. The excellent correlation between the T_t (DSC) peak and the α_t loss peak indicates that the latter arises from motions within the crystal phase associated with the crystal-crystal phase transition. The third and fourth runs indicate the effect of annealing above the temperature of the α_t transition on the shapes of the DSC curves. The α_t peak essentially disappears and the α peak becomes much less marked. Table IV-I indicates temperature location of the DSC peaks for H-1,2 subjected to the thermal histories of Figure 28.

Figure 29 shows the temperature dependence of E' and E" for H-1,5 in the glass transition region. The sample quenched at -20°C clearly shows well separated α and α_t peaks. However, the sample annealed at 138°C for 24 hours (approximately 20°C below the melting point) shows no evidence of either an α or α_t peak and, instead, a new peak appears at the much higher temperature of 80°C. The solution grown material which is presumably of very high crystallinity again shows no α or α_t peak but a shoulder appears at 100°C.

Figure 30 adds considerably to the picture of the H series relaxation phenomena in the glass transition region. The thermal histories of the samples in Figure 30 were identical to those of the DSC curves, Figure 28. The E" temperature dependence for the first run reveals a rather asymmetric α peak which consists of overlapping mechanisms. E' for this run shows the beginning of a sharp decrease corresponding to T_g, but does not show the subsequent maximum associated with the α_t peak. E' does level off above the α region, however, and this, together with the exotherm observed in the DSC experiment for such samples (Figure 28), indicates crystallization taking place. However, this sample does not undergo an α_t relaxation within the time scale of the experiment and no DSC endotherm below the melting point is observed. In sharp contrast to this is the behavior observed in the second run. Here may be observed both the α and α_t peaks, well separated, with the α_t peak accompanied by the maximum in E" already commented upon. The third run shows only a single broad peak which presumably arises from the merging of the α peak with other mechanisms. The temperature dependence of E' for the third run is quite typical of the behavior of semicrystalline polymers around T_g. No maximum in E' is observed. The annealed sample behaves in a comparable manner to the annealed H-1,5 of Figure 29. The 90° loss peak evidently arises from motions within the crystal phase although the exact nature of these motions is still unclear. For the moment, we content ourselves with labeling this peak α_c'.

Figure 31 shows the temperature dependence of E' and E" for a H-1,2 sample quenched at -40°C and then

stored at room temperature for one month. Again, the α and α_t peaks are in evidence for the -40°C quenched sample while the α_t peak is absent for the aged sample. Evidently, the crystal-crystal phase transition associated with the α_t peak requires a certain amount of nuclei to be present. Presumably, fast quenching does not allow time for nuclei to form and so the α_t relaxation does not occur within the time scale of the experiment.

Figure 32 brings together dynamic mechanical, DSC and volume-temperature data in the glass transition region for H-1,5. In the quenched sample, which shows no α_t transition, the volume-temperature plot shows a distinct break associated with T_g and then a pronounced levelling off associated with crystallization as evidenced by the DSC exotherm. The sample cooled to room temperature, on the other hand, shows very little volume change associated with the α_t transition. This implies that the volume change in going from one crystalline modification to the other must be small.

It remains to inquire into the nature of the crystal-crystal phase transition associated with the α_t relaxation. Takayanagi[43] has indicated, for the case of nylon 6, that a crystal structure change from a monoclinic to a hexagonal unit cell takes place above T_g. If a similar mechanism is operative in the H series, there should be a change in the lattice spacings observed by x-ray analysis. Table IV-II shows that such a change does indeed occur in going from quenched to annealed H-1,2. The details of the analysis are incomplete as yet, but the indication of the essential correctness of the mechanism is strong.

There are several results to further explain the origin of the α_t relaxation. H-1,4 and H-1,10 exhibited smaller relative magnitudes, $E_u - E_r$ for the α_t relaxation than did the other members of the H series. Figure 33 is a plot of $E_u - E_r$ versus n for the α_t relaxation and a zig-zag trend is apparent with the exception of H-1,2 and H-1,3. Members of the H series with even n have lower values of $E_u - E_r$ for the α_t relaxation than do members of the series with odd n.

Figure 34 is the infrared spectra of two samples of H-1,2, one of which was quenched at -78°C and the other of which was annealed at 90°C. The prominent shoulder around 3420 cm^{-1} in the quenched sample which arises from the free hydrogen N-H stretching mode almost disappears for the annealed sample. Also, the peak around 3290 cm^{-1} is shifted to a lower frequency in the case of the annealed sample. This result indicates that the concentration of free N-H groups gradually decreases during the annealing process.

Figure 35 shows the fiber period of the H series versus n, including the theoretical fiber period calculated on the assumption that the chains are in the all trans planar conformation. Agreement is obtained only in the case of H-1,4, while the other members of the H series seem to be in a conformation which is slightly less extended than the all trans conformation. Zahn[5] has reported that H-1,4 exists in a planar zigzag form while Saito, et.al.[6], have reported that H-1,5 exists in a twisted form similar to the γ form of polyamides. This twisted conformation allows complete hydrogen bonding to occur. Vogeslong[42] suggested that the adjacent molecular segments of a γ form may all be in the same direction

rather than inverted and that as a result the hydrogen bonds are not normal to the chain axis, as in the α and the β forms, but are tilted. The experimental results show good agreement with the data reported by Zahn and Saito. This indicates that the H series exists in a twisted chain conformation similar to the γ form of polyamides. A phase transition from the α form to the γ form of polyamides occurs during the annealing process to form complete hydrogen bonding. This idea may be applicable to explain the α_t relaxation of the H series.

On the basis of the chemical structure shown in Figure 36, H-1,4 and H-1,10 can form perfect hydrogen bonding even in the case of the parallel and antiparallel allignment of the chain directions in the all trans conformation. The H series members with odd n cannot form completely hydrogen bonded sheets if the chains are in the all trans planar conformation. The shift of the infrared N-H hydrogen bonded stretching mode to lower frequencies on annealing may be consistent with the idea that the α form undergoes crystal phase transition to the γ form during the annealing process in order to form completely hydrogen bonded structures.

As expected from the chemical structure of H-1,4, this polymer can form completely hydrogen bonded sheets with chains in the planar trans conformation and thus the magnitude of the α_t relaxation should be much smaller in the case of H-1,4.

Thus it is concluded that the α_t relaxation arises from motions associated with the phase transition from the α form to the γ form similar to the case of polyamides. The "driving force" is the tendency to form completely hydrogen bonded structures.

In contrast to the very complex behavior displayed by the H series, the DP and 4M series are much more straightforward. Figure 39 shows the temperature dependence of E' and E'' for DP-1,5 in the glass transition region. Sample 1, which was quenched from the melt to -78°C, shows no evidence of crystallinity measured either by the x-ray or DSC method. Its relaxation behavior is typical of that of amorphous polymers in which a sharp loss peak associated with the glass transition is observed accompanied by a large decrease in the storage modulus. As the degree of crystallinity increases from samples 1 through 3 (sample 1 = 0%, sample 2 = 25%, sample 3 = 36% from DSC) the α peak broadens considerably and also increases in temperature from about 100°C for the quenched sample to about 120°C for the annealed sample. The broadening of relaxation peaks associated with T_g and their decrease in magnitude with increasing crystallinity is well known and has been observed, for example, by Takayanagi[37] for polyethylene terephthalate. The increase in the α peak temperature with increasing crystallinity, although generally a small effect, is also not uncommon and is attributed to the bracing effect exerted on the amorphous regions by the presence of crystallites.

The 4M series, as might be expected on the basis of its wholly amorphous character, shows essentially no change in the magnitude, shape or temperature location of the α peak on annealing.

The α_c Relaxation

The α_c relaxation appears as a small shoulder about 40 to 50°C below the melting point for the H and DP series. It is completely absent in the amorphous 4M series and on this basis is associated with motions

occurring in the crystal phase. It is especially prominent for well annealed samples as may be seen in Figures 29, 36 and 39.

The α_c relaxation did not show reproducibility upon repeated tests while the α relaxation associated with the segmental motion in the amorphous region did show reproducibility. This indicates the α_c relaxation motion may be associated with motions involving the crystalline region.

Hirota, et.al.[44], have reported a dielectric loss peak which they labeled α_i located around 95°C to 100°C at 110 Hz for H-1,4. This temperature location is almost consistent with that of the mechanical α_c peak. They concluded that the α_i relaxation was associated with motions arising from interfacial polarization at the boundaries between the crystalline and amorphous regions.

CHAPTER V

THERMAL PROPERTIES OF POLYURETHANES

Experimental

A. Thermal Analysis.

Melting point, T_m, cold crystallization temperature, T_c, solid-solid phase transition temperature, T_t, and glass transition temperature, T_g, were all determined by Differential Scanning Calorimetry (Perkin Elmer Model DSC 1-B). The scanning speed was 10°C per minute in all cases. The temperature of the peak maxima (endotherms) or the peak minima (exotherms) were taken as the temperature of the transitions. In the case of the glass transition, the midpoint of the transition was chosen to represent T_g. The schematic feature of DSC curve is

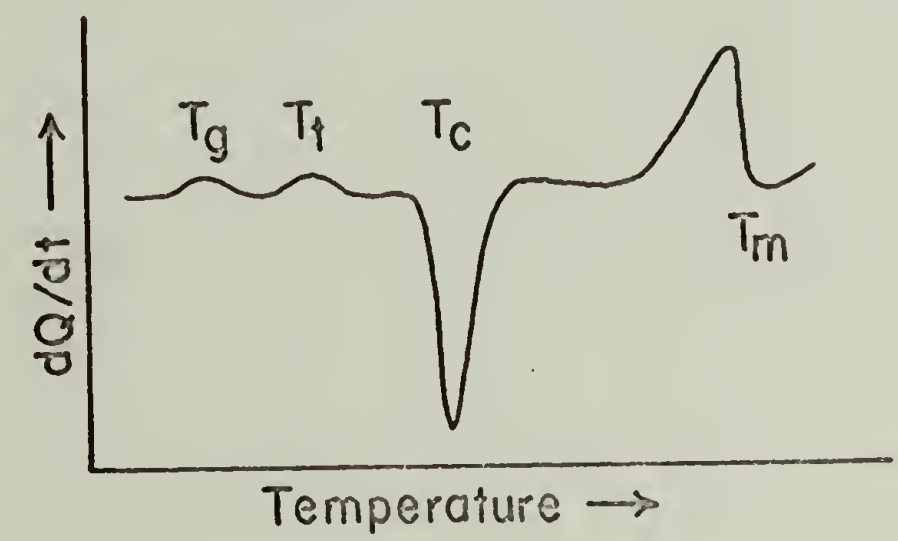

B. Heat of Fusion.

Experimental heats of fusion, $\Delta H_f(E)$ were calculated from the area under the DSC melting endotherms. Pure titanium metal was used as a standard. Theoretical heats of fusion, $\Delta H_f(T)$ were calculated by two methods, (1) the diluent method and (2) the x-ray method. Both methods will be discussed in detail later. Phenanthrene was used as a diluent

for the melting point depression experiments. In these experiments melting points were taken to be the temperatures at which the melting endotherms returned to the base line.

C. Degree of Crystallinity.

X-ray measurements were accomplished by means of a radial scanning method. The x-ray absorption as a function of Bragg angle for the completely amorphous H series polymers were obtained by scanning the polymers above their melting points. The corresponding data for the DP series was obtained by scanning samples which had been quenched from the melt in dry ice-alcohol. Such samples showed no melting endotherm by DSC. The air scattering was subtracted from the absorption data and incoherent scattering was ignored under the assumption that its contribution to the total scattering was negligible.

The degree of crystallinity was obtained from

$$\text{Degree of Crystallinity} = 1 - \frac{(\text{Integrated Absorption})_{\text{amorphous}}}{(\text{Integrated Absorption})_{\text{total}}}$$

Melting Points and Glass Transition

A. Melting Points.

The melting points of the DP and H series are collected in Table V-I[46]. There are scattered references to the melting points of some of these polymers in the literature[47,48,49]. The melting point of H-1,4, for example, is quoted as 180°C[47] in excellent agreement with our value of 182°C. In both series it is seen that the T_m's decrease in a zigzag fashion with increasing methylene sequence in the repeat unit.

The zigzag phenomenon has been observed before, both in the case of nylons containing even and odd numbers of methylene groups in the repeat unit and in the case of low molecular weight hydrocarbons of even and odd chain lengths. The effect is attributed to packing efficiency with the even numbered members packing more efficiently on the basis of geometrical considerations and thus melting higher than the odd numbered members.

The zigzag behavior of the melting points can be discussed more quantitatively on the basis of statistical thermodynamics.

We construct a canonical ensemble from N statistical chain segments. The ensemble volume is V and its temperature is T. The partition function for the ensemble is then

$$Q\ (N,\ V,\ T) = N!\ \prod_i \frac{p_i^{\,n_i}}{n_i!}$$

where p_i is defined as $Ce^{-E_i/kT}$ where E_i is the internal energy of the ith statistical segment, n_i is the number of statistical segments in the ith subsystem, $\sum_i n_i = N$ is the total number of statistical segments.

The Helmholtz free energy, A, is given by the following well-known equation.

$$A = -\ kT \ln Q$$

$$= -\ kT \left[\ln N! + \sum_i (n_i\ p_i - \ln n_i!) \right]$$

Introducing Stirling's equation for n_i sufficiently large,

$$A = - kT \left[N \ln N + \sum_i n_i \ln \frac{P_i}{n_i} \right]$$

The entropy is given by

$$S = - \left(\frac{\partial A}{\partial T}\right)_{V,N}$$

$$= k \left[N \ln N + \sum_i n_i \ln \frac{P_i}{n_i} \right] + kT \sum_i n_i \frac{1}{P_i} \left(\frac{\partial p_i}{\partial T}\right)_{V,N}$$

Since

$$p_i = Ce^{-E_i/kT}$$

$$\left(\frac{\partial p_i}{\partial T}\right)_{V,N} = \frac{E_i}{kT^2} \; p_i$$

$$S = k \left[N \ln N + \sum_i n_i \ln \frac{P_i}{n_i} \right] + \frac{1}{T} \sum_i n_i E_i$$

therefore

$$\Delta S = k \sum_i \ln \left(\frac{p_i^{\,p_i}}{p_c^{\,p_c}} \right)^N + \frac{1}{T} N \, \Delta \overline{E}$$

$$= Nk \sum_i \ln \left(\frac{p_i^{\,p_i}}{p_c^{\,p_c}} \right) + \frac{1}{T} N \, \Delta \overline{E}$$

Also

$$E = A + TS = \sum_i n_i \, E_i = N \, \overline{E}$$

The enthalpy (ΔH) and entropy (ΔS) changes during the melting process are

$$\Delta S = S_{\text{melt at equilibrium}} - S_{\text{crystal}}$$

$$\Delta H = H_{\text{melt at equilibrium}} - H_{\text{crystal}}$$

In order to derive S_{crystal} we formally state that all the subsystems are in the crystalline state,

$$S_{\text{crystal}} = k \left[N \ln N + \sum_c n_c \ln \frac{p_c}{n_c} \right] + \frac{1}{T} N \, \overline{E}$$

where the summation is now over the subsystem in the crystalline state and $\overline{E}$ refers to the average of the internal energy of the crystal

$$\Delta S = S_{\text{melt at eq.}} - S_{\text{crystal}}$$

$$= k\left[N \ln N + \sum_i n_i \ln \frac{p_i}{n_i} \right] + \frac{1}{T} N \overline{E}_{\text{eq.}}$$

$$- \left\{ k\left[N \ln N + \sum_c n_c \ln \frac{p_c}{n_c} \right] + \frac{1}{T} N \overline{E}_{\text{crystal}} \right\}$$

$$= k \left[\sum_i n_i \ln p_i - \sum_c n_c \ln p_c \right]$$

$$- k \left[\sum_i n_i \ln n_i - \sum_c n_c \ln n_c \right]$$

$$+ \frac{1}{T} N \left[\overline{E}_{\text{eq.}} - \overline{E}_{\text{crystal}} \right]$$

If each ith state is equivalent to the ith level, that is, the degeneracy of the ith level is always one, then

$$\Delta S = k \sum_i \ln \frac{p_i^{n_i}}{p_c^{n_c}} + \frac{1}{T} N \Delta\overline{E}$$

$$n_i = p_i N$$

$$n_c = p_c N$$

Finally we can obtain

$$\Delta S = Nk \sum_i \ln \frac{P_i}{P_c} + \frac{1}{T} N \Delta \overline{E}$$

where

$$P_i = p_i^{p_i}, \; P_c = p_c^{p_c}$$

Also the enthalpy is

$$H = E + PV$$

For the solid state the pressure and the volume change during the melting process can be ignored.

$$\Delta H = \Delta E + V\Delta p + p\Delta V \simeq \Delta E$$

We arbitrarily break the melting process down into two distinct steps.

(1) Conformational changes from the all trans "crystalline" conformation to the random coil "liquid" conformation. It is assumed that no translation of chain segments with respect to one another takes place during this step.

(2) Translation of chain segments with respect to one another.

Schematically

$$\text{crystal state} \xrightarrow[\Delta H_1]{\Delta S_1} \text{liquid "1"} \xrightarrow[\Delta H_2]{\Delta S_2} \text{liquid "2"}$$

ΔS_1 arises from the fact that more conformations are available to the molecules in the "liquid 1" state than in the crystal state. ΔH_1 arises from energy differences among the various conformational isomers. ΔS_2 arises from the translational motion of chain segments while ΔH_2 arises from the changes intermolecular interactions (hydrogen bonding) as a result of this translational motion. The total change of entropy and enthalpy from the crystalline state to the molten state is

$$\Delta S_m = \Delta S_1 + \Delta S_2$$

$$= N\,k \sum_i \ln \frac{P_i}{P_c} + \frac{1}{T} N\,\Delta\bar{E} + \Delta S_2$$

$$\Delta H_m = \Delta H_1 + \Delta H_2 = N\,\Delta\bar{E} + \Delta H_2$$

Since the Gibbs free energy of the melt and of the crystal are equal at the melting point, we have

$$G = H - T\,S$$

$$\Delta G_m = \Delta H_m - T_m\,\Delta S_m = 0$$

$$T_m = \frac{\Delta H_m}{\Delta S_m}$$

$$= \frac{N\,\Delta\bar{E} + \Delta H_2}{Nk \sum_i \ln \frac{P_i}{P_c} + \frac{1}{T} N\,\Delta\bar{E} + \Delta S_2}$$

The structures of the polyurethanes used in these experiments are

H Series 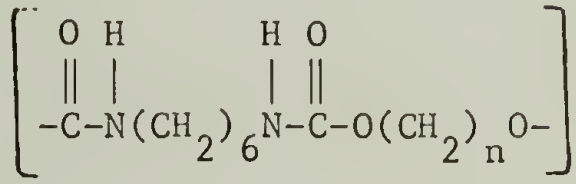 n=2-10

DP Series 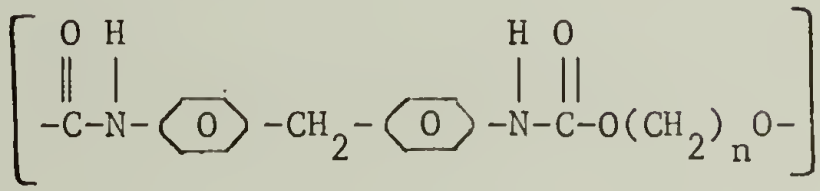 n=2-10

It is reasonable to consider that the number of possible conformation states increases with increasing methylene sequence length, n. This means that T_m decreases with n and this tendency is shown in Table V-I ignoring the zigzag fashion. The polarities of the chains with even n

cancel each other in the crystalline region but with odd n the chain polarities are additive. Also, hydrogen bond formation for even n is easier than that for odd n. These ideas predict that the crystalline region with even n is more stable than that with odd n, that is, the values of ΔH_2 for even n are higher than those for odd n. The zigzag tendency of T_m may thus be concerned with the ΔH_2 difference between even n and odd n. The possible change of P_i/P_c and ΔH_2 may make the melting temperatures decreased in the zigzag fashion with increasing n. Also, the melting points of the DP series are higher than those of the H series because the stiff diphenyl group in the main chain leads to low values of P_i/P_c.

B. The Glass Transitions.

The T_g's for the three series are summarized in Table V-I. As expected, the DP series shows highest T_g's, reflecting the influence of the "stiff" diphenylmethane group. In addition, the T_g's of the DP series decrease in regular fashion with increasing methylene sequence lengths (increasing n) in the repeat unit. This is due to the increased mobility introduced by the presence of these methylene sequences. It is possible to regard the phenomenon as arising from the fact that the polymer becomes more polymethylene-like with increasing methylene sequence length.

We can apply an equilibrium model[50-53] which has as its basis restricted internal rotation to describe the behavior of the glass transition region. This naturally leads to a physical picture wherein at low temperatures ($T<T_g$), the molecular segments are localized in a

potential energy well and undergo torsional vibrations. On the other hand, at extremely high temperatures ($T>T_g$), the motion tends to approach free rotation about single bonds in the polymer chain. The region of interest lies intermediate to these two extremes, i.e., when $T \simeq T_g$.

The potential energy is considered to be a function of the angle of rotation about a given bond. The potential energy hindering rotation is assumed to be separable into an internal and an external part. Thus the total potential energy would have the following general form:

$$V = \frac{1}{2} V_i \ (1 - \cos n\phi) + \frac{1}{2} V_e \ (1 - \cos (m\phi + a)) + \text{constant}$$

where V_i and V_e are the respective intramolecular and intermolecular barrier heights, n and m are the corresponding potential energy periodicities, ϕ is the angle of rotation out of the chosen plane of reference, and "a" is a possible phase difference in the angular distribution of the minima.

In the case of the tetrahedral carbon atoms, a particularly simple case arises when m=n=3 and a=0

$$V = \frac{1}{2} (V_i + V_e) \ (1 - \cos 3\phi)$$

$$= \frac{1}{2} V_m \ (1 - \cos 3\phi)$$

where

$$V_m = V_i = V_e$$

The Hamiltonian for the rotation about the jth bond treated classically is

$$H_r = \frac{1}{2I_j}\left(P_\theta^{\,2} + \frac{P_\phi^{\,2}}{\sin^2\theta}\right) + V$$

where P_θ and P_ϕ are momentums about the angles θ and ϕ, respectively, and I_j is the moment of inertia of jth bond.

The classical partition function about the jth bond is

$$Q_{j\ \mathrm{class}} = \frac{1}{h^2}\int_{P_\phi}\int_{P_\theta=-\infty}^{+\infty}\int_{\phi=0}^{2\pi}\int_{\theta=0}^{\pi} e^{-H_r/kT}\, d\theta\, d\phi\, dP_\theta\, dP_\phi$$

$$= \frac{\pi I_j kT}{h^2}\int_0^{2\pi} e^{-V/kT}\, d\phi$$

Then the total partition function is

$$Q_{total} = \prod_j Q_{j\ \mathrm{class}}$$

The energy is derived using the above total partition function

$$E = kT^2 \left(\frac{\partial \ (\ln Q_{total})}{\partial T} \right)_{V,N}$$

Therefore the heat capacity, C_v, is derived as a function of temperature

$$C_v = \left(\frac{\partial E}{\partial T} \right)_V$$

If we plotted the heat capacity derived from this partition function against temperature, a maximum would be observed around $V_m \simeq 5\ kT_{max}$. It is now proposed to identify T_{max} with T_g, which leads to the result that the glass temperature is proportional to the total barrier height energy corresponding to the stiffness of the chain backbone. The stiffness of the chain backbone decreases with n and therefore V_m decreases with n. This relationship indicates that T_g decreases with n as detected experimentally.

If we apply copolymer idea for the DP series the T_g's of many copolymers may be represented by the empirical equation[54]

$$\frac{1}{T_g} = \frac{w_1}{T_{g1}} + \frac{w_2}{T_{g2}}$$

where T_g is the glass transition of the copolymer, T_{g1} is the glass transition of one homopolymer, and T_{g2} is the glass transition of the other homopolymer. w_1 and w_2 are the weight fraction of homopolymers one and two in the copolymer. The DP series may be regarded somewhat arbitrarily as a copolymer of methylene and diphenylurethane. According to this view the repeat unit of homopolymer one is

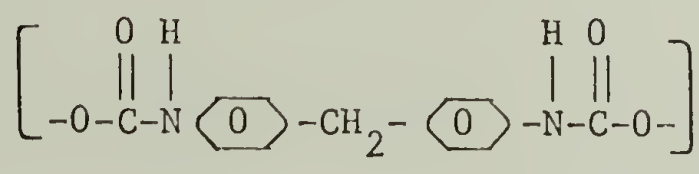

and that of homopolymer two is $[-CH_2-]$.

Figure 38 is a plot of $1/T_g$ versus w and it is seen that a fairly good straight line results with an extrapolated value of T_{g2} of -115°C. It has been established by a number of workers[54] that the T_g of polymethylene is approximately -120°C, in excellent agreement with the extrapolated value. It should be noted that the intermolecular hydrogen bonds which undoubtedly exist in these polymers seem to play a rather minor role in determining T_g, at least in the samples studied.

The situation is quite different in the case of the 4M series. Since the diisocyanates monomer is unsymmetrical, it can enter the chain in more than one configuration. This introduces sufficient disorder in the structure to make packing into a crystal lattice difficult and thus the 4M series is amorphous, at least without prolonged annealing at elevated temperatures. It would appear that the same trends should be noted with the 4M series as with the DP series since increasing the number of methylene units in the repeat unit should lead to increased chain backbone mobility in an analogous fashion to the effect in the DP series.

Examination of Table V-I shows, however, that the T_g's for the 4M series behave in an irregular manner. The reason for this is not entirely clear at this time. One possibility is the effect of water. All of these series are hydrophilic, but the effect is somewhat more pronounced in the 4M series, probably because of the amorphous nature of this series. Caution was taken to exclude water but it is certainly possible that traces might remain. Water is an extremely effective plasticizer for nylons so that the irregularities observed in the 4M series may be due to a similar cause. A second possibility is that the various polymers in the 4M series may have different concentrations of intermolecular hydrogen bonds. Changes in the level of hydrogen bonding are known to have significant effects on T_g's and a study has been made of this effect on a series of copolymers of various methacrylates containing hydroxyl groups[55].

It was found that T_g decreased markedly as the concentration of hydrogen bonding hydroxyl groups decreased. The situation in the 4M series may be similar. An infrared study is presently in progress to attempt to obtain quantitative information about the hydrogen bonding in all the series investigated. If this explanation for the irregular T_g behavior is correct, it leads to the conclusion that intermolecular forces play a dominant role in determining T_g in the 4M series while chain mobility is the important factor in both the DP and H series.

Cold Crystallization and Solid-Solid Transition

Figure 39 shows DSC curves for H-1,2 subjected to three different thermal treatments. Every quenched sample of the H series exhibits a

very sharp, large exothermic peak, just above T_g. The peak temperatures, T_c's, are summarized in Table V-II. Such behavior is common to many polymers which have been quenched from the melt to below T_g. As an example may be cited the case of polyethylene terephthalate. This exothermic peak is associated with the crystallization of amorphous material made possible by the enhanced segmental motion occuring above T_g. Table V-II shows that T_c decreases with increasing n. This behavior is to be expected since T_g also decreases with increasing n and chain mobility allowing crystallization to take place occurs at progressively lower temperatures with increasing n.

As shown in Figure 39, a small endothermic peak appears above T_g for the samples of the second run after heating up to T_c. The temperatures of those peaks, T_t's, are collected in Table V-II. These values are insensitive to methylene sequence length. This behavior is in contrast to the strong dependencies of T_g and T_m on n for the H series. It thus appears that chain stiffness is unimportant in the mechanism of this T_t transition. According to the dynamic mechanical[45] and infrared results[56], this mechanism may be similar to the change from the α crystalline form to the γ crystalline form in nylon 66. This crystal-crystal phase transition is accompanied by an increase in the degree of hydrogen bonding.

Heat of Fusion and Entropy of Fusion

Figure 40 shows the melting point depression due to the presence of diluent. In these experiments, phenanthrene was used as the diluent. From the well-known thermodynamic expression for the melting point depression[58], the theoretical heat of fusion, $\Delta H_f(T)$ is calculated by

extrapolation of plot of $(1/T_m - 1/T_m^\circ)/$ versus ϕ_1/T_m to $\phi_1/T_m = 0$.

$$\frac{\left(\frac{1}{T_m} - \frac{1}{T_m^\circ}\right)}{\phi_1} = \frac{R}{\Delta H_f(T)}\left(\frac{v_2}{v_1}\right)\left[1 - \left(\frac{Bv_1}{R}\right)\phi_1/T_m\right]$$

where ϕ_1 is the volume fraction of phenanthrene; v_1 and v_2 are the molar volumes of phenanthrene and polymer, respectively; and B is the interaction parameter.

The results are shown in Figure 41. They give a quite good straight line and the $\Delta H_f(T)$'s were calculated from the extrapolation of this line to $\phi_1/T_m = 0$. These values are listed in Table V-III. $\Delta H_f(T)$'s for the H series are 37-39 cal/g and those for the DP series are 32-34 cal/g. These values are quite similar to those of the nylons which are structurally similar to the H series and to those of polyesters similar in structure to the DP series[57]. $\Delta H_f(T)$'s of the nylons are 43-45 cal/g and those of the polyesters are 33-36 cal/g.

The $\Delta H_f(T)$'s may be obtained independently by using the degree of crystallinity as determined by x-ray measurements. The method is outlined below.

$$\chi = \frac{\Delta H_f(E)}{\Delta H_f(T)}$$

where χ is the degree of crystallinity and $\Delta H_f(E)$ is the heat of fusion measured experimentally.

Figures 42 and 43 show the x-ray intensity curve as a function of the Bragg angle as measured by the radial scanning method. The lower -·-·- line arises from the reflections of the amorphous region and the ------ line at the low Bragg angle is the air scattering intensity which has already been subtracted. The weight of the amorphous and crystalline regions respectively are given by the following equations.

$$m_a = k_a \int I(\theta_a)\, d\theta$$

$$m_c = k_c \int I(\theta_d)\, d\theta$$

If $k_a/k_c = 1$

$$\chi = \frac{m_c}{m_a + m_c} = \frac{\int I(\theta_c)\, d\theta}{\int I(\theta_a)\, d\theta + \int I(\theta_c)\, d\theta}$$

In this experiment the upper and the lower limits of integration were assumed 14.5° and 3.5° for 2θ using a molybdenum target, respectively. $\Delta H_f(T)$ can be calculated using both χ's from the x-ray measurements and the $\Delta H_f(E)$ from the DSC measurements. The calculated values are summarized in Table V-III. These values are consistent with the $\Delta H_f(T)$'s

obtained from the diluent method as well as the data of Dole[57]. $\Delta H_f(T)$'s are plotted versus n in Figures 44, 45 and 46. $\Delta H_f(T)$ values show a zigzag behavior with increasing methylene sequence length, n, except DP-1,6. The T_m's also exhibit this zigzag tendency as already pointed out.

From the equation derived above

$$\Delta H_f(T) = \Delta H_m = N\,\Delta\overline{E} + \Delta H_2$$

ΔH_2 may be expected to be a strong function of the polarity and the formation of hydrogen bonding in the crystalline regions. Samples with even n have higher $\Delta H_f(T)$'s than those with odd n due to the cancellation of the polarity effects and the possibility of more perfect formation of hydrogen bonding. Also, hydrogen bonding formation is most possible for n=4 and 10 according to the chemical structures and this may be expected experimentally[56]. Higher values of $\Delta H_f(T)$ of n=4 or 10 are in agreement with this idea.

$\Delta H_f(T)$'s for the annealed materials are higher than those for the rapidly cooled materials at room temperature. This is probably due to the formation of larger crystallite or more perfect crystals accompanying the annealing process. The differences between values of the $\Delta H_f(T)$'s for the annealed and the rapidly cooled samples are larger for the H series than for the DP series. This may arise from the fact that the rapidly cooled H series contains an unstable crystalline form[45,49] as

discussed in Chapter IV of this thesis. The H series undergoes a solid-solid phase transition to a more stable crystal form during annealing. No such transition takes place in the DP series. Additional differences in the $\Delta H_f(T)$'s between the H series and the DP series may arise from the fact that the packing efficiency is probably higher in the H series than in the DP series.

At the melting temperature

$$\Delta G_m = \Delta H_m - T_m \Delta S_m = 0$$

$$\Delta S_f(T) = \Delta S_m = \frac{\Delta H_m}{\Delta T_m} = \frac{\Delta H_f(T)}{\Delta T_m}$$

We can calculate the entropy of fusion from the equation mentioned above using $\Delta H_f(T)$ and T_m. $\Delta S_f(T)$ values are summarized in Table V-III and are also plotted in Figures 44, 45 and 46. $\Delta S_f(T)$'s of polymethylene terephthalates are around 1.9 cal/bond deg. The experimental values of $\Delta S_f(T)$'s lie for the DP and H series are again quite consistent with these values.

The relatively larger values of $\Delta S_f(T)$ for the H series than the DP series as shown in Figure 46 may arise from the fact that the DP series is less susceptible to conformational rearrangements in the melt than the H series due to the presence of the diphenylmethane group of the chain backbone.

CHAPTER VI

STRUCTURE-MECHANICAL PROPERTY RELATIONSHIPS IN ETHYLENE METHACRYLIC ACID COPOLYMERS AND THEIR SALTS

Introduction

Recently there has been a considerable amount of interest in a class of copolymers which are based on a polyolefin and a carboxylic acid[59]. The two are copolymerized in such a way that the carboxylic acid groups are pendant from the main chain at intervals along it. The concentration of carboxylic acid groups present has a very great effect on the properties of the copolymer as might be expected. However, an even greater effect is produced if the acid groups are ionized to form the carboxylate salt. In the case of relatively low levels of acid group concentration, the effect of ionization is to greatly increase the melt viscosity, the ultimate tensile strength and the optical clarity of the copolymer among other things[60]. In addition, the per cent crystallinity is reduced significantly. At higher levels of acid group concentration, ionization produces materials so resistant to flow that they are intractable and it is necessary to resort to the techniques of powder metallurgy in order to prepare useable samples[61].

Despite the considerable amount of reported work, there is no completely satisfactory explanation for the low temperature ($T \simeq -120°C$) γ relaxation in semicrystalline ethylene polymers. Schmieder and Wolf[62], Oakes and Robinson[63] and Woodward and collaborators[64,65] all observed the γ relaxation in polyethylene of varying crystallinity and attributed it to short range motion in the amorphous areas. Wilbourn[66] demonstrated

that the γ transition is more general, occuring in polymers of widely different types containing at least four methylene sequences. Schatzki[67] then proposed his now famous "crankshaft" model for γ relaxations in the amorphous regions. Boyer[68], summing up the work done to 1963, favored this model and concluded that the γ peak does indeed arise in the amorphous areas, a conclusion also reached by Bohn[69]. More recently, Andrews and Hammack[70] presented a new model for the γ transition, assigning it to amorphous phase motions. Iwayanagi and Sakurai[71] have given additional support to a local mode amorphous motion but discount the Schatzki model.

On the other hand, Pechold, et.al.[72], Sinnott[73], Illers[74] and Takayanagi[75] have all presented evidence for a γ relaxation mechanism involving defects in the crystalline regions. Peterlin and co-workers[76,77] have given evidence which they suggest shows that the relaxation is related to crystallinity, not through internal defects, but due to disordered regions in the chain fold plane. This is also claimed by Wada, et.al.[78], for single crystals.

The available evidence thus leads to the reasonable hypothesis that in semicrystalline systems the γ relaxation may, in fact, consist of contributions from both the amorphous and crystalline regions. This suggestion was first made by Cole and Holmes[79] and later by Boyer[80]. Sinnott[73] pointed out an unresolved shoulder on the low temperature side of the γ peak for both melt-crystallized and solution grown single crystals of high density polyethylene and suggested that the γ region may be a superposition of two peaks. Hoffmann, et.al.[81], have shown that the γ relaxation in poly(chlorotrifluoroethylene) can be decomposed into γ_a

and γ_c regions which are associated with the amorphous and crystalline phases respectively and suggest that polyethylene should show similar behavior. Matsuoka and co-workers[82] have proposed that the γ relaxation in polyethylene may arise in either, or both, the crystalline or amorphous regions, depending on the method of preparation of the sample.

We have been studying a unique semi-crystalline ethylene copolymer containing a small amount of copolymerized methacrylic acid. By ionizing the acid moieties with Groups I and II cations, large changes in the properties of this material are observed. These groups exist exclusively in the amorphous regions and show their influence on mechanical relaxations arising in the amorphous regions. Thus their presence allows a method of distinguishing processes with amorphous and crystalline contributions. In this report, we examine the unusual behavior of the γ relaxation region and submit evidence for the coexistence of two distinct γ relaxation mechanisms, one arising in the crystalline regions and the other due to motions in the amorphous areas.

Experimental

The parent poly(ethylene-co-methacrylic acid) polymer was prepared from a commercial material supplied by E. I. duPont deNemours and Company and is identical to that used in our previous studies[83,84]. This material has a weight average molecular weight of about 300,000, a methacrylic acid content on the purified material of 4.1 mole per cent (by oxygen analysis), and a degree of methyl branching (by infrared), similar to low density branched polyethylene (approximately 25 branches per 1000 carbon atoms).

Schematically, the structure of the copolymer is

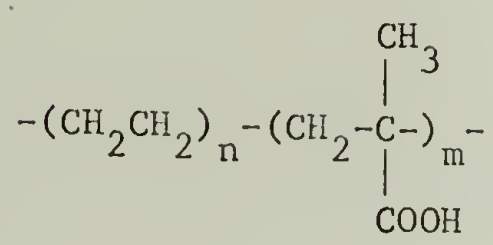

with n equal to 25 on the average for m equal to one.

The acid groups were ionized to various levels (generally about 20, 50 and 75% ionization) with lithium, sodium and calcium salts. We have described the ionization procedure in previous reports[83]. Films were prepared by pressing at 150°C (~180°C for the calcium salts) for five minutes at ~10,000 psi. Samples were quenched by direct immersion of the mold in a dry ice-ethanol bath immediately after removal from the press. Annealed films were prepared by heating the quenched material in nitrogen at 95°C for 24 hours and cooling slowly.

The real and imaginary parts of Young's modulus were obtained on a Vibron dynamic viscoelastometer in the temperature range -180°C to -60°C which completely encompasses the γ transition spectrum. The data reported in this work is for determinations made at a constant, forced frequency of 110 Hz.

Crystallinities were determined by an x-ray radial scan method using both copper and molybdenum targets. The per cent crystallinity was calculated by decomposition of the peaks in a plot of intensity vs Bragg angle into crystalline and amorphous contributions[85].

Results and Discussion

A copolymer of ethylene and methacrylic acid containing only 4.1 mole per cent of acid units would be expected to behave in a similar manner to polyethylene itself since such a small concentration of acid groups leads to a copolymer which is, in fact, very largely polyethylene. It is, therefore, instructive to examine the viscoelastic response of branched polyethylene in the temperature range investigated and to use this as a basis for the discussion of the response of the acid copolymer and its salts. Branched polyethylene is chosen as the model because the acid copolymer is prepared by a high pressure, free radical process and this is known to lead to chain branching. At relatively low frequencies, branched polyethylene exhibits three main relaxations in the low temperature range investigated and these are most easily observed by plotting the loss modulus as a function of temperature. When this is done, three peaks appear corresponding to the three relaxations: the α peak at approximately 50°C, the β peak at -20°C and the γ peak at -150°C. The molecular motions responsible for these relaxations remain a matter of some controversy. Inasmuch as attention is to be focused on the β and γ relaxations in the copolymer and its salts, the mechanisms responsible for these only will be discussed. The magnitude of the β relaxation in branched polyethylene definitely depends on the concentration of branches present and is thus associated with them. On the basis of the results of several authors[86,87] the motion responsible for the β peak seems to be microbrownian segmental motion involving the branches and occuring in the amorphous phase. In other words, it is a type of glass transition and

may be thought of as the glass transition of the copolymer consisting of ethylene sequences and branches. In the case of the γ peak it seems clear that we are dealing with a composite peak consisting of two distinct relaxation mechanisms[82]. The two peak maxima occur at -140°C and -110°C. The low temperature maximum has been stated[82] to involve motion of defects in the crystalline phase while the high temperature maximum is associated with local motions in the amorphous phase. In the case of polyethylene, the two γ processes are generally not resolvable and this had led to considerable confusion in earlier literature discussion of the γ relaxation.

With the above discussion as a basis, it is now possible to turn to the relaxations observed in the acid copolymer and its salts. The overall features have been given[83] and, in the temperature range of interest, the ionized copolymers exhibit four main relaxation regions, while the acid exhibits three. This is shown for a series of annealed samples of varying degrees of ionization with sodium in Figure 47. The data were obtained with a torsion pendulum at a nominal frequency of 1 Hz. Inspection of the figure shows that the α relaxation moves to somewhat higher temperatures with increasing ionization while the β' relaxation decreases in magnitude with increasing ionization. On the other hand, the β relaxation is entirely absent in the acid copolymer and increases in magnitude with increasing ionization. The temperature range of Figure 47 is insufficient to completely resolve the γ relaxation but this will be dealt with more fully later. As indicated above, the relaxation will not be discussed further and we shall proceed to a discussion of the β', β and γ relaxations.

A. The β' Relaxation.

The significant results concerning the β' relaxation indicated in Figure 47 are the peak temperature and the fact that the magnitude of the β' relaxation decreases in direct proportion to the decrease in the concentration of the unionized acid groups. This latter immediately indicates that the molecular motion responsible for the β' relaxation involves the carboxylic acid groups. An infrared study of these groups[84] indicates that they exist almost entirely in the form of interchain, hydrogen bonded dimers in the temperature range of the β' relaxation. This structure may be schematically represented as

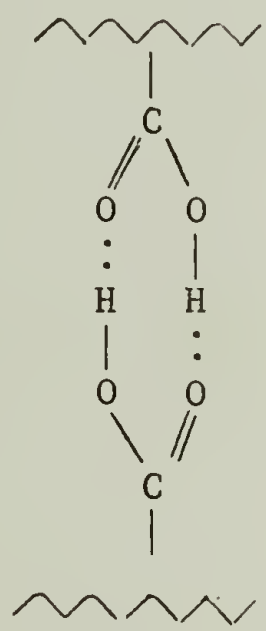

Temperature dependent infrared studies[84] show that the behavior of the acid groups is quantitatively comparable to that of low molecular weight carboxylic acids with an enthalpy of dissociation of the dimers equal to 11.8 kcal $mole^{-1}$. Thus we are led to the conclusion that the carboxylic acid dimers act as crosslinks in the temperature range of the β relaxation. They are relatively weak crosslinks and also labile ones, inasmuch as they break and reform reversibly. The picture that emerges is that

the amorphous phase consists of ordinary branched polyethylene crosslinked by acid dimers. On this basis, the β' relaxation is easily interpretable as being due to the same molecular process involved in the β relaxation in branched polyethylene, namely microbrownian segmental motion, but the temperature of the relaxation is increased by the presence of the acid dimer crosslinks which act to restrict this motion and thus to raise the temperature of the loss peak from about -20°C to about +20°C. It is quite possible that the β' relaxation also involves the breaking and reforming of the dimer units. Striking confirmation of the proposed mechanism has been provided by the work of Otocka and Kwei[88]. These authors worked with ethylene-acrylic acid copolymers containing varying amounts of acid units. In this study it was found that the temperature of the β' relaxation and the β relaxation in branched polyethylene is linearly dependent on the density of dimer units present. The calculation is carried out assuming that all dimer units are present in the amorphous phase which they undoubtedly are since, among other things, they would not be expected to be able to fit into the polyethylene crystal lattice for steric reasons. The above relationship is that of Fox and Loshaek and gives the effect of covalent crosslinks on the glass transition temperature of amorphous polymers. It thus seems clear that the molecular motions responsible for the β' loss peak in the acid copolymers is well understood.

B. <u>The β Relaxation</u>.

Figures 48 and 49 are plots of the loss modulus as a function of temperature for lithium, sodium and calcium salts of comparable degrees of ionization. In the case of the quenched salts (Figure 48), it may be

seen that the temperature of maximum loss is comparable for all three salts but that the breadth of the relaxation differs. (Quenching is defined as removing samples from the press at 130°C to 150°C and immediately plunging them into dry ice.) It is, of course, somewhat unexpected at first sight that ionization should produce a β relaxation at a lower temperature than is found in the acid copolymer, and that the nature of the cation should have no significant effect on the temperature of the β relaxation. Attempts have been made to explain this behavior[83,89] and it has been proposed[89] that ionization results in the formation of a new phase or domain consisting of regions of ionic groups embedded in an amorphous hydrocarbon matrix which is then connected to the crystalline phase. The system is thus composed of three phases - the polyethylene crystal phase, the amorphous phase consisting of branched polyethylene plus any unionized acid groups, and the ionic phase. The β relaxation in the ionized copolymers then arises from the amorphous hydrocarbon phase and is thus identical to the β relaxation in branched polyethylene. According to this view, the reason for the increase in magnitude of the β relaxation with increasing ionization is due to the fact that ionization leads to an increase in the amount of amorphous hydrocarbon phase present. The ionic domains themselves are not involved in the relaxation at all. An examination of Figures 48 and 49, however, indicates that the different cations do affect the shape of the β relaxation significantly. In both the annealed and quenched cases, the calcium salt gives a much narrower relaxation region than the sodium or lithium salts. (Annealing is carried out by holding the samples at 95°C for 24 hours followed by slow cooling

to room temperature.) The effect is particularly marked in the case of the quenched samples. It seems, therefore, that the ionic groups do contribure to the β relaxation to some extent with the calcium ions perhaps contributing less than the sodium or lithium ions. The sharpening of the relaxation peaks on annealing would be explained on the basis that the annealing process leads to more perfect segregation of the ionic domains from the amorphous hydrocarbon domains. The divalent calcium ions are possibly more restrictive to motion than the monovalent lithium and sodium leading to the relative sharpness of the β relaxation in the calcium salt.

C. The γ Relaxation.

Plots of log E" versus 1/T in the γ relaxation region are given in Figure 50 for annealed samples of the unionized polymer and a calcium-ionized derivative. These plots are typical of all the samples studied. It can be shown[90] that the strength of the relaxation mechanism taking place in the γ region should be proportional to the area under the curve, assuming the process is of the Arrhenium type. In this case, the relaxation times are described by

$$\tau = \tau_o \exp (\Delta H^{\ddagger}/RT)$$

Then, the relaxation strength, ΔE, is given by the equation

$$E_u - E_r = \Delta E = \frac{2\Delta H^{\ddagger}}{\pi R} \int E''d\ (1/T)$$

where E_u and E_r are the storage moduli immediately before and after the relaxation region, ΔE is the relaxation magnitude and E'' is the loss modulus as a function of $1/T$.

$\Delta H^{\ddagger}$ is the apparent activation energy. In this treatment it is assumed constant throughout the relaxation region. Dielectric determinations[91], coupled with the mechanical data presented here, confirm that the γ relaxation processes have an Arrhenius dependency and that $\Delta H^{\ddagger}$ has about the same value for each process.

If the relaxation process takes place in either the crystalline or amorphous regions exclusively, there should be some straightforward relationship between the peak area, as given by the value of the integral, and either χ, the degree of crystallinity, or $1-\chi$. Analysis of the areas and comparison with crystallinities did not uncover any such relationship. Moreover, since the γ peak is far removed from the perturbing influence of any other transitions, we would also expect a symmetrical distribution of relaxation times if only one mechanism is involved. It is clear, however, that the peaks are asymmetric and, in fact, show a prominent shoulder on the low temperature side. These features suggest that the relaxation is, in reality, two closely related mechanisms partially superimposed on each other.

We then decomposed the γ peak into two separate peaks by assuming symmetry around a line drawn through the high temperature peak maximum and constructing the second peak by differences. The method is illustrated in Figure 51 for the unionized polymer. This procedure results in two separated peaks, which we designate as γ_a, the high temperature

peak, and γ_c, the low temperature peak. The maximum in γ_c coincides with the shoulder on the undecomposed curve.

The area of γ_c for all the samples is plotted in Figure 52 as a function of χ. The area increases linearly with a slope directly proportional to χ only, and does not depend on level of ionization, type of cation or thermal history, except insofar as the latter affects the overall degree of crystallinity. Recent studies on these copolymers in our laboratory and by others[91] have uncovered large changes in the amorphous phase behavior, particularly in the β transition region, caused by changes in ionization level, cation type and thermal treatment. Thus, the independence of the γ_c area with these variables leads us to conclude that this is a relaxation occuring exclusively in the polyethylene crystalline regions. That the crystalline regions are composed only of the polyethylene segments of the chain is supported by the findings of Otacka[88] on poly(ethylene-co-acrylic acid) systems and by the results of Bodily and Wunderlich[92] using polyethylene copolymers containing vinyl acetate groups. Both conclude that the comonomer is excluded from the crystalline regions.

The γ_a peak area is plotted in Figure 53 as a function of $1-\chi$. Again, there is a linear relation between the strength of the absorption and the amount of amorphous material, with some apparent dependence on the chemical nature of the groups in the amorphous areas. We therefore assign the γ_a relaxation to the amorphous regions of the polymer.

Although we cannot assign specific mechanisms to these processes, several features should be pointed out. Our preliminary microscopic and

DSC examinations suggest that the nature of the crystalline morphology is complex and is significantly different depending on whether the samples are quenched or annealed. Furthermore, this work, as well as more complete electron microscopy studies by Davis, et.al.[93], on similar systems, show drastic changes in the crystalline morphology on ionization. Since the γ_c relaxation is unaffected by thermal treatment or degree of ionization per se, this mechanism must involve motions in the crystal phase.

Our data contains one disturbing but highly interesting aspect with regard to the γ_c transition: the failure of the line in Figure 52 to extrapolate to zero area at $\chi = 0$. It is possible that this is a result of some systematic error in area and crystallinity measurements. However, we feel this is not the case based on re-examination of the data and the possible errors involved. Sinnott, in his examination of polyethylene single crystals[73], plotted the area of the γ peak against the NMR mobile fraction and found a similar failure to extrapolate to zero area. He suggested this may be due to an unresolved lower temperature relaxation. No evidence for a lower temperature peak in the neighborhood of the γ relaxation was found in our work.

We believe it more likely that the data shown in Figure 52 is a demonstration of the origin of the γ_c relaxation in more than one kind of crystal defect. In the discussion that follows, we will advance the hypothesis that the γ_c relaxation occurs both in the interior of the crystal lattice and in the side surfaces. Hoffmann has suggested that the γ_c mechanism in poly(chlorotrifluoro ethylene) may involve twisting

of chain segments adjacent to row defects in the crystal. This model is appealing since it explains the observed increase in γ_c with annealing by showing that the additional insertion of chain ends drawn into the crystal during annealing increases the row vacancy defect concentration. These defects result in an unsymmetrical potential field around the chain segments adjacent to the vacancy. The γ_c relaxation is a result of these local chain segments twisting or flip-flopping in and out of the vacancy. We add to this concept the suggestion that there will also be a similar unsymmetrical potential field for chains on the side surfaces of the crystallites as a result of vacancies at the crystal-amorphous boundary plane. These vacancies may exist as imperfections on the growth faces of the crystal where many chains are entering and leaving the ordered lattice structure. Alternatively, there may be vacancies in the amorphous areas adjacent to the crystal face which provide sites for twist motions of segments of crystallized chains. The important consequence of this postulated model is that the contribution of surface defect motion to the total γ_c relaxation strength should be large at small crystal volumes where the ratio of surface area to volume is large. However, as the crystal size increases due to lateral growth, the contributions of surface defect motions will become proportionately smaller and eventually interior defect motions will swamp the effects of surface defects. When this occurs, the relaxation strength is then a linear function of crystal volume.

The form of the contributions of each of these motions can be represented in a qualitative way by the following relationship:

$$\psi(E'') = f\ (\text{internal defect motion}) + g\ (\text{side surface defect motions})$$

where $\psi(E'')$ is some function of the total relaxation strength of the γ_c region in a plot of the loss modulus versus reciprocal temperature. The functions f and g should involve both the specific strength of the relaxation modes and the concentration of defects of each type. It becomes apparent, then, that f is proportional to the volume of the crystal, while g is proportional to the side surface area. Thus

$$\psi(E'') = f\ (\text{crystal volume}) + g\ (\text{side surface area})$$

To examine the forms of each of these contributions, we postulate as a simple model of the crystal, a square box having a side length "a" and a height "ℓ." The volume of the box, V, and the side surface area, A, are given by:

$$V = \ell a^2$$

and

$$A = 4\ell a$$

The equation mentioned above, $\psi(E'')$, is now rewritten in terms of crystal volume or size:

$$\psi(E'') = f(V) + g(V^{1/2})$$

To apply this equation to the data shown in Figure 52, we identify the V terms with degree of crystallinity, χ. Although admitting that this is a teneuous identification, we justify it by the fact that all samples were prepared from the melt in exactly the same way and, therefore, should have approximately the same number of crystal nuclei. Thus we can identify differences in degree of crystallinity with differences in crystal size. When this is done, $\psi(E'')$ may then be rewritten as:

$$\psi(E'') = f(\chi) + g(\chi^{1/2})$$

The data in Figure 52 is replotted in Figure 54 along with a curve representing the above equation, $\psi(E'')$. Values for the functions f and g were selected to fit the curve to the data points. Inspection of Figure 54 shows that the treatment described above is a way of accommodating both the data observed and the fact that at zero crystallinity the γ_c relaxation strength should also vanish. We are attempting to develop a technique for preparing samples of lower crystallinity to experimentally check the curvilinear portion of the curve.

The γ_a mechanism appears to arise only from short-range local motions of polyethylene segments in the amorphous phase. The specific relaxation strength, calculated as the γ_a area per unit volume of amorphous material, is plotted against degree of ionization in Figure 55. It is seen that there is no dependency on either the ionization level of the chemical

nature of the comonomer groups. This is in dramatic contrast to the behavior of the β region where the longer range motions of amorphous phase polyethylene segments are controlled by ionization and comonomer structure. It is interesting to note that the γ_a mechanism occurs at a higher temperature than the γ_c motions, [T_{max} (γ_a) = -129°C; T_{max} (γ_c) = -163°C]. The same result was also observed for PCTFE[91]. This must indicate that the size of the vacancies in the amorphous regions are somewhat smaller than those in the crystal.

TABLE I-I

Conditions of the Polymerizations

Polymerization Temperature (°C)/Reflux Time (hr.)

	Diisocyanates		
Diols	Hexamethylene	4,4'-Methylene Diphenyl	4-Methyl Meta-phenylene
1,2	121/11.0	113/1.33	90/1.0
1,3	121/15.0	113/3.0	90/1.2
1,4	121/24.0	113/2.0	90/2.0
1,5	121/18.0	113/1.33	90/1.16
1,6	121/24.0	113/1.95	90/1.33
1,7	125/30.0	113/8.0	90/1.1
1,8	121/24.0	113/1.5	90/1.4
1,9	121/26.0	113/4.0	90/2.0
1,10	121/24.0	113/1.33	90/2.5

TABLE I-II

Conditions for Purification of Diols and Weight Corresponding to 0.1021 mole

Diols	Boiling Points (°C)	Melting Points (°C)	Weight Corresponding to 0.1021 mole(g)
1,2	77/4.5 mmHg	-17.4	6.20
1,3	199/760 mmHg		7.60
1,4	96/1.9 mmHg	16	9.012
1,5	95/0.8 mmHg	-18	10.414
1,6	250/760 mmHg	42	11.816
1,7	172/20 mmHg	63	13.220
1,8	250/760 mmHg	43	14.624
1,9	169/14 mmHg	46	16.026
1,10	179/11 mmHg	71	17.428

TABLE I-III

Solubilities of Polyurethanes at Room Temperature

Solvents	H Series	DP Series	4M Series
Trifluoro Acetic Acid	+	+	+
C_6H_5-CN	-	-	+
$(C_2H_5)_3N$	-	-	+
CH_2=CH-C=CN	-	-	+
CH_2=Cl_2	-	-	x
$CHCl_3$	-	-	+
CCl_4	-	-	x
Quinoline	-	-	x
Pyridine	-	+	x
m-cresol	+	+	+
Dioxane	-+	x	+
Dimethyl Sulfoxide	-	+	x
THF	x	x	+
Acetone	x	x	+
DMF	-	x	x
Sulfuric Acid	+	+	+

- insoluble
-+ swollen
+ soluble
x not observed

TABLE I-IV

Carbon, Hydrogen and Nitrogen Analysis for the Various Series of Polyurethanes (%)

	Experimental			Theoretical		
Series	H	C	N	H	C	N
H-1,2	8.01	52.64	11.98	7.82	52.22	12.15
H-1,5	8.44	56.87	10.02	8.26	57.42	10.31
H-1,10	9.42	66.22	7.62	8.90	66.92	7.32
DP-1,2	5.30	64.88	8.69	5.13	65.42	8.97
4M-1,2	5.84	52.31	9.90	4.50	54.00	12.62

TABLE I-V

Viscosity Average Molecular Weight

H Series	[η]	$M_v \times 10^{-4}$
H-1,2	.775	5.80
H-1,3	.776	5.88
H-1,4	.859	6.63
H-1,6	.876	7.20
H-1,7	.664	4.48
H-1,9	.734	5.33
H-1,10	1.090	9.81

$K = 5.52 \times 10^{-4}$

$a = .66$

TABLE IV-I

Activation Energies in the α Region (kcal/mole)

Diols	H Series	DP Series	4M Series
1,2	123	172	180
1,3	138		86
1,4	100	189	115
1,5	113	123	73
1,6	101	102	110
1,7	88	88	90
1,8	86	99	88
1,9	98	114	112
1,10	94	109	95
1,2 Annealed	84		
1,5 Annealed	87		
1,10 Annealed		85	127

TABLE IV-II

Temperature Location of the DSC Peaks for H-1,2 Subjected to the Various Thermal Histories

		T_g	T_c	T_t	Relative area of T_c/m_g
1st Run	Quenched liq. N_2	39.5	68.0	-	48.0
	-70	40.3	68.3	-	43.5
	-50	40.0	69.0	-	42.8
	-37	38.8	67.2	-	37.6
	-18	38.6	67.4	-	37.2
	0	38.7	67.2	-	39.2
	19	38.0	67.0	-	41.8
	Slow Cool	38.5	-	-	
2nd Run	liq. N_2	45.0	-	72.0	
	-70	45.2	-	73.0	
	-50	45.0	-	74.4	
	-37	46.0	-	73.5	
	-18	46.7	-	77.2	
	0	48.0	-	76.2	
	19	48.0	-	72.3	
	Slow Cool	49.8	-	-	
3rd Run	liq. N_2	45.0		72.0	

TABLE IV-III

Lattice Distances of the Quenched and Annealed H-1,2 Samples

Annealed d(Å)		Quenched d(Å)	
13.39	S	13.42	S
6.92	W	6.88	VW
4.69	W		
4.45	M	4.50	W
4.27	VS	4.08	VS
3.89	W	3.95	M
3.72	W	3.68	W
3.44	W	3.28	W
2.82	VW	2.80	VW
2.45	VW	2.45	VW

TABLE V-I

Melting Points and Glass Transition Temperatures (°C)

	H Series		DP Series		4M Series	
Diols	Regular	Annealed	Regular	Annealed	Regular	Annealed
MELTING POINTS						
1,2	163	167	237			
1,3	157	161	227			
1,4	175	180		232		
1,5	150	155	187	189		
1,6	165	165	194	197		
1,7	145	146		191		
1,8	153	157	194	196		
1,9	147	147	186	190		
1,10	155	154	186	192		
GLASS TRANSITION TEMPERATURES						
1,2	42		139		52	59
1,3	31		119		72	76
1,4	25		108		42	58
1,5	20		95	85	62	66
1,6	16		91	68	32	43
1,7	12			81	61	63
1,8	10		79	64	64	66
1,9	6		72	64	62	65
1,10	6		72	64	18	40

TABLE V-II

Temperatures of the Peaks of T_c and T_t (°C)

	T_c (Exotherms)	T_t (Endotherms)
H-1,2	94	56
H-1,3	75	55
H-1,4	41	59
H-1,5	47	58
H-1,6	36	59
H-1,7	43	55
H-1,8	35	58
H-1,9	29	58
H-1,10	23	55

TABLE V-III (1)

Experimental Heat of Fusion $\Delta H_f(E)$, Theoretical Heat of Fusion $\Delta H_f(T)$ and Theoretical Entropy of Fusion $\Delta S_f(T)$

		X-Ray Method			Diluent Method	
H Series	$\Delta H_f(E)$ (cal/g)	$\Delta H_f(T)$ (kcal/mole)	$\Delta H_f(T)$ (cal/g)	$\Delta S_f(T)$ (cal/bond.deg)	$\Delta H_f(T)$ (cal/g)	$\Delta S_f(T)$ (cal/bond.deg)
1,2 Regular	9.2	8.07	35	1.32	38	1.39
Annealed	12.5	9.68	42	1.01	46	1.12
1,3 Regular	9.7	8.05	33	1.25		
Annealed	14.6	10.01	41	1.55		
1,4 Regular	13.5	10.58	41	1.48		
Annealed	17.6	11.37	44	1.57		
1,5 Regular	12.0	10.38	38	1.65	39	1.48
Annealed	12.7	9.53	35	1.31	40	1.37
1,6 Regular	16.8	12.02	42	1.52		
Annealed	18.6	12.28	43	1.56		
1,7 Regular	10.9	10.51	35	1.33		
Annealed	13.1	10.80	36	1.36		
1,8 Regular	14.4	10.92	38	1.28		
Annealed	15.9	13.21	42	1.62		
1,9 Regular	10.2	10.51	32	1.19		
Annealed	14.1	12.12	37	1.37		
1,10 Regular	13.3	11.64	34	1.24	37	1.37
Annealed	14.6	13.68	40	1.45	43	1.30

TABLE V-III (2)

Experimental Heat of Fusion $\Delta H_f(E)$, Theoretical Heat of Fusion $\Delta H_f(T)$ and Theoretical Entropy of Fusion $\Delta S_f(T)$

		X-Ray Method			Diluent Method	
DP Series	$\Delta H_f(E)$ (cal/g)	$\Delta H_f(T)$ (kcal/mole)	$\Delta H_f(T)$ (cal/g)	$\Delta S_f(T)$ (cal/bond.deg)	$\Delta H_f(T)$ (cal/g)	$\Delta S_f(T)$ (cal/bond.deg)
1,2 Regular	13.1	7.78	35	1.38		
Annealed	15.9	8.02	36	1.42		
1,3 Regular	11.2	8.03	34	1.34		
Annealed	16.8	8.27	35	1.37		
1,4 Regular	9.0	8.50	34	1.30		
Annealed	13.2	9.27	37	1.41		
1,5 Regular	7.9	8.20	31	1.27	32	1.31
Annealed	11.3	8.98	34	1.39	37	1.36
1,6 Regular	9.2	8.36	30	1.20		
Annealed	11.7	9.18	33	1.30		
1,7 Regular	8.4	8.48	29	1.15		
Annealed	6.9	8.78	30	1.18		
1,8 Regular	11.6	9.81	32	1.27		
Annealed	13.9	11.01	36	1.38		
1,9 Regular	10.2	9.94	31	1.19		
Annealed	10.9	10.79	34	1.29		
1,10 Regular	7.9	11.03	33	1.26	34	1.30
Annealed	13.9	12.35	37	1.40	40	1.36

CAPTIONS FOR FIGURES

1. Temperature dependence of tanδ at 110 Hz for the 4M series in the γ relaxation region.
2. Dependence of the temperature of the γ peak maxima at 110 Hz on n, the number of CH_2 units in the diol part of the repeat units for E", T_{max} (γ - E"), and tanδ, T_{max} (γ - tanδ). Also included are corresponding temperatures of peak maxima for polyethers (⊖) and polymethylene terephthalates (PMT) (⊖).
3. The activation energy of the γ relaxation ($\Delta H^{\ddagger}(\gamma)$) as a function of n, the number of CH_2 units in the diol part of the repeat units for all three series.
4. Maximum intensity of the tanδ peak of the γ relaxation at 110 Hz as a function of n, the number of CH_2 units in the diol part of the repeat units for all three series.
5. Maximum intensity of the E" peak of the γ relaxation at 110 Hz as a function of n, the number of CH_2 units in the diol part of the repeat units for all three series.
6. Temperature dependence of tanδ and E" in the γ region at 110 Hz for H-1,2 subjected to the thermal treatments indicated in the figure.
7. Temperature dependence of tanδ and E" in the γ region at 110 Hz for H-1,5 subjected to the thermal treatments indicated in the figure.
8. Temperature dependence of tanδ and E" in the γ region at 110 Hz for DP-1,5 subjected to the thermal treatments indicated in the figure.
9. Temperature dependence of tanδ and E" in the γ region at 110 Hz for 4M-1,5 subjected to the thermal treatments indicated in the figure.

10. Temperature dependence of E" at 110 Hz for various members of the 4M series showing the δ relaxation.

11. Temperature dependence of E" at 100 Hz for 4M-1,2 and 4M-1,5 in the γ relaxation region.

12. Temperature dependence of E" at 100 Hz for H-1,2 and H-1,5 in the γ relaxation region.

13. E" vs 1/T for H-1,5 in the γ relaxation region illustrating the decomposition of the peak into the γ_1 and γ_3 peaks.

14. (a) Dependence of the temperature of the γ peak maxima at 110 Hz on n, the number of CH_2 units in the diol part of the repeat units for E". The peak temperatures of the γ_3 relaxation were assumed to be independent of n and to be located at the same temperature as the γ_3 peak of H-1,2. The γ_1 relaxation temperatures for the various members of the H series were assumed to be identical to those of the corresponding polyesters. (b) Relative magnitude, $E_u - E_r$, vs n for the H series in the γ_1 and γ_3 region.

15. Temperature dependence of E' and E" at 110 Hz for 4M-1,10. This illustrates the effect of water on several of the relaxation peaks.

16. Temperature dependence of tanδ at 110 Hz for 4M-1,10 showing the effect of both water and D_2O on the relaxation peak.

17. Temperature dependence of E" at 110 Hz for 4M-1,10 which absorbed hexanol. Also temperature dependence of E" for the annealed and regular 4M-1,10 are shown to compare with the behavior of E" for the 4M-1,10 - hexanol system.

18. Temperature dependence of E' and E" of 4M-1,5 and 4M-1,10 polymers containing water and heavy water.

19. Temperature dependence of E' and E" for a decanol-water and a diisocyanate-water mixture sandwiched between thin polystyrene films and also the stretched 4M-1,10 (drawn ratio 300%).

20. Temperature dependence of E" for the 4M-1,10 polymer which was purified by precipitation by pouring its acetone solution into water and absorbed water and heavy water.

21. Temperature dependence of tanδ at 110 Hz for the H and DP series which was rapidly cooled at room temperature and annealed.

22. Maximum intensity of the tanδ peak of the β relaxation at 110 Hz as a function of n, the number of CH_2 units in the diol part of the repeat units for all three series.

23. (a) Dependence of the temperature of the β maximum at 110 Hz on concentrations of water for E". (b) Schematic explanation of the overlapping peaks which arise from motions associated with water molecules (the β_w relaxation) and hydrogen bonded parts (the β relaxation).

24. Temperature dependence of E' and E" for H-1,5, DP-1,5, and 4M-1,5.

25. Temperature dependence of tanδ at 3.5 Hz for DP-1,5 and 4M-1,5 in the β and β_ϕ relaxation region.

26. Comparison of DSC transition temperatures and α loss peaks as a function of n for the DP and 4M series.

27. Comparison of DSC transition temperatures and α and α_t loss peaks as a function of n for the H series.

28. DSC curves for H-1,2 subjected to various thermal treatments.

29. Temperature dependence of E' and E" for H-1,5 subjected to various thermal treatments.

30. Temperature dependence of E' and E" for H-1,5 subjected to the thermal treatments of Figure 4.

31. Temperature dependence of E' and E" for H-1,2 subjected to the following thermal treatments: 1. Quenched from the melt to -40°C. 2. Quenched from the melt to -78°C and then maintained at room temperature for one month.

32. Dynamic mechanical, volume temperature and DSC data for H-1,2 in the glass transition region.

33. Relative magnitude, $E_u - E_r$, vs n for the H series in the α_t region. Areas under a plot of E" vs 1/T were calculated with an assumption that there were no relaxation mechanisms on the higher temperature side of the α_t relaxation.

34. Infrared spectra of two samples of H-1,2 which were quenched at -78°C and annealed at 98°C.

35. Dependence of fiber periods of the H series vs n, the number of CH_2 units in the diol part of the repeat units. Also included are corresponding fiber periods calculated on the assumption that the chains are in the all trans planar conformation.

36. (a) Chemical structure of H-1,2, H-1,3 and H-1,4. (b) Conditions of hydrogen bonding for the various crystalline forms of the H series.

37. Temperature dependence of E' and E" for DP-1,5 in the glass transition region.

38. A plot of $1/T_g$ vs w for the DP series.

39. DSC curves for H-1,2 subjected to three different thermal treatments.

40. Thermograms of H-1,2 and DP-1,5 alone and mixed with phenanthrene.

41. Plot of melting point depression of H-1,2 and DP-1,5 - diluent (phenanthrene) mixture against volume fraction of the diluent.

42. X-ray intensity curve of the annealed H-1,10 sample as a function of the Bragg angles. Dotted lines indicate air scattering intensity which has already been subtracted.

43. X-ray intensity curve of the annealed DP-1,10 sample as a function of the Bragg angle.

44. Plot of theoretical heat of fusion, $\Delta H_f(T)$, and entropy of fusion, $\Delta S_f(T)$, as a function of n for the H series.

45. Plot of theoretical heat of fusion, $\Delta H_f(T)$, and entropy of fusion, $\Delta S_f(T)$, as a function of n for the DP series.

46. Plot of average theoretical heat of fusion and average entropy of fusion as a function of n for the H and DP series.

47. Temperature dependence of the logarithmic decrement at 1 Hz of annealed ethylene-methacrylic acid copolymers ionized with sodium. The percentage of acid groups ionized are given on the curves.

48. Temperature dependence of E" in the β relaxation for quenched sodium, lithium and calcium salts of an ethylene-methacrylic acid copolymer at a frequency of 110 Hz.

49. Temperature dependence of E" in the β relaxation region for annealed sodium, lithium and calcium salts of ethylene-methacrylic acid copolymer at a frequency of 110 Hz.

50. E" vs 1/T for a calcium salt and the unionized copolymer in the relaxation region.

51. E" vs 1/T for the unionized copolymer in the γ region illustrating the decomposition of the peak into the γ' and γ peaks.

52. Area of the γ_c peak vs degree of crystallinity, χ, for the unionized copolymer and its sodium, lithium and calcium salts.

53. Area of the γ_a peak vs amorphous fraction, $(1 - \chi)$, for the unionized copolymer and its sodium, lithium and calcium salts.

54. Area of the γ_c peak vs degree of crystallinity, χ, for the unionized copolymer and its sodium, lithium and calcium salts.

55. Specific relaxation strength of the γ_a peak vs per cent ionization for the unionized copolymer and its sodium, lithium and calcium salts.

B I B L I O G R A P H Y

1. J. H. Saunders, Rubber Chem. and Technology 33, 1259 (1960).
2. O. Bayer, Angew. Chem. A59, 275 (1947).
3. F. Saunder, High Polymer 16, "Polyurethanes, Chemistry and Technology, Interscience, New York, 1965.
4. D. J. Lyman, Review in Macromol. Chem. 1, 191 (1966).
5. H. Zahn and V. Winter, Kolloid-Z. 128, 142 (1952).
6. Y. Saito, H. Ito, M. Koyama and S. Kinoshita, Preprint of the 17th Annual Meeting of High Polymer Society, Japan (1968).
7. D. J. Layman, J. Heller and M. Barlow, Makromol. Chem. 84, 64 (1965).
8. R. Eppe, E. W. Fisher and H. A. Stuart, J. Polymer Sci. 34, 721 (1959).
9. W. Kern, J. Danidonitz, K. J. Rauterkas and G. F. Schmidt, Makromol. Chem. 43, 106 (1961).
10. Y. M. Boyarchuk, L. Y. Raproport, V. N. Nikitin and N. P. Apukhtina, Vysokomol. Soyed. 7, 778 (1965).
11. S. Hirata, S. Saito and T. Nakajima, Kolloid-Z. 212, 109 (1966).
12. G. W. Becker and H. Obert, Kolloid-Z. 152, 1 (1957).
13. K. H. Illers and H. Jacobs, Makromol. Chem. 39, 234 (1960).
14. H. Jacobs and E. Jenckel, Makromol. Chem. 43, 132 (1961).
15. A. G. Goren, Senior Thesis, University of Massachusetts, 1968.
16. H. Saito, Bull. Chem. Soc. Japan 39, 2335 (1966).
17. M. Takayanagi, K. Imada and T. Kajiyama, J. Polymer Sci. C15, 263 (1966).
18. I. M. Ward, J. Macromol. Sci. B1(4), 667 (1967).

19. G. P. Michailov and T. I. Bousevn, Polymer Sci. USSR 6, 1971, 1979 (1964).

20. H. Hendus, G. Schnell, H. Thurn and K. Wolf, Ergeb. Exakt. Naturw. 31, 5 (1959).

21. K. M. Sinnott, J. Polymer Sci. 42, 3 (1960).

22. J. G. Powles, B. I. Hunt and D. J. H. Sandiford, Polymer 5, 505 (1964).

23. For a review of the mechanical data on polyurethanes through 1965 see: Anelastic and Dielectric Effects in Polymeric Solids by N. G. McCrumb, B. E. Read and G. Williams, Wiley, New York, 1967, Chapter 12.

24. T. F. Schatzki, J. Polymer Sci. 57, 496 (1962).

25. S. Matsuoka, Y. Ishida and C. J. Aloisio, presented at IUPAC International Symposium on Macromolecular Chem., Tokyo, Sept. 1966.

26. L. W. McKenna, T. Kajiyama and W. J. MacKnight, Macromolecules, in press.

27. J. D. Hoffmann, G. Williams and E. Passaglia, J. Polymer Sci. C14, 173 (1966).

28. R. E. Wetton and G. Williams, Trans. Faraday Soc. 61, 2132 (1965).

29. C. M. Davis and J. Jarzynski, Advan. Mol. Relaxation Process 1, 155 (1967).

30. M. C. Shen and J. D. Strong, J. Appl. Phys. 38, 4197 (1967).

31. S. Matsuoka, J. H. Daane and C. J. Aloisio, Preprint presented at 5th International Congress on Rheology, Kyoto, Japan, 1968.

32. G. Honjo and K. Shimaok, Acta. Cryst. 10, 710 (1957).

33. K. Shimaoka, J. Phys. Soc. Japan 15, 106 (1960).

34. K. H. Illers, Makromol. Chem. 38, 168 (1960).

35. A. J. Curtis, Progr. Dielectrics 2, 31 (1960).

36. J. Kolarik and J. Janacek, J. Polymer Sci. C16, 414 (1967).

37. M. Takayanagi, Mem. Fac. Eng. Kyushu Univ. 23, No 1 (1963).

38. T. Kajiyama, S. Togami, Y. Ishida and M. Takayanagi, J. Polymer Sci. B3, 103 (1965).

39. E. Rashton and G. Russel, Brit. Elec. Ind. Res. Assoc. Rept. 355 (1956).

40. G. Nemethy and H. Seheraga, J. Chem. Phys. 36, 3382 (1962).

41. K. H. Illers and H. Breuer, Kolloid-Z. 176, 110 (1961).

42. D. C. Vogeslong, J. Polymer Sci. A1, 1055 (1963).

43. N. Neki and M. Takayanagi, Rept. Prog. Polymer Phys. Japan 8, 281 (1965).

44. S. Hirota, S. Saito and T. Nakajima, Kolloid-Z. 212, 109 (1966).

45. T. Kajiyama and W. J. MacKnight, Macromolecules, in press.

46. W. J. MacKnight, M. Yang and T. Kajiyama, Analytical Chemistry, p. 99, R. S. Porter and J. F. Johnson, Eds., Plenum, New York, 1968.

47. R. Hill and E. E. Walker, J. Polymer Sci. 3, 49 (1948).

48. D. J. Lyman, J. Polymer Sci. 45, 49 (1960).

49. K. Saotome and H. Komoto, J. Polymer Sci. A1, 119 (1967).

50. B. Wunderlich, J. Polymer Sci. C1, 41 (1963).

51. K. S. Pitzer and W. D. Gwim, J. Chem. Phys. 10, 428 (1942).

52. N. Davidson, Statistical Mechanics, McGraw Hill, New York, 1962.

53. S. M. Ellerstein, J. Polymer Sci. B1, 443 (1963).

54. L. E. Nielsen, Mechanical Properties of Polymers, Reinhold, New York, 1962.

55. A. V. Tobolsky and M. C. Shen. J. Phys. Chem. 67, 1886 (1963).

56. T. Kajiyama and W. J. MacKnight, to be published.

57. M. Dole, Advances in Polymer Sci. 2, 224 (1960).

58. P. J. Flory, Principles of Polymer Chemistry, Cornell Univ. Press, Ithaca, New York, 1953.

59. Symposium on Solid Ionic Forces, San Francisco ACS Meeting, April, 1968.

60. R. W. Rees and D. J. Vaughn, Polymer Preprints 6, 296 (1968).

61. L. E. Nielsen, Polymer Preprints, April, 1968.

62. K. Schmieder and K. Wolf, Kolloid-Z. 134, 149 (1953).

63. W. G. Oakes and D. W. Robinson, J. Polymer Sci. 14, 505 (1954).

64. D. E. Kline, J. A. Sauer and A. E. Woodward, J. Polymer Sci. 22, 455 (1956).

65. C. W. Deeley, D. E. Kline, J. A. Sauer and A. E. Woodward, J. Polymer Sci. 28, 109 (1958).

66. A. H. Wilbourn, Trans. Faraday Soc. 54, 717 (1958).

67. T. F. Schatzki, J. Polymer Sci. 57, 496 (1962).

68. R. F. Boyer, Rubber Chem. and Technology 36, 1303 (1963).

69. L. Bohn, Rheol. Acta 3, 212 (1964).

70. R. D. Andrews and T. J. Hammack, J. Polymer Sci. 13, 565 (1954).

71. S. Iwayanagi and I. Sakurai, J. Polymer Sci. C15, 29 (1966).

72. W. S. Pechold, S. Blasenbrey and S. Woerner, Kolloid-Z. 189, 14 (1963).

73. K. M. Sinnott, J. Appl. Phys. 37, 3385 (1966).

74. K. H. Illers, Rheol. Acta 3, 194 and 202 (1964).

75. M. Takayanagi, Proceedings of the Fourth International Congress on Rheology, 1963, Wiley, New York, 1964, p. 161.

76. H. G. Olf and A. Peterlin, Paper presented to Division of High-Polymer Physics, American Physical Society, Durham, March, 1966; cf. Bulletin of the American Physical Soc. 11, 213 (1966).

77. E. W. Fischer and A. Peterlin, Makromol. Chem. 74, 1 (1964).

78. Y. Wada, K. Tsuge, K. Arisawa, Y. Ohzawa, K. Shida, Y. Hotta, R. Hayakawa and T. Nishi, J. Polymer Sci. C15, 101 (1966).

79. E. A. Cole and D. R. Holmes, J. Polymer Sci. 46, 245 (1960).

80. R. F. Boyer, J. Polymer Sci. C14, 3 (1966).

81. J. D. Hoffman, G. Williams and E. Passaglia, J. Polymer Sci. C14, 173 (1966).

82. S. Matsuoka, Y. Ishida and C. J. Aloisio, Paper presented at IUPAC International Symposium on Macro. Chem., Bokyo, Sept. 1966.

83. W. J. MacKnight, L. W. McKenna and B. E. Read, J. Appl. Phys. 38, 4208 (1967).

84. W. J. MacKnight, L. W. McKenna, B. E. Read and R. S. Stein, J. Phys. Chem. 72, 1122 (1968).

85. J. L. Matthews, H. S. Peiser and R. S. Richards, Acta Cryst. 2, 85 (1949).

86. D. K. Kline, J. A. Sauer and A. E. Woodward, J. Polymer Sci. 22, 455 (1956).

87. S. Matsuoka, S.P.E. Transactions.

88. E. P. Otacka and T. K. Kwei, Macromolecules 1, 244 (1968).

89. R. Longworth and D. J. Vaughn, Polymer Preprints, April 1968.

90. B. E. Read and G. Williams, Trans. Faraday Soc. 57, 1979 (1961).

91. B. E. Read, private communication.

92. D. Bodily and B. Wunderlich, J. Polymer Sci. A-2, 4, 25 (1966).

93. H. A. Davis, R. Longworth and D. J. Vaughn, Am. Chem. Soc. Polymer Preprints 9, No. 1, 515 (1968).

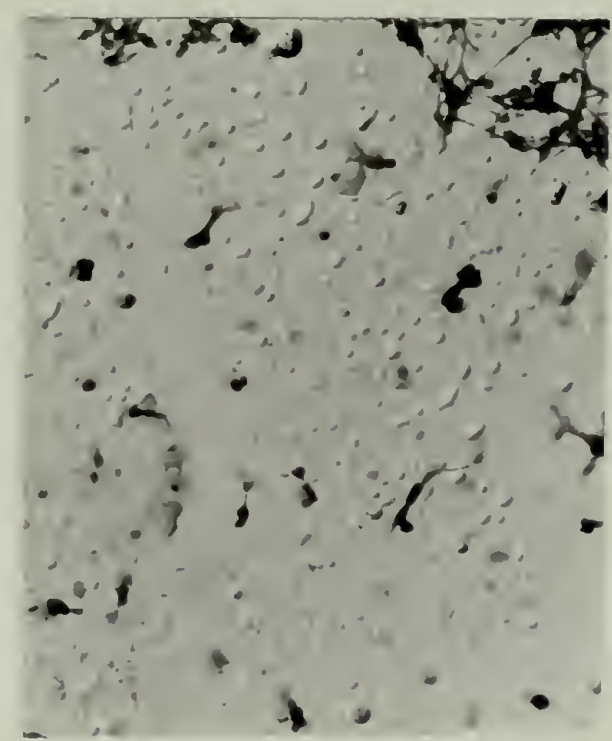

(a)

dry

(b)

water 35 wt. %

Electron Micrograph of a Surface Replica of 4M-1,10 Sample
(X9200)

Plate 1

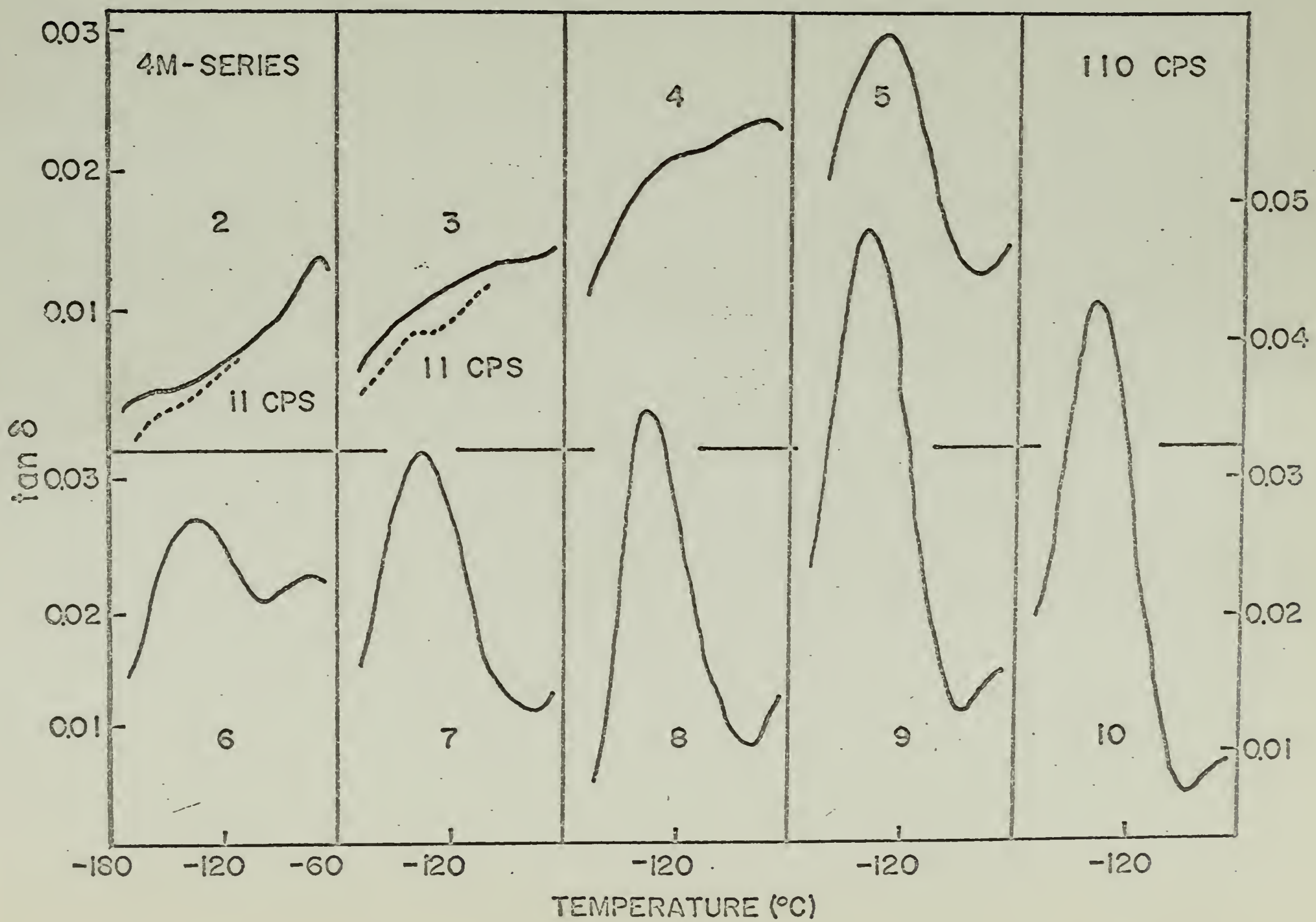
4M-SERIES
110 CPS
2
3
4
5
11 CPS
11 CPS
6
7
8
9
10
tan δ
0.03
0.02
0.01
0.05
0.04
0.03
0.02
0.01
-180
-120
-60
-120
-120
-120
-120
TEMPERATURE (°C)

Figure 1

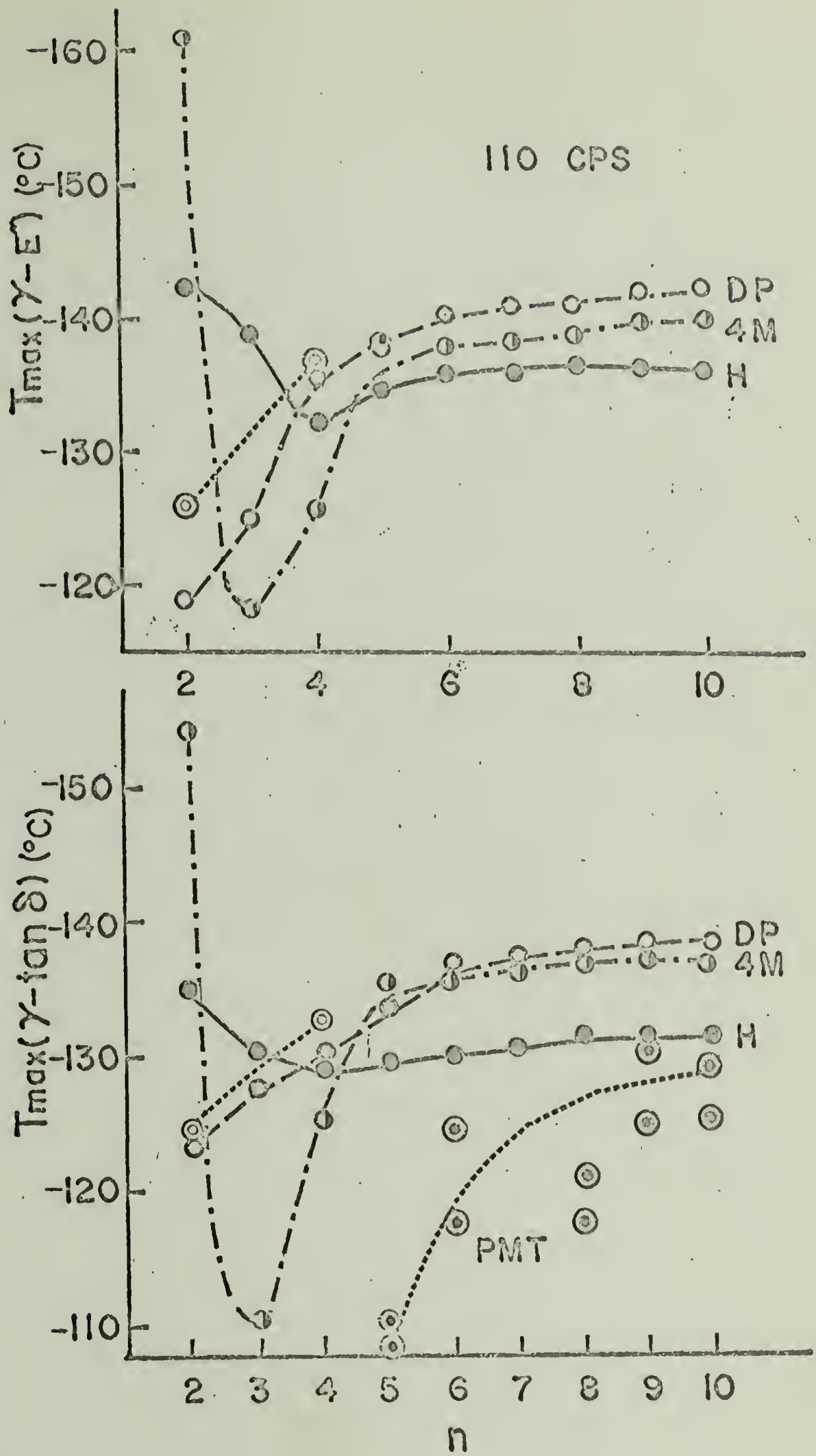
110 CPS
Tmax(γ-E) (°C)
-160
-150
-140
-130
-120
DP
4M
H
2
4
6
8
10
Tmax(γ-tan δ) (°C)
-150
-140
-130
-120
-110
DP
4M
H
PMT
2
3
4
5
6
7
8
9
10
n

Figure 2

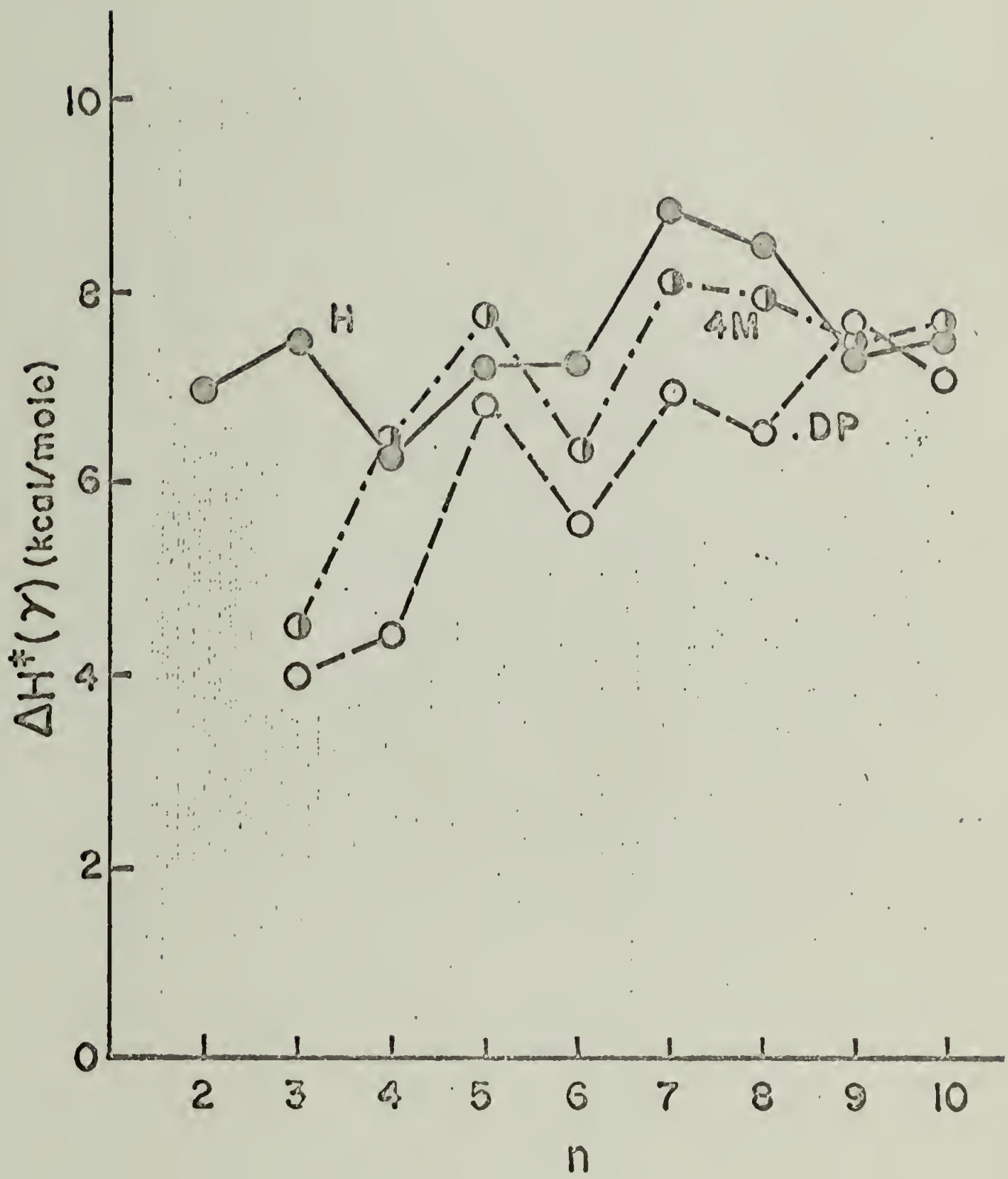

Figure 3

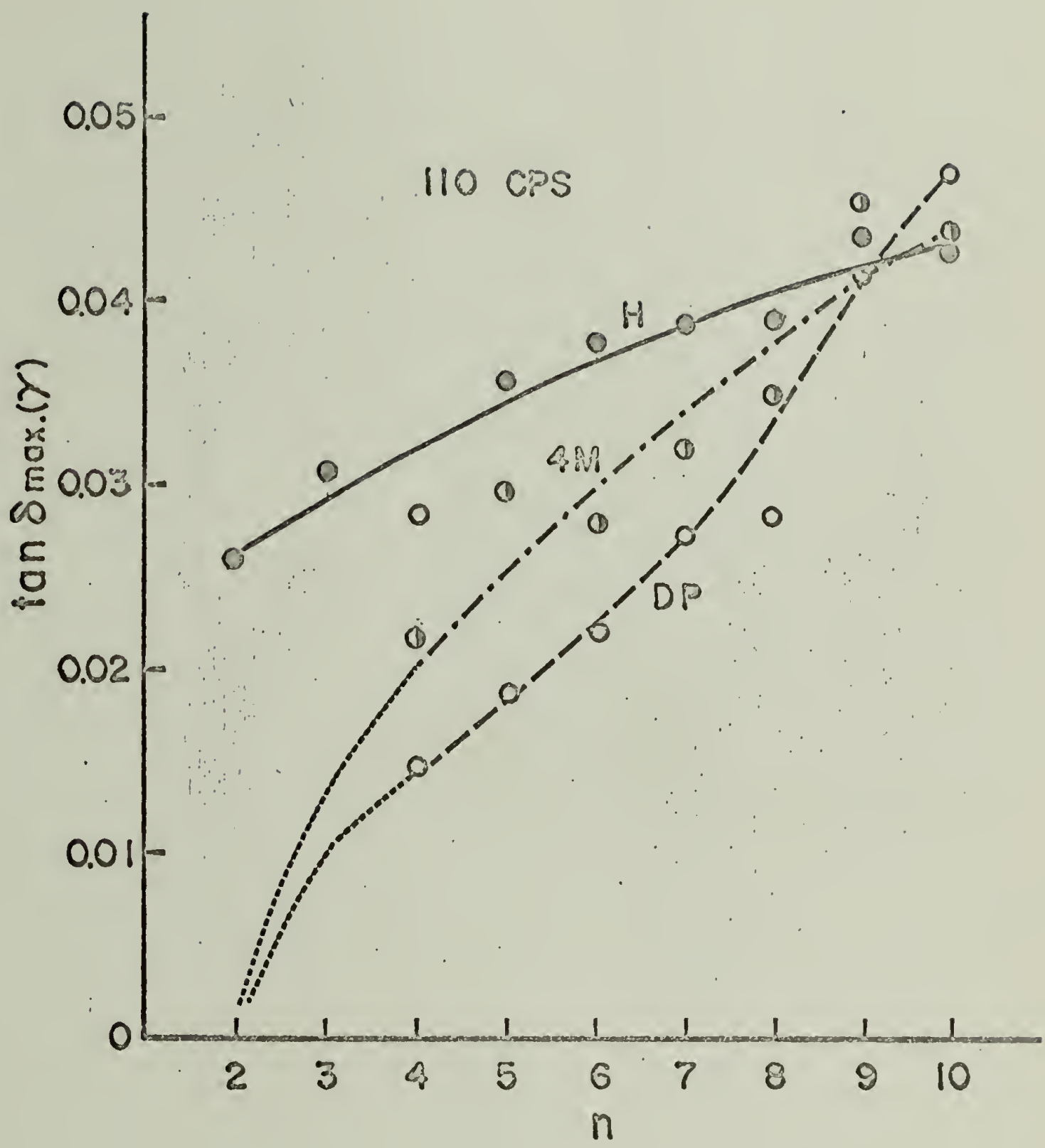

Figure 4

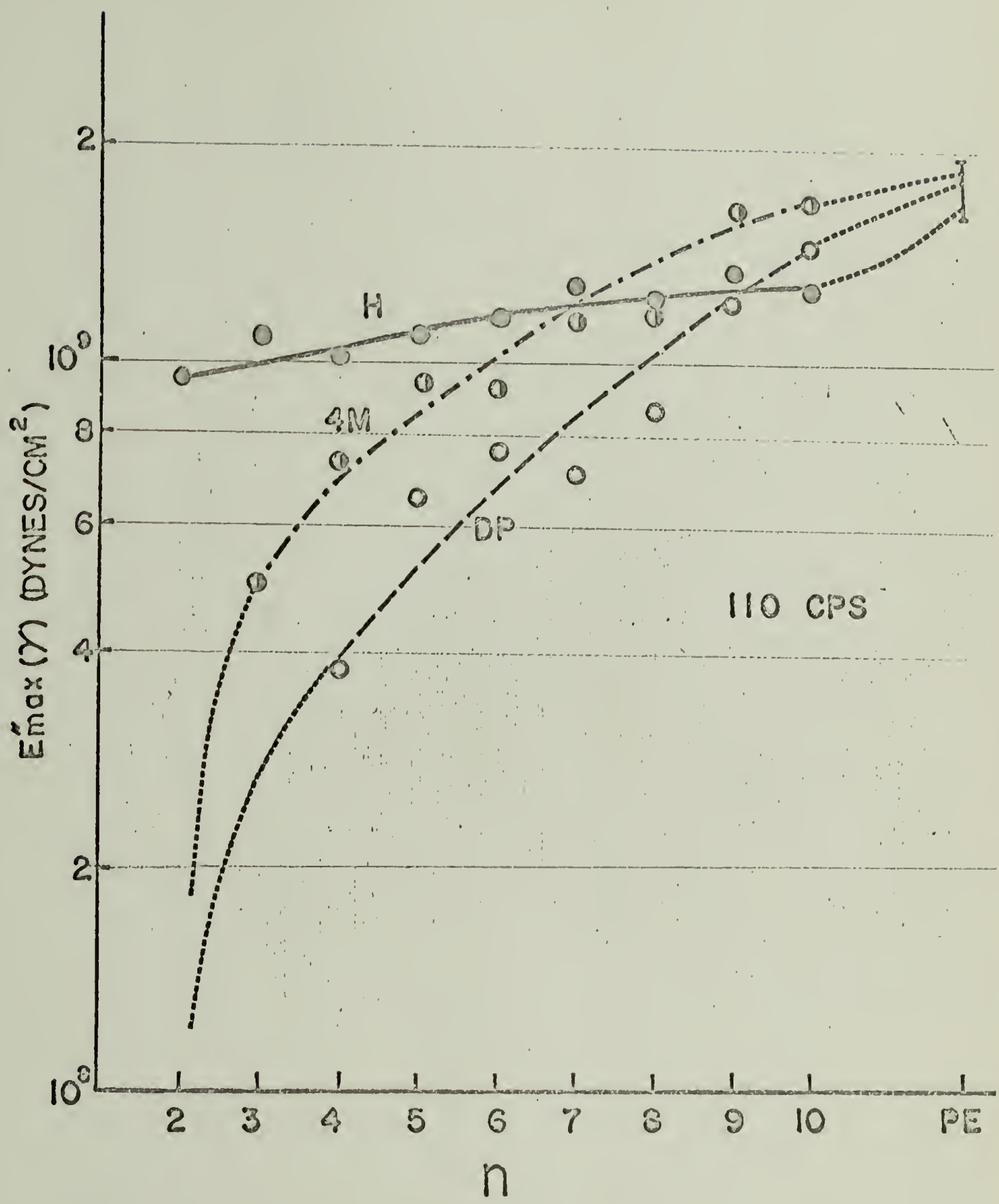

Figure 5

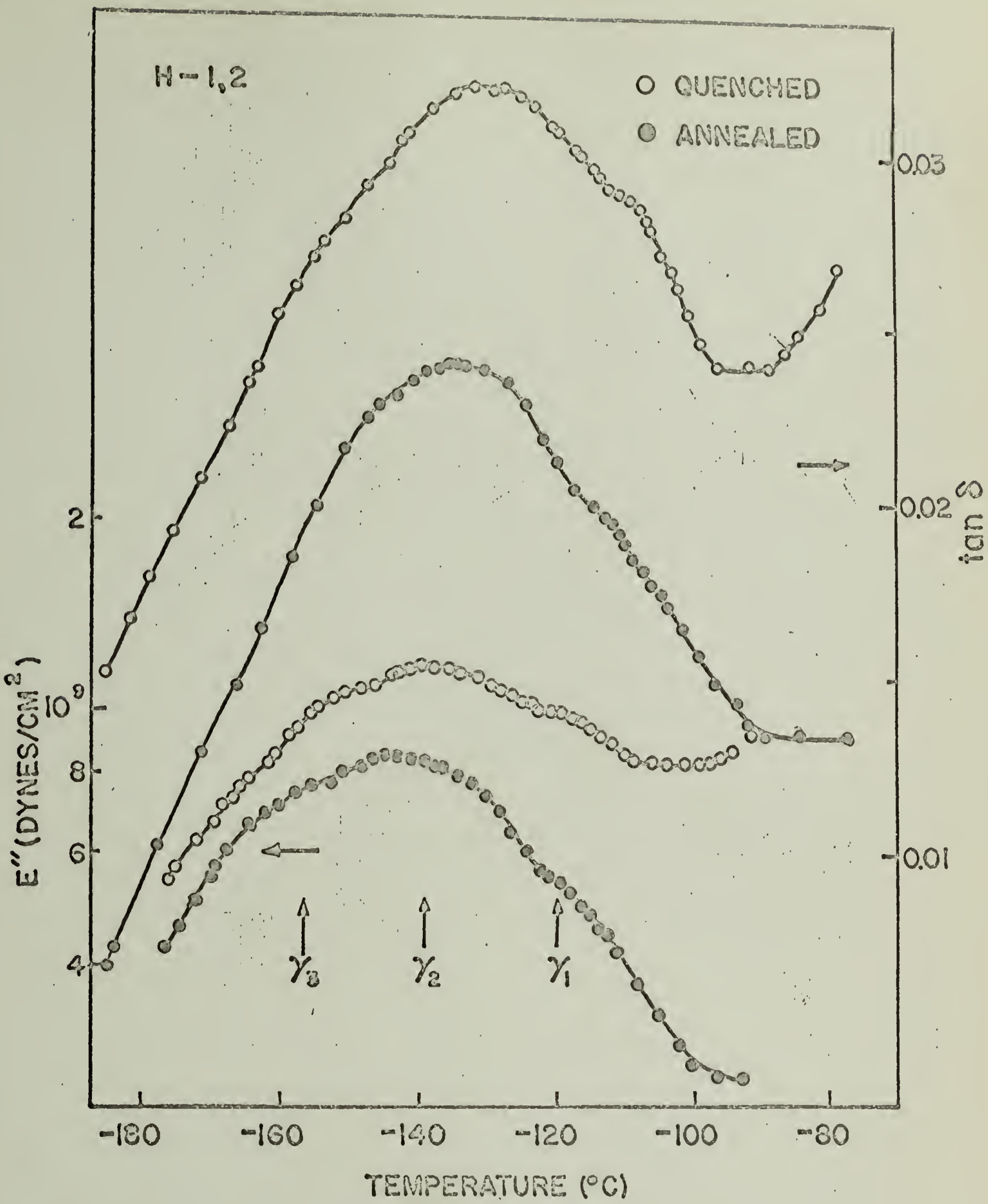
H-1,2
QUENCHED
ANNEALED
E'' (DYNES/CM²)
10⁹
2
1
8
6
4
tan δ
0.03
0.02
0.01
γ3
γ2
γ1
-180
-160
-140
-120
-100
-80
TEMPERATURE (°C)

Figure 6

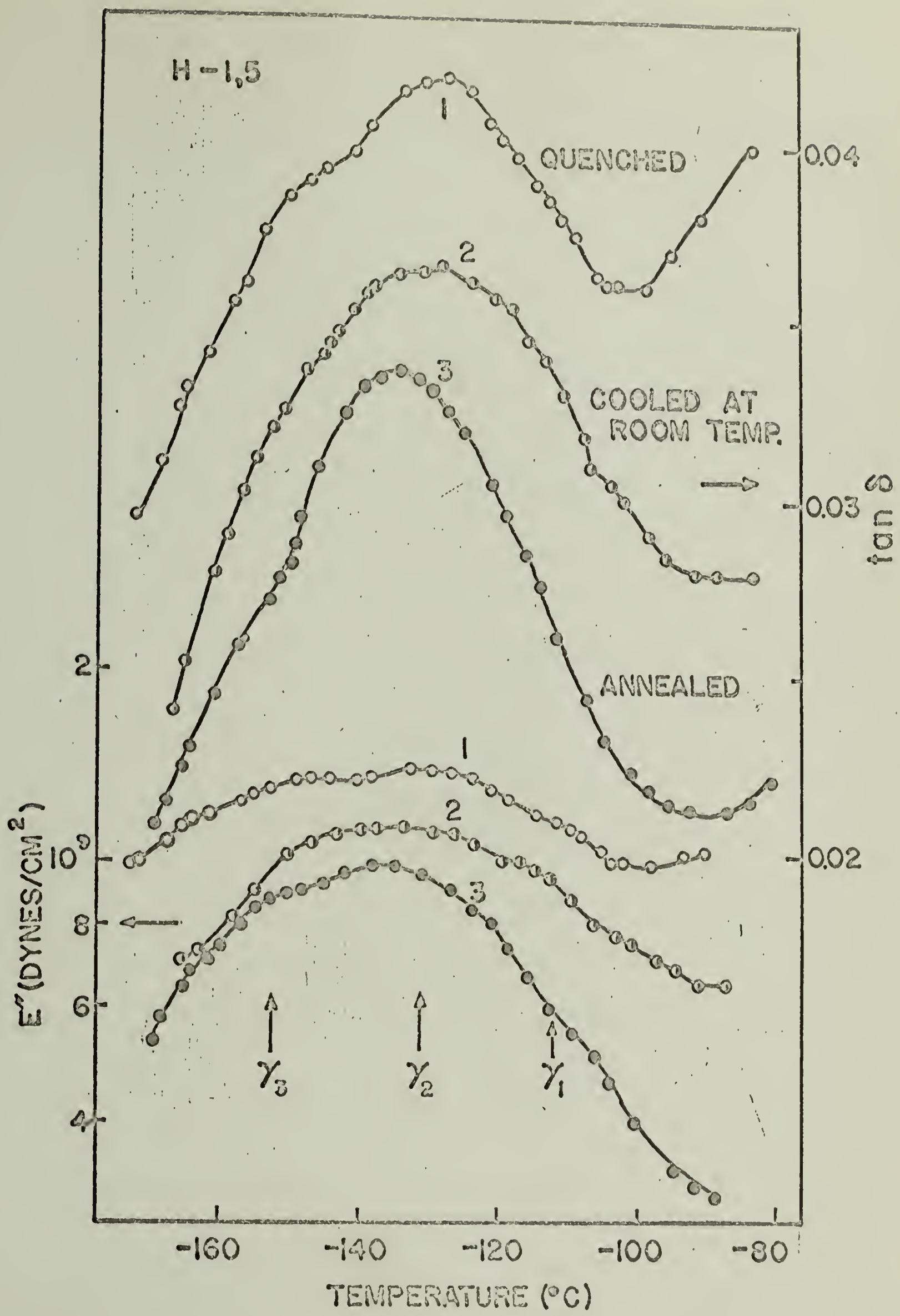
H-1,5
QUENCHED
COOLED AT ROOM TEMP.
ANNEALED
1
2
3
0.04
0.03
0.02
tan δ
2
10^9
8
6
4
E'(DYNES/CM^2)
γ3
γ2
γ1
-160
-140
-120
-100
-80
TEMPERATURE (°C)

Figure 7

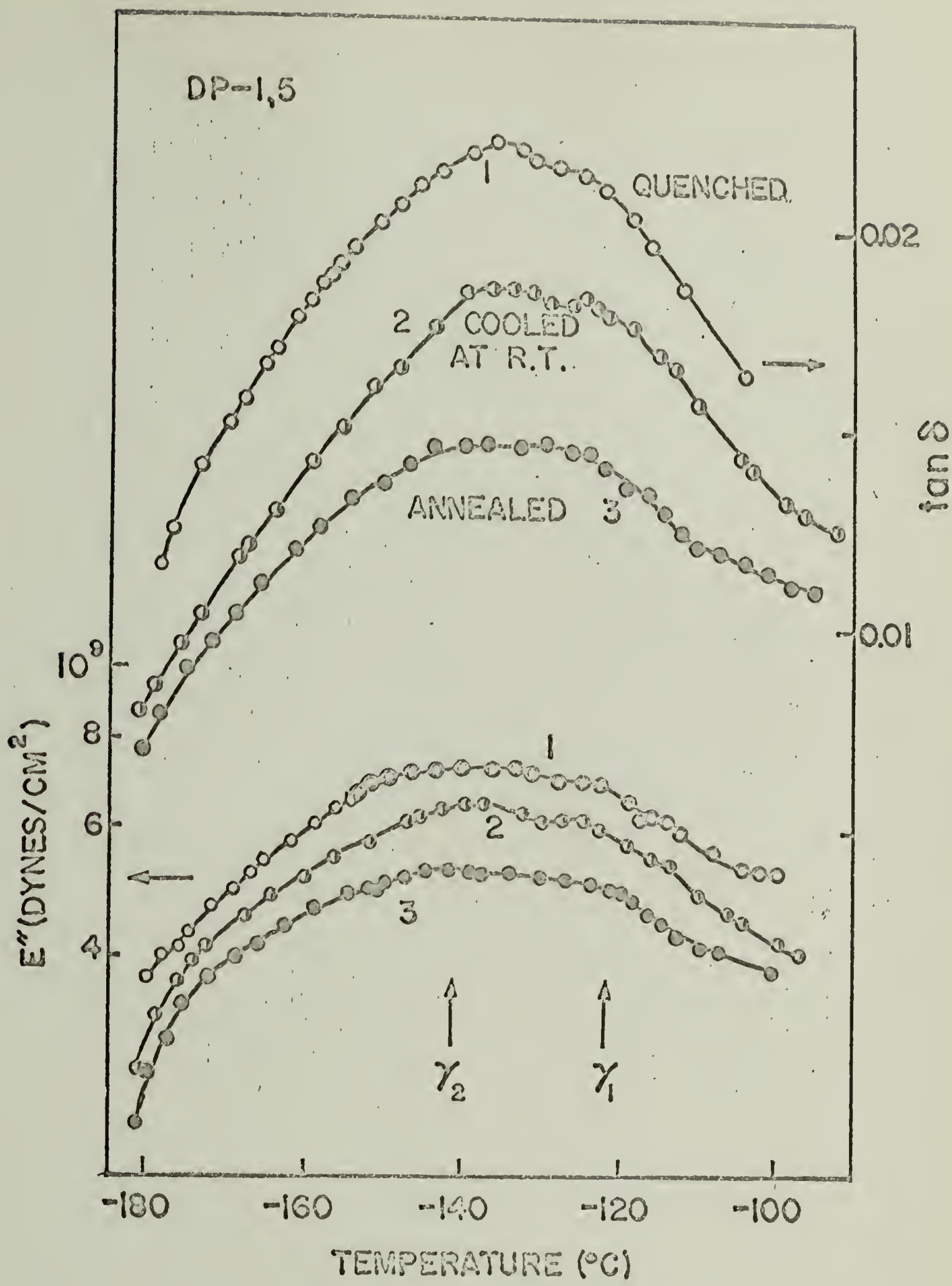
DP-1,5
QUENCHED
1
2
COOLED
AT R.T.
ANNEALED
3
0.02
0.01
tan δ
10^9
8
6
4
E''(DYNES/CM^2)
γ_2
γ_1
-180
-160
-140
-120
-100
TEMPERATURE (°C)

Figure 8

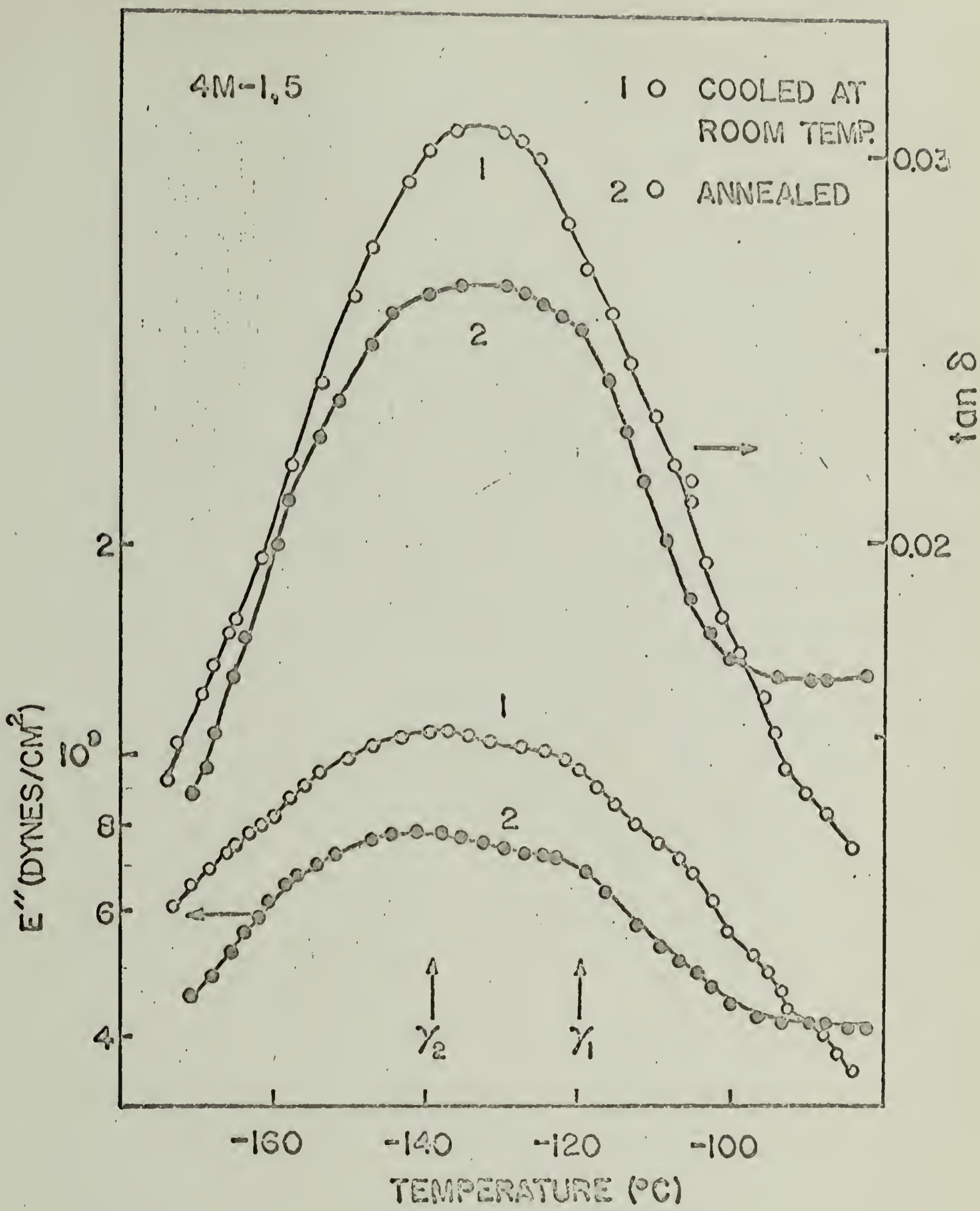
4M-1,5
1 O COOLED AT ROOM TEMP.
2 O ANNEALED
1
2
1
2
γ_2
γ_1
E'' (DYNES/CM^2)
10^9
8
6
4
2
tan δ
0.03
0.02
-160
-140
-120
-100
TEMPERATURE (°C)

Figure 9

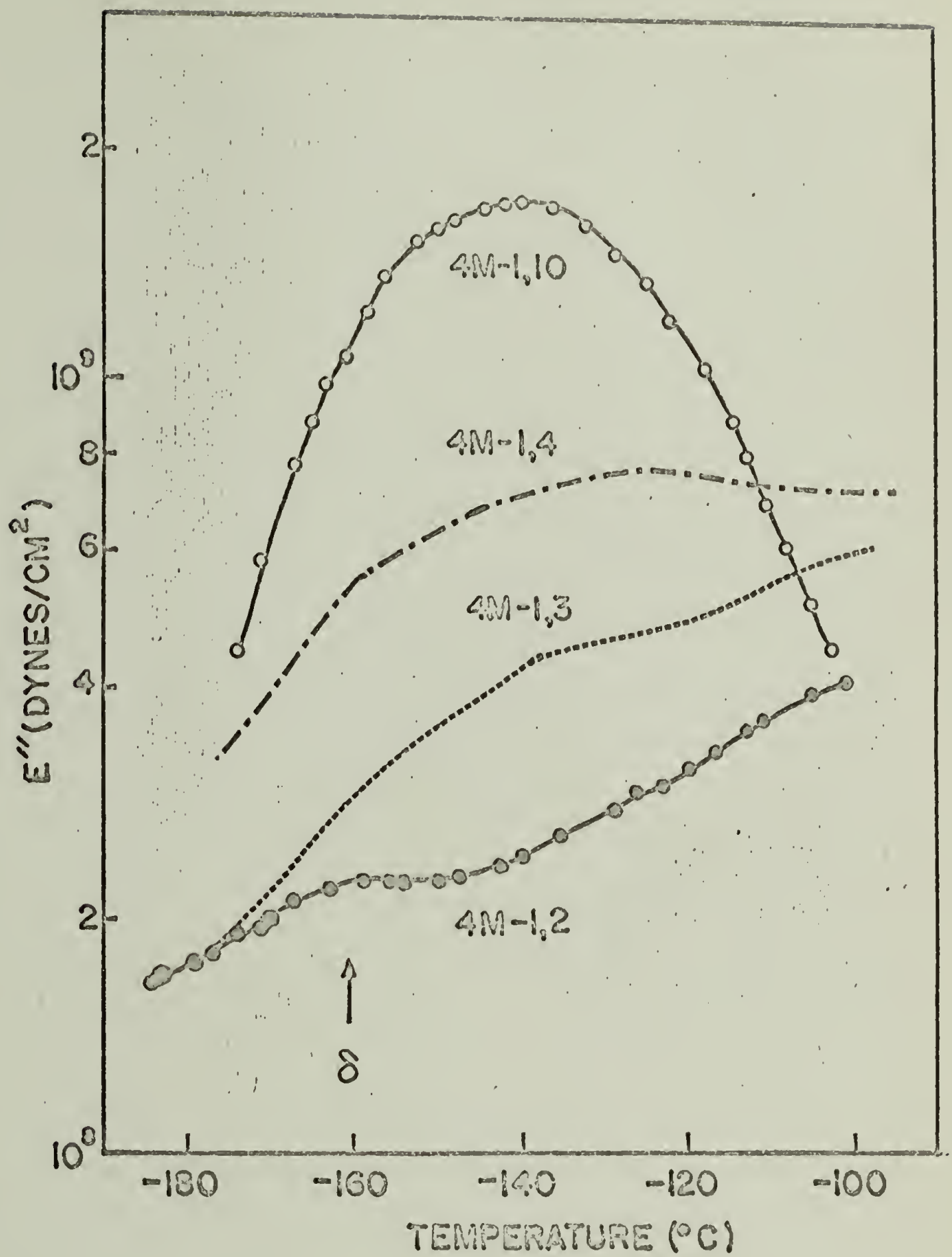
4M-1,10
4M-1,4
4M-1,3
4M-1,2
δ
E''(DYNES/CM²)
2
10⁰
8
6
4
2
10⁰
-180
-160
-140
-120
-100
TEMPERATURE (°C)

Figure 10

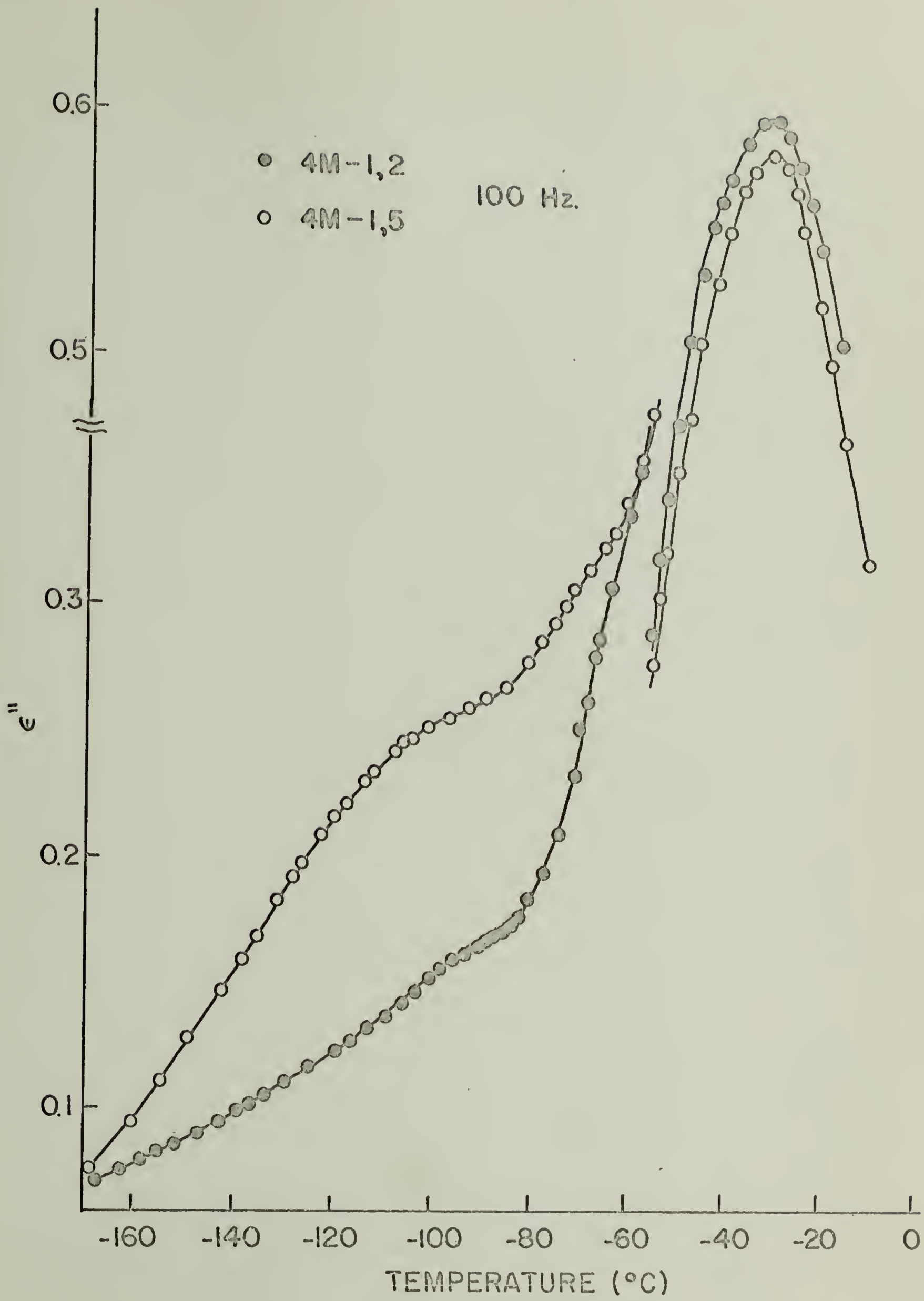
0.6
0.5
0.3
0.2
0.1
ε''
4M-1,2
4M-1,5
100 Hz.
-160
-140
-120
-100
-80
-60
-40
-20
0
TEMPERATURE (°C)

Figure 11

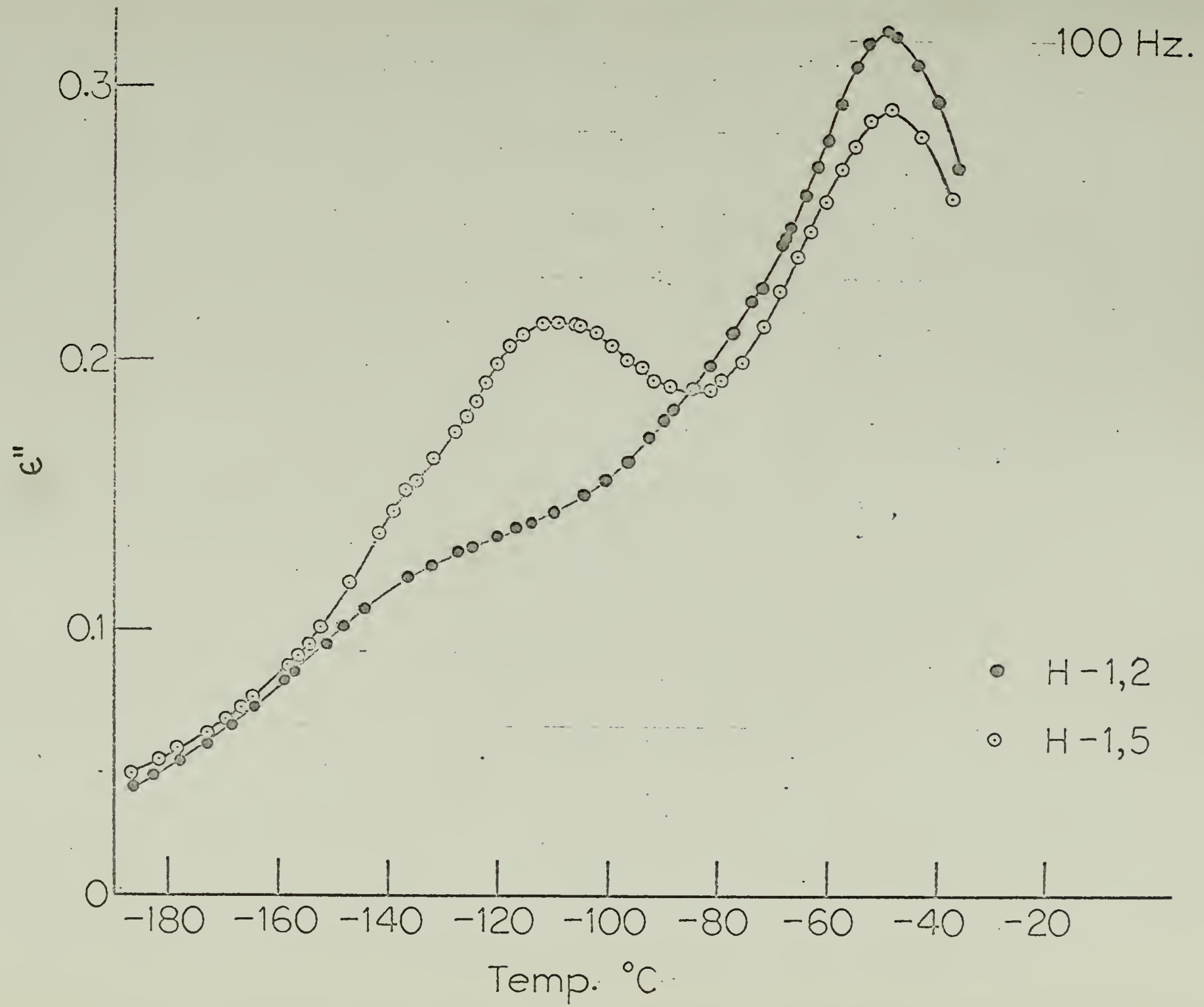

Figure 12

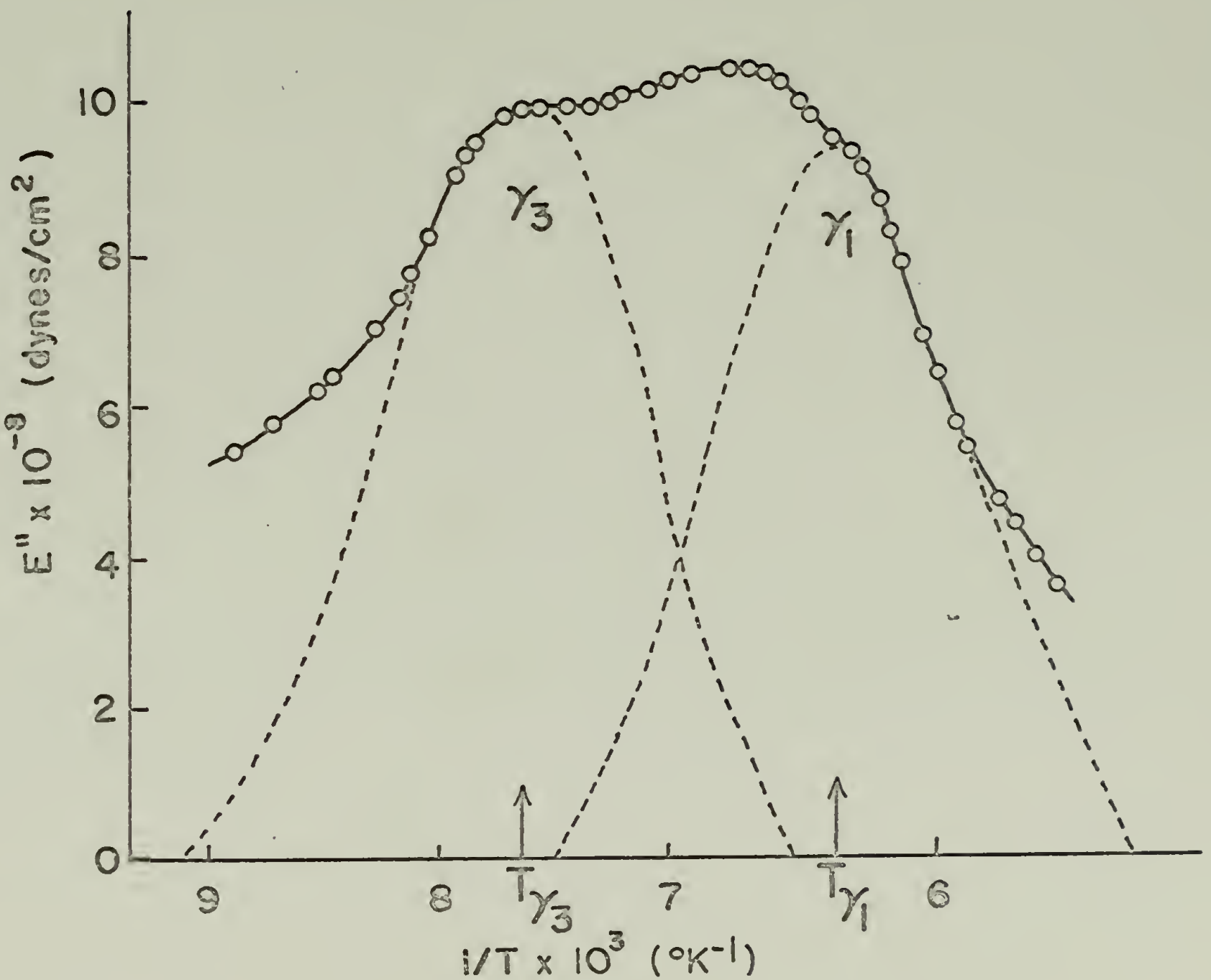

Figure 13

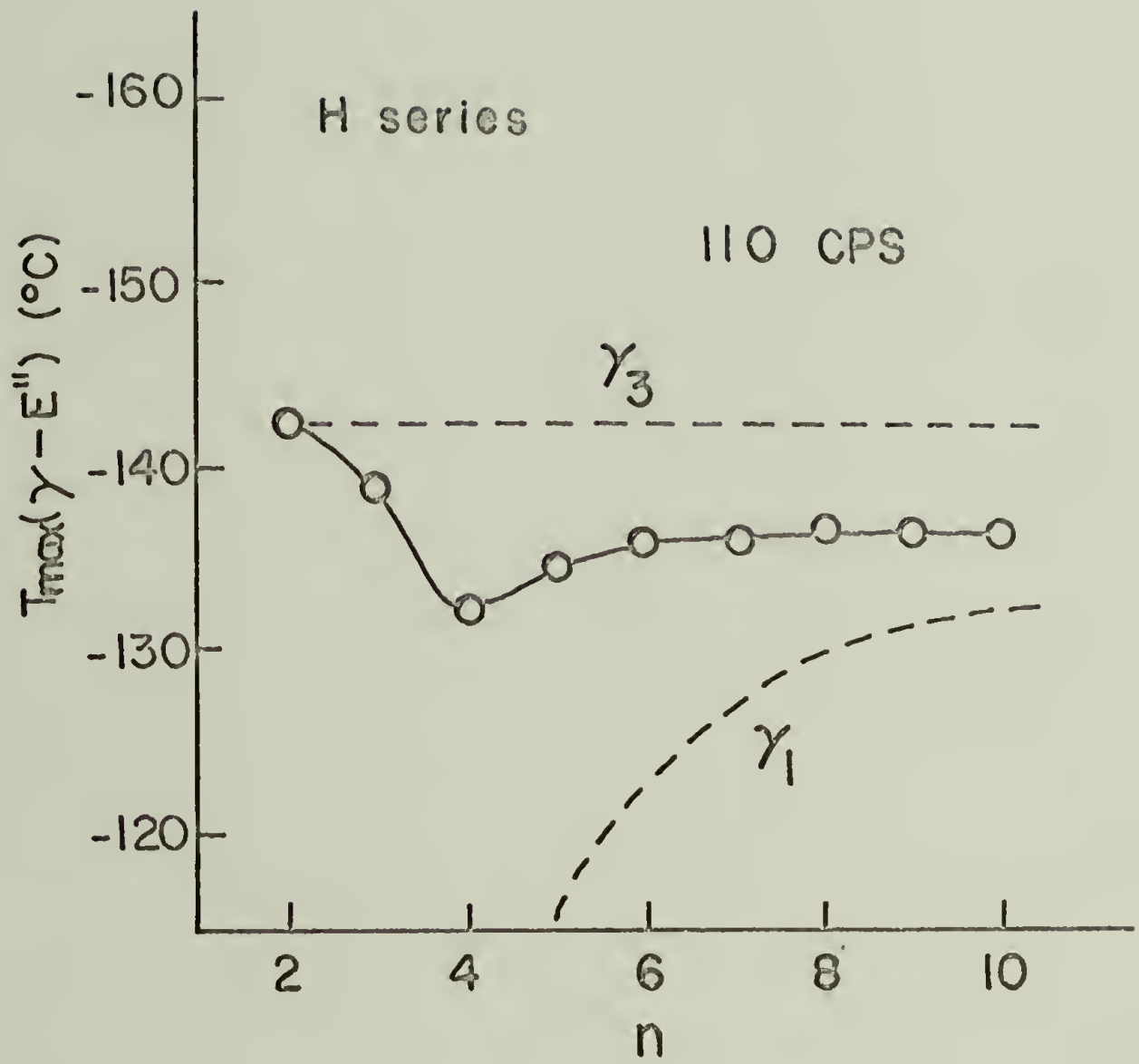
H series
110 CPS
γ_3
γ_1
$T_{max}(\gamma - E'')$ (°C)
-160
-150
-140
-130
-120
2
4
6
8
10
n

Figure 14(a)

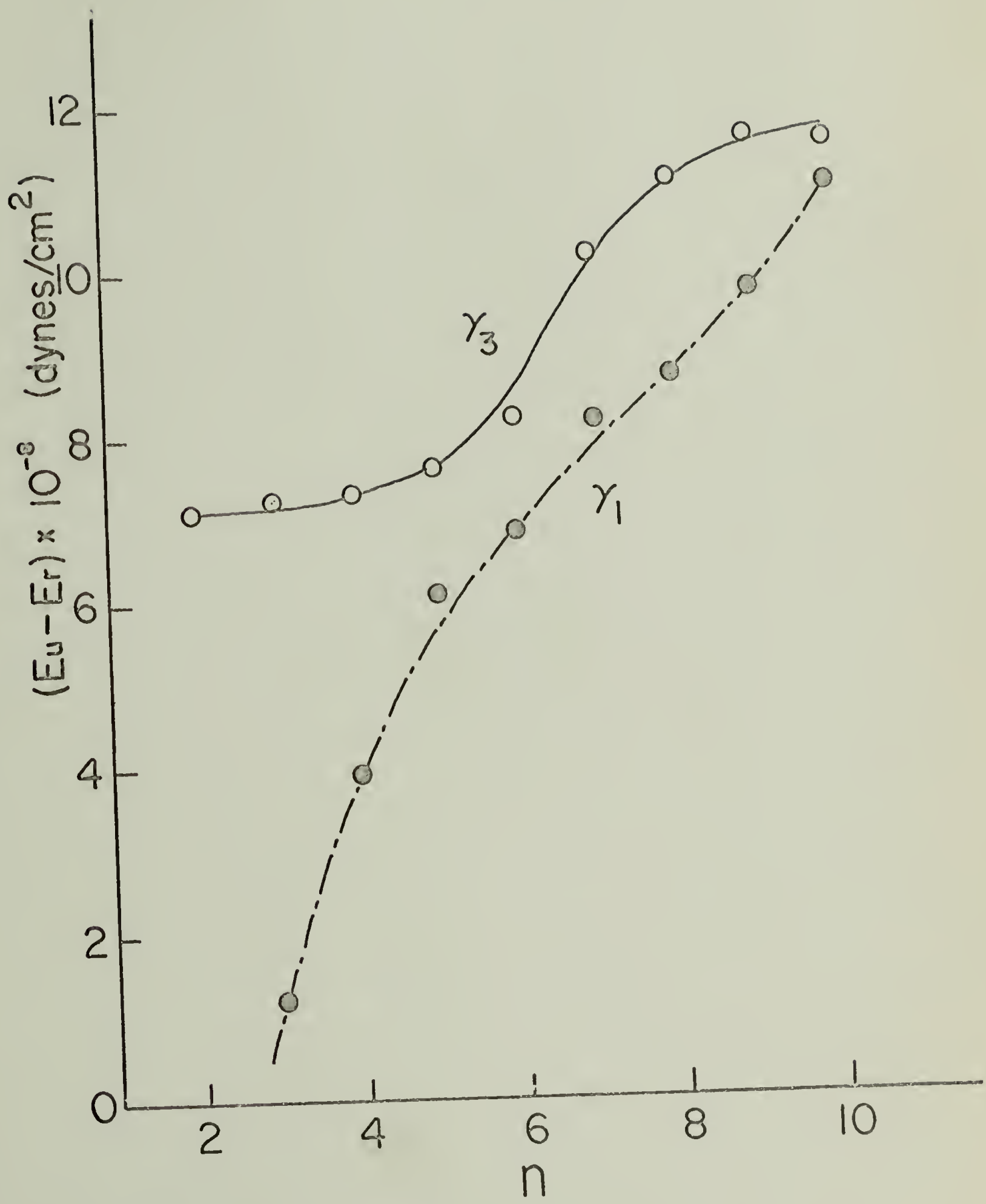

Figure 14(b)

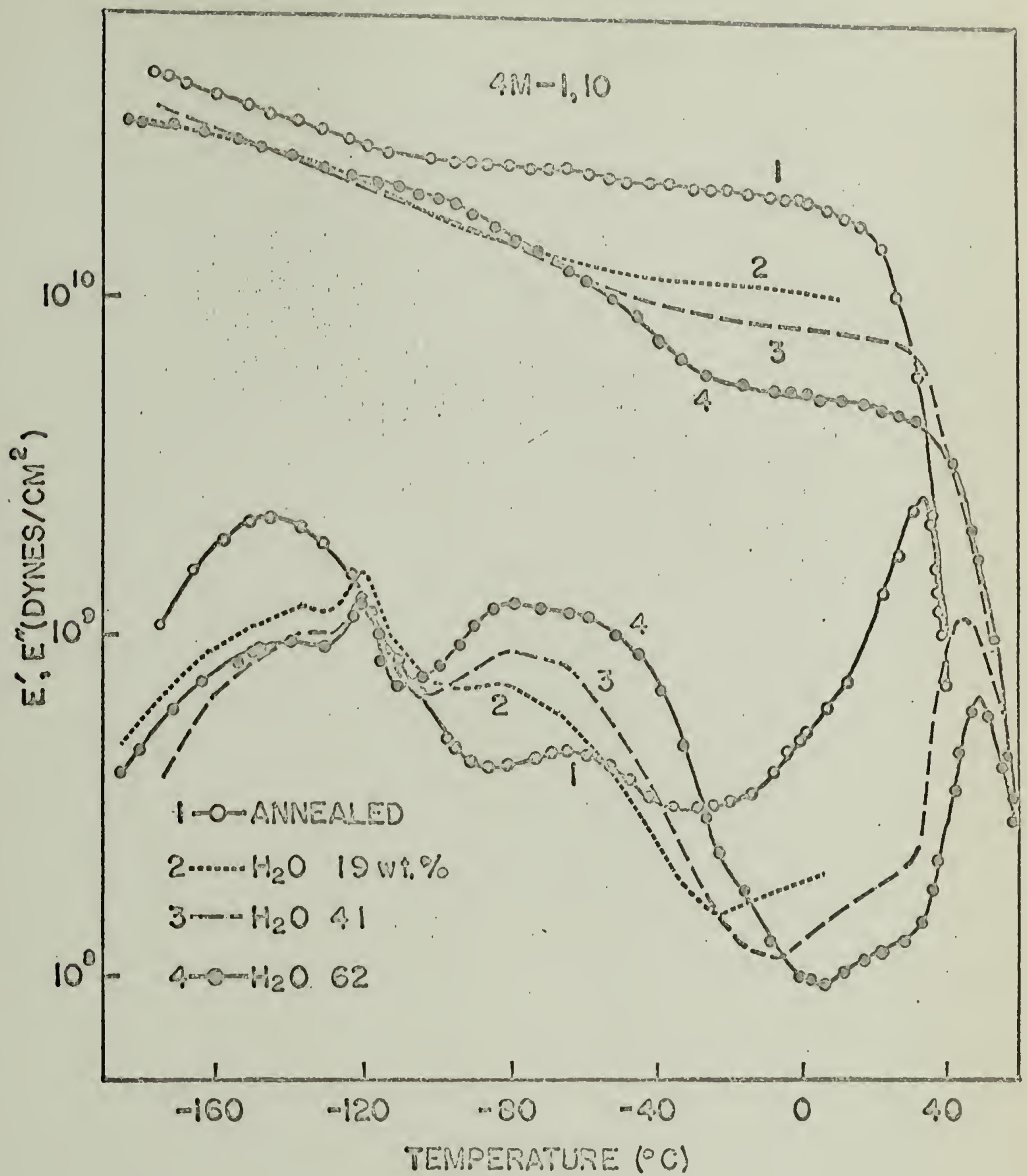
4M-1,10
1
2
3
4
10^{10}
10^{9}
10^{8}
E', E"(DYNES/CM^2)
1—o—ANNEALED
2·····H_2O 19 wt.%
3——H_2O 41
4—o—H_2O 62
-160
-120
-80
-40
0
40
TEMPERATURE (°C)

Figure 15

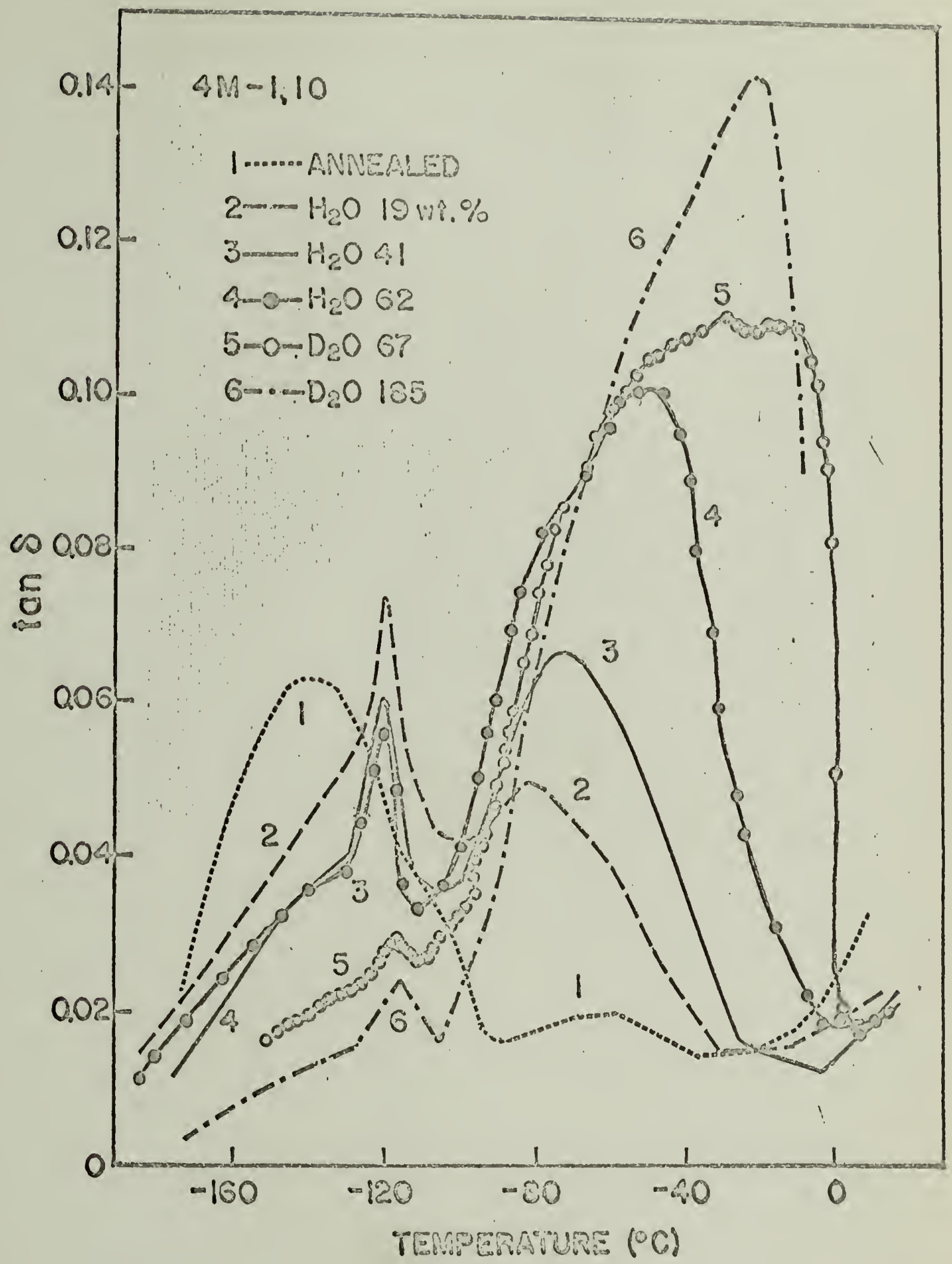
4M-1,10
1 ANNEALED
2 H_2O 19 wt.%
3 H_2O 41
4 H_2O 62
5 D_2O 67
6 D_2O 185
tan δ
0.14
0.12
0.10
0.08
0.06
0.04
0.02
0
-160
-120
-80
-40
0
TEMPERATURE (°C)

Figure 16

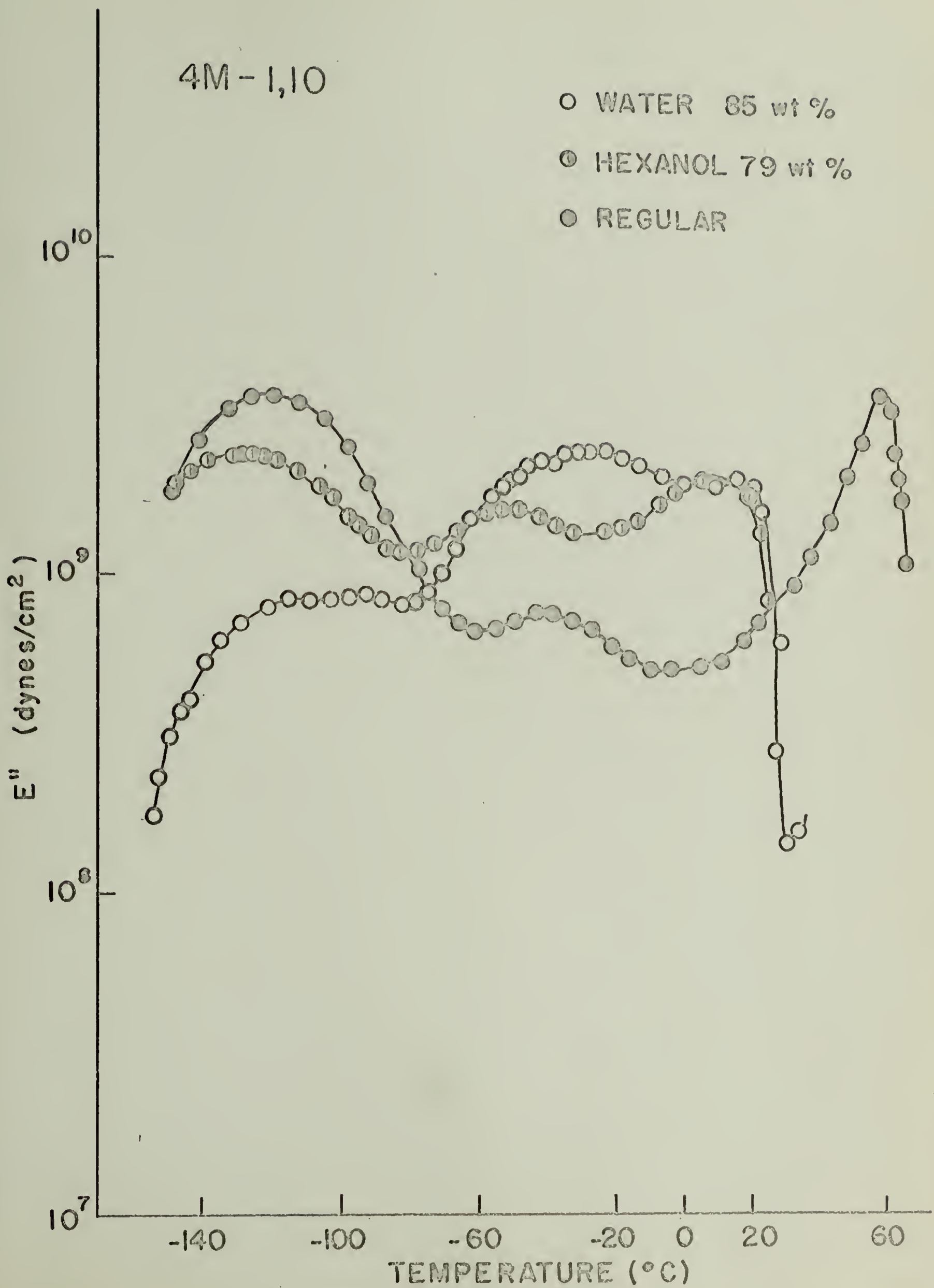
4M - 1,10
WATER 85 wt %
HEXANOL 79 wt %
REGULAR
10^{10}
10^{9}
10^{8}
10^{7}
E" (dynes/cm^2)
-140
-100
-60
-20
0
20
60
TEMPERATURE (°C)

Figure 17

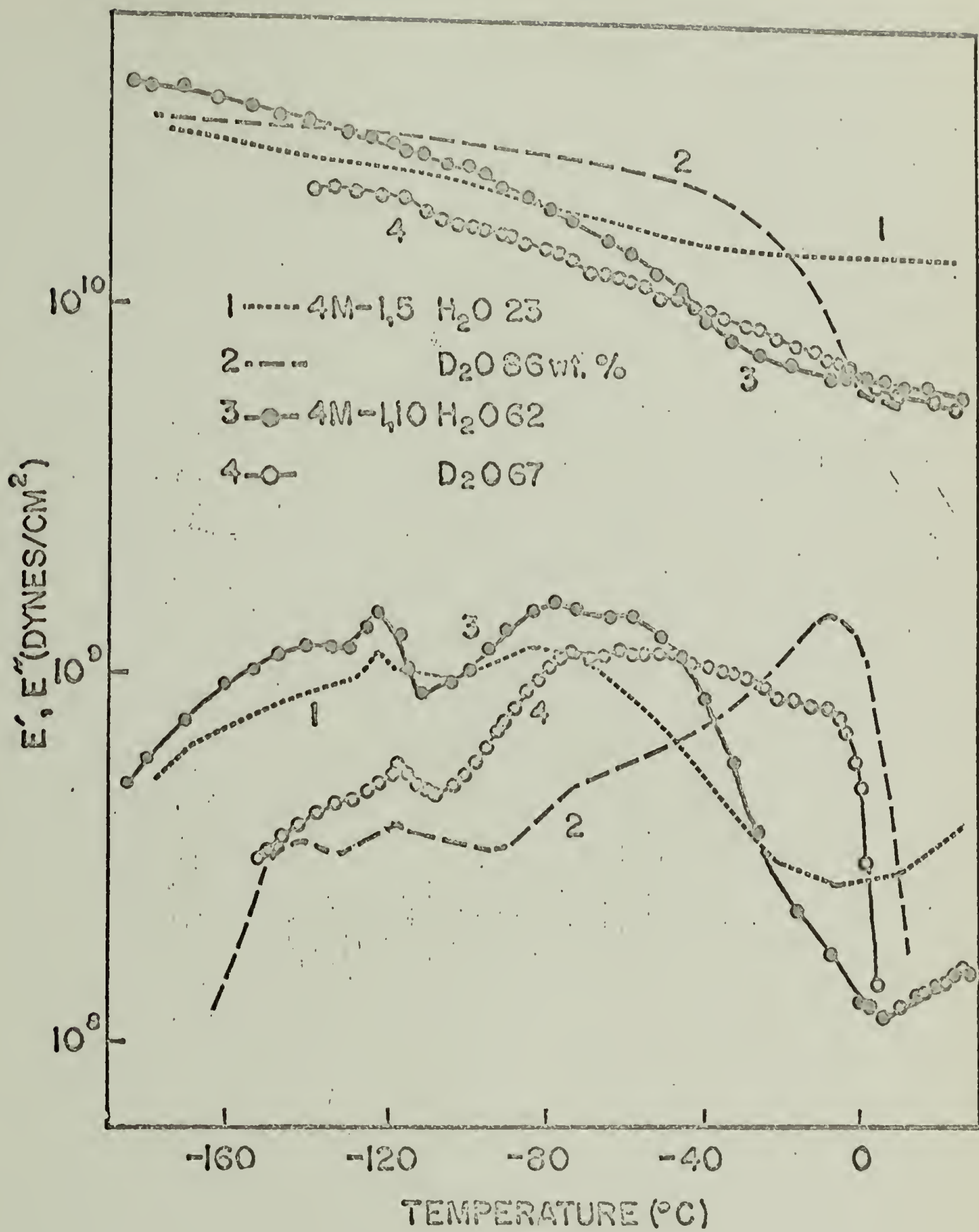
1 4M-1,5 H_2O 23
2 D_2O 86 wt. %
3 4M-4,10 H_2O 62
4 D_2O 67
10^{10}
10^{9}
10^{8}
E', E" (DYNES/CM^2)
-160
-120
-80
-40
0
TEMPERATURE (°C)

Figure 18

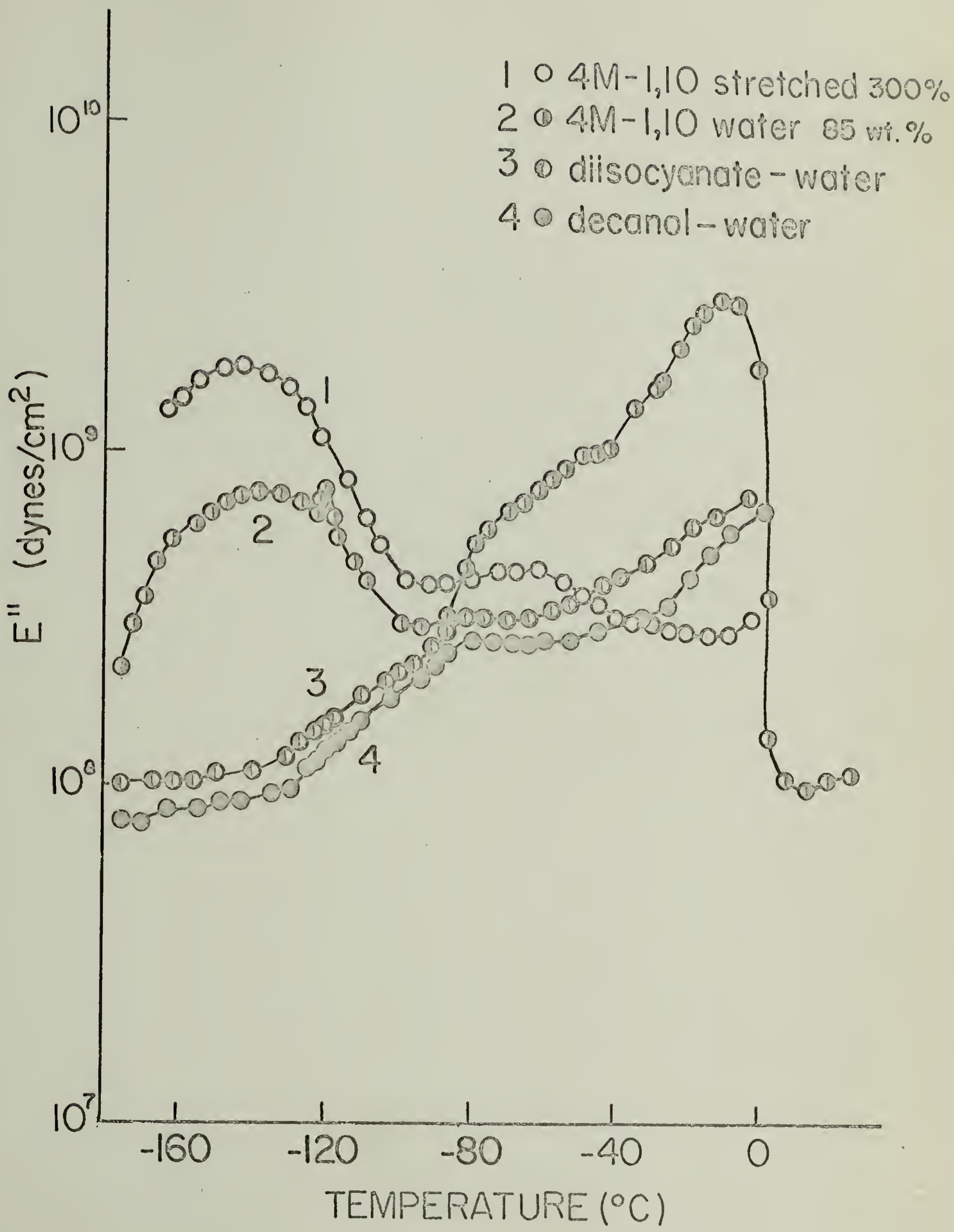
1 ○ 4M-1,10 stretched 300%
2 ◐ 4M-1,10 water 85 wt.%
3 ◐ diisocyanate - water
4 ◐ decanol - water
E'' (dynes/cm²)
10¹⁰
10⁹
10⁸
10⁷
1
2
3
4
-160
-120
-80
-40
0
TEMPERATURE (°C)

Figure 19

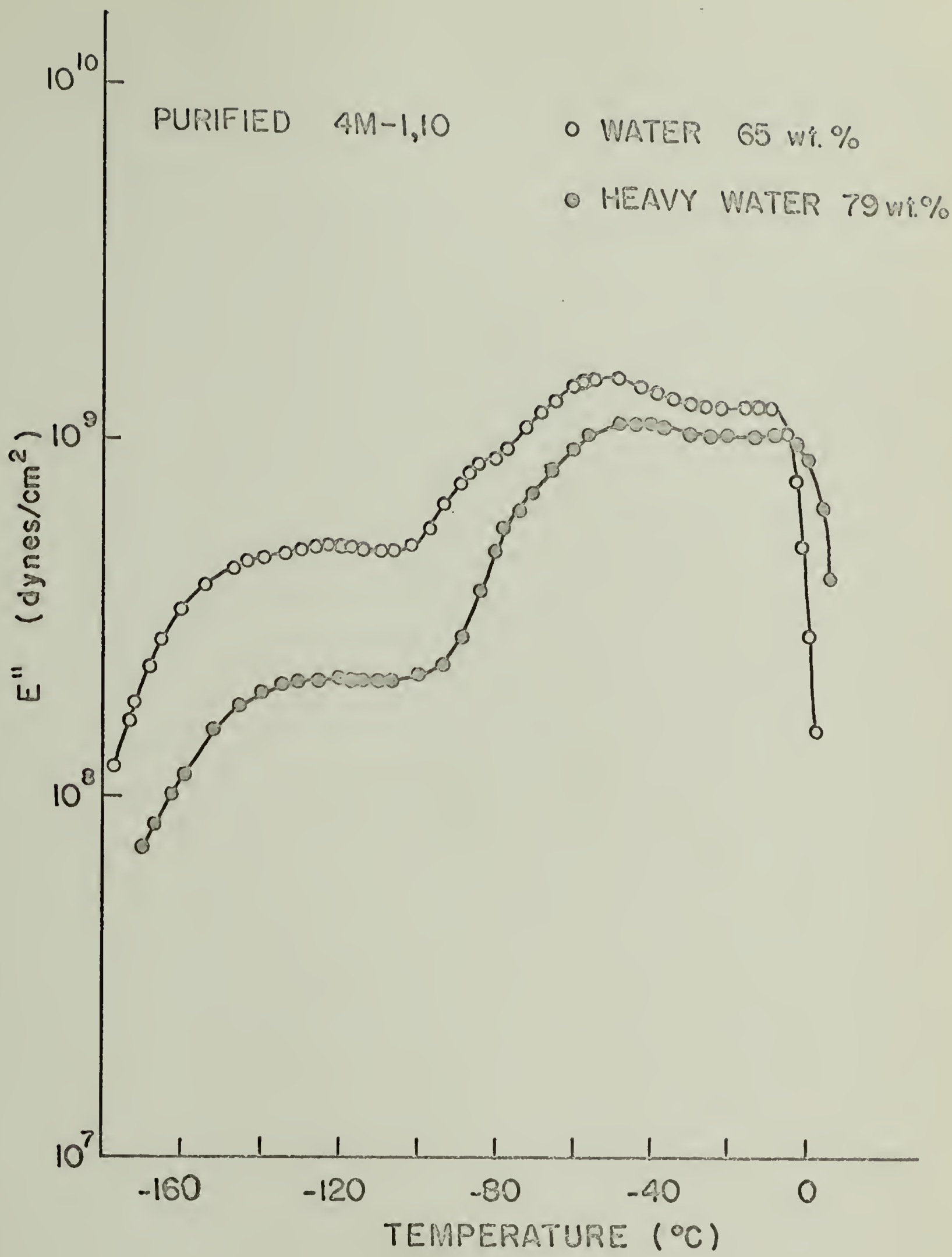
PURIFIED 4M-1,10
o WATER 65 wt. %
⊙ HEAVY WATER 79 wt.%
E'' (dynes/cm²)
10¹⁰
10⁹
10⁸
10⁷
-160
-120
-80
-40
0
TEMPERATURE (°C)

Figure 20

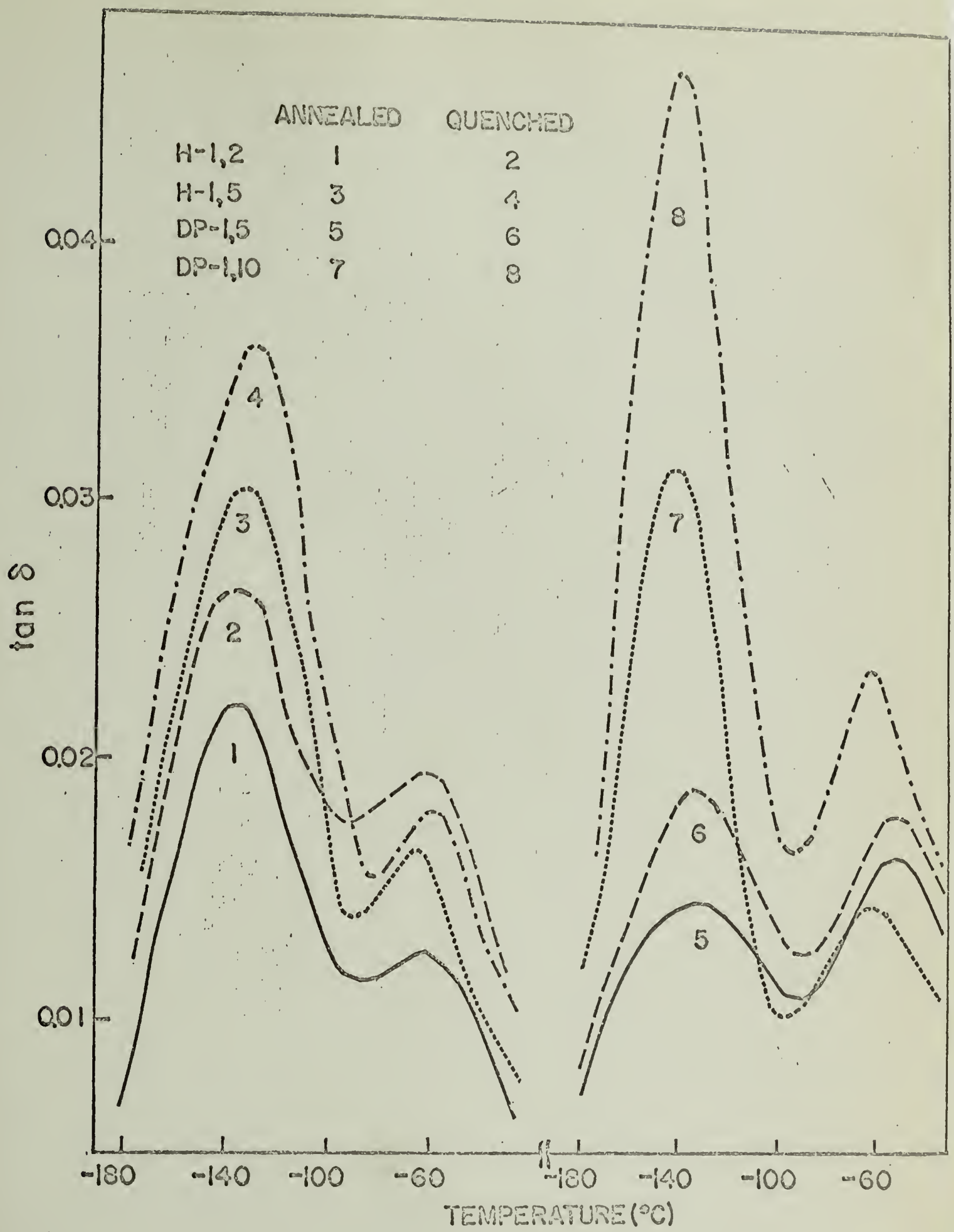
ANNEALED
QUENCHED
H-1,2 1 2
H-1,5 3 4
DP-1,5 5 6
DP-1,10 7 8
0.04
0.03
0.02
0.01
tan δ
-180
-140
-100
-60
-180
-140
-100
-60
TEMPERATURE (°C)

Figure 21

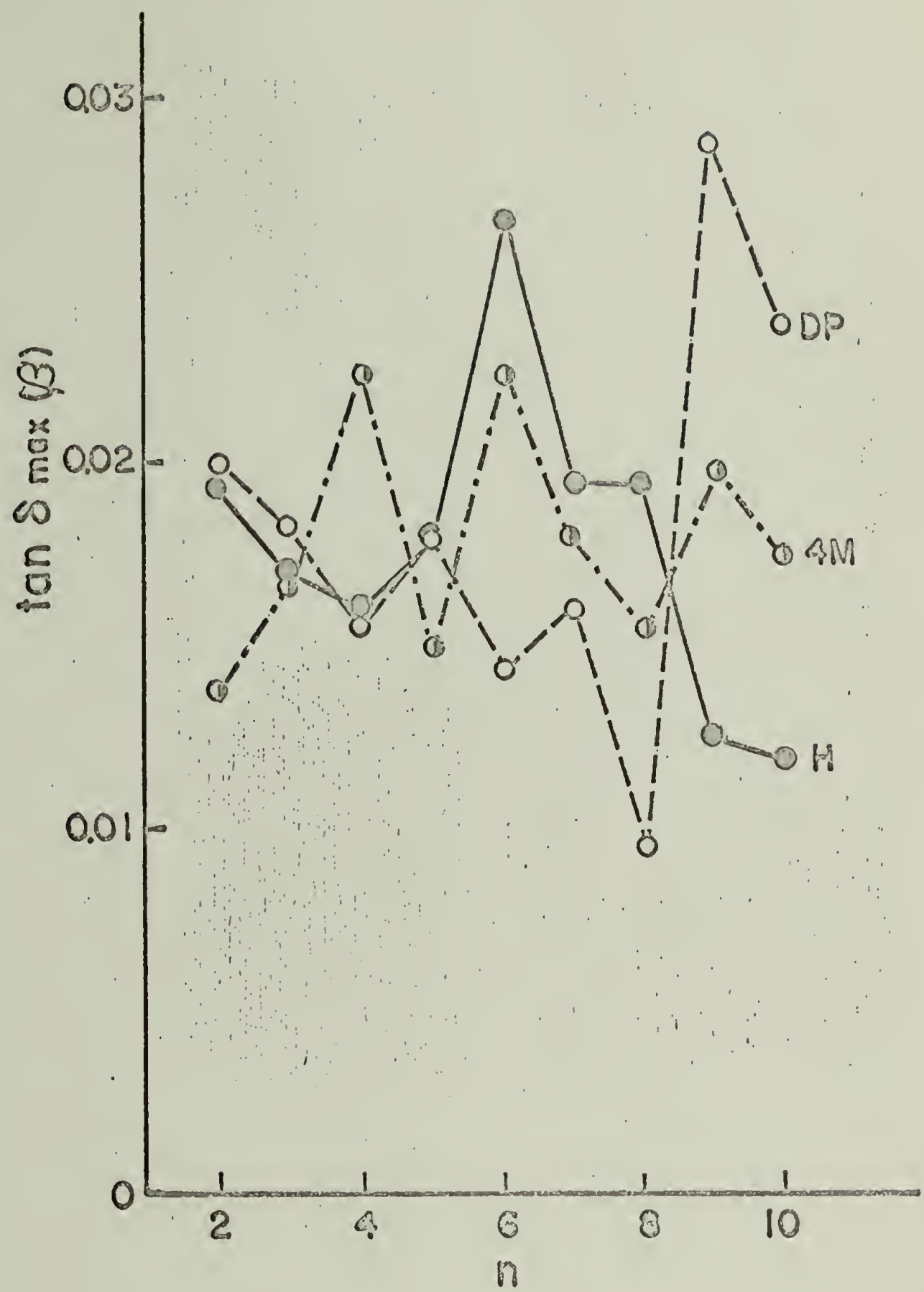

Figure 22

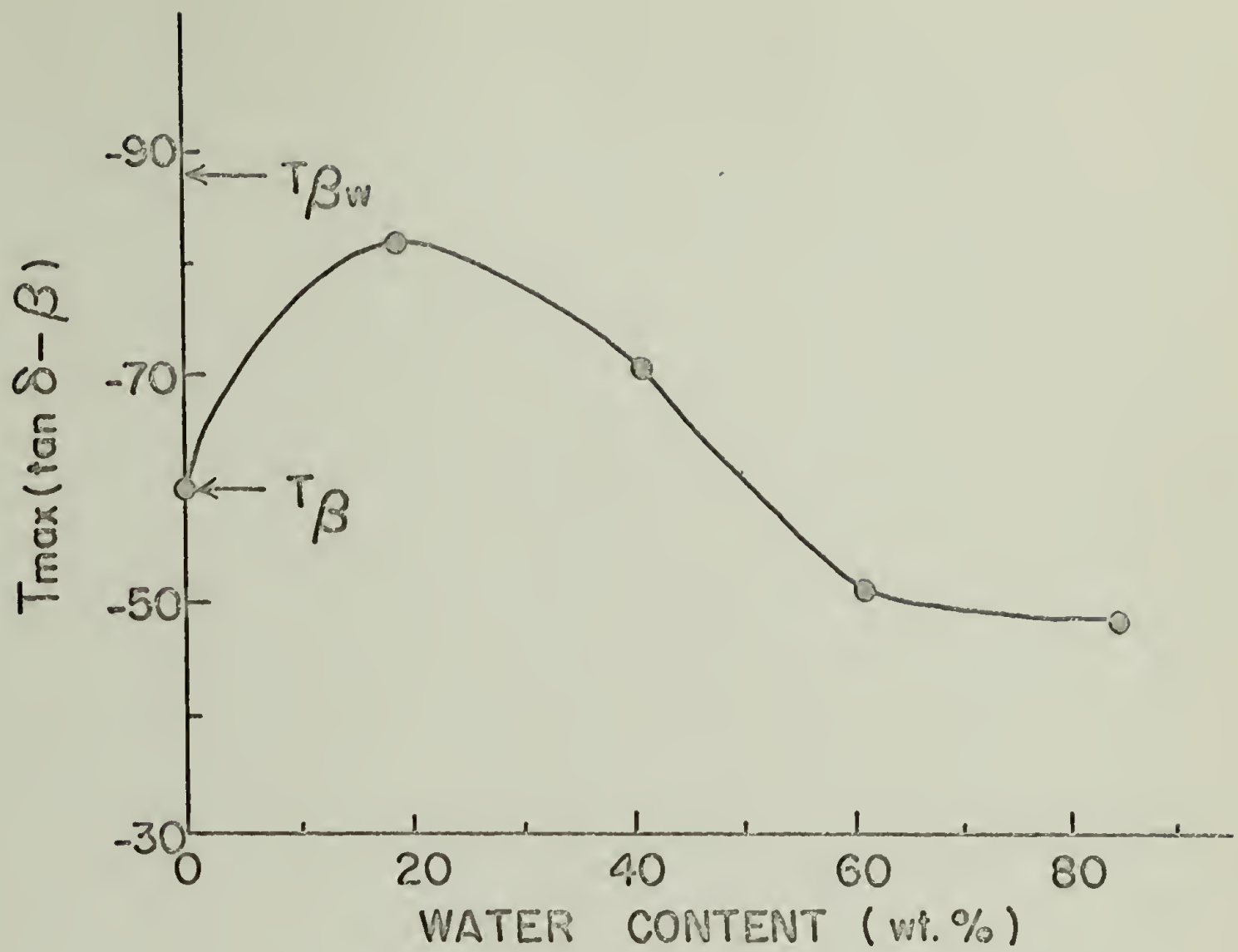
-90
-70
-50
-30
$T_{\beta w}$
T_{β}
T_{max} (tan $\delta - \beta$)
0
20
40
60
80
WATER CONTENT (wt. %)

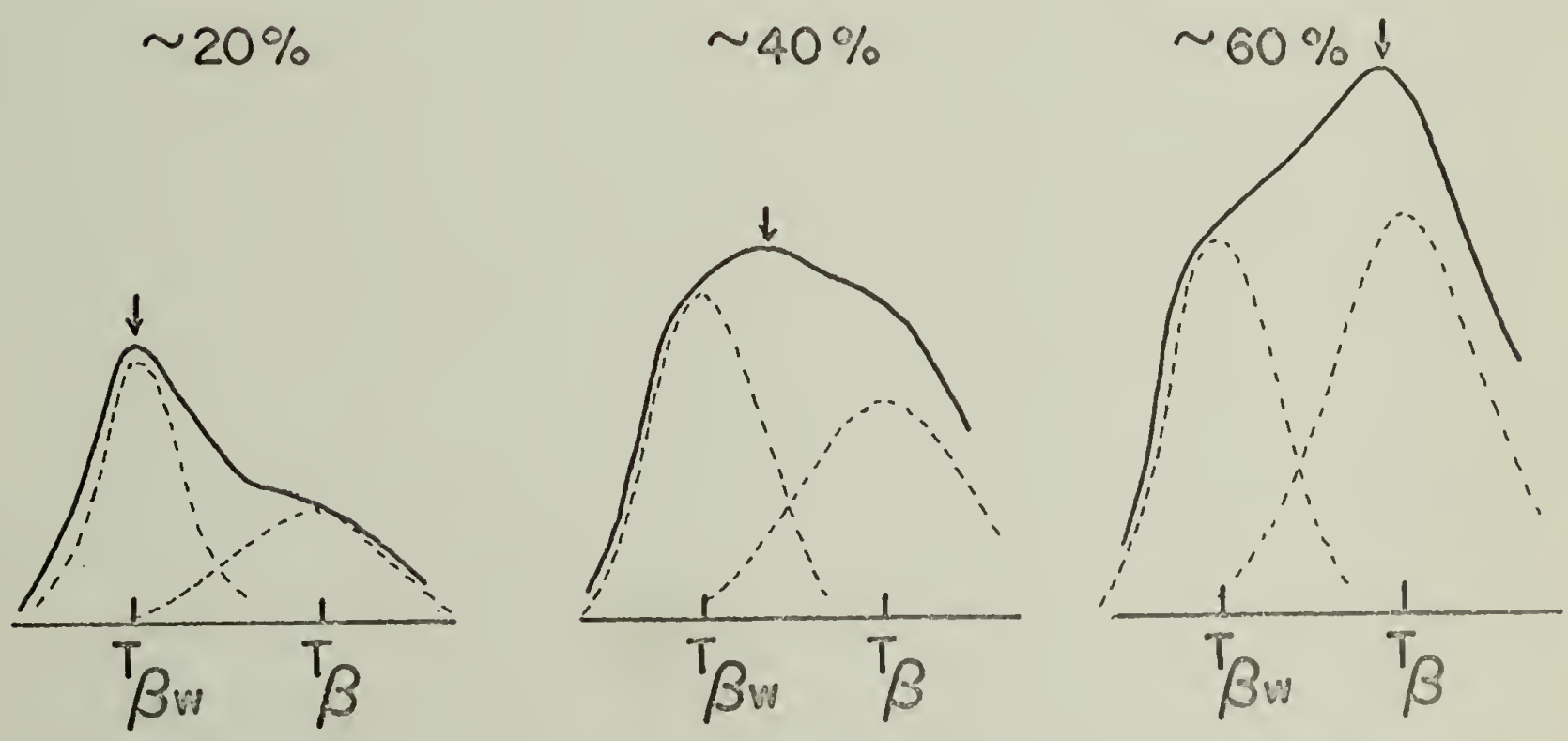
~20%
~40%
~60%
$T_{\beta w}$
T_{β}
$T_{\beta w}$
T_{β}
$T_{\beta w}$
T_{β}

Figure 23

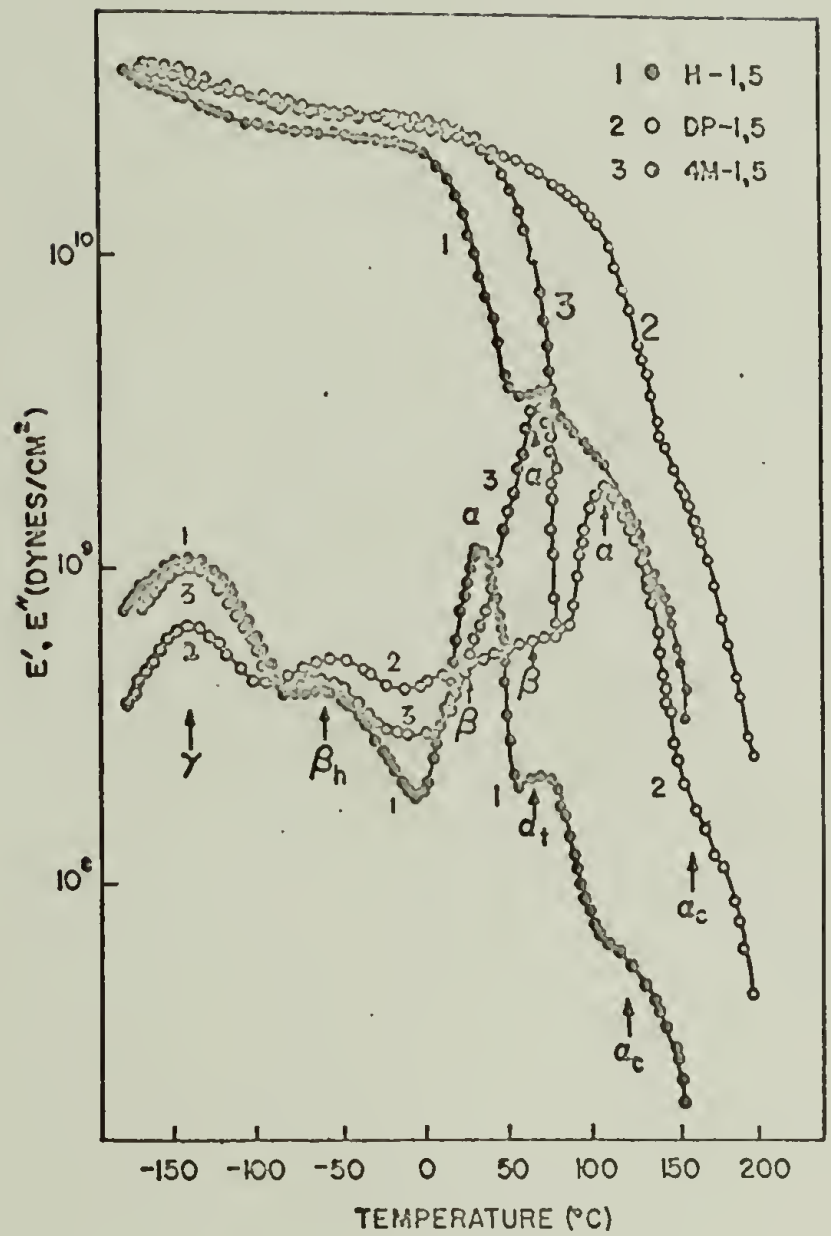
1 ● H-1,5
2 ○ DP-1,5
3 ○ 4M-1,5
E', E'' (DYNES/CM²)
10¹⁰
10⁹
10⁸
-150
-100
-50
0
50
100
150
200
TEMPERATURE (°C)
γ
βh
β
a
at
ac

Figure 24

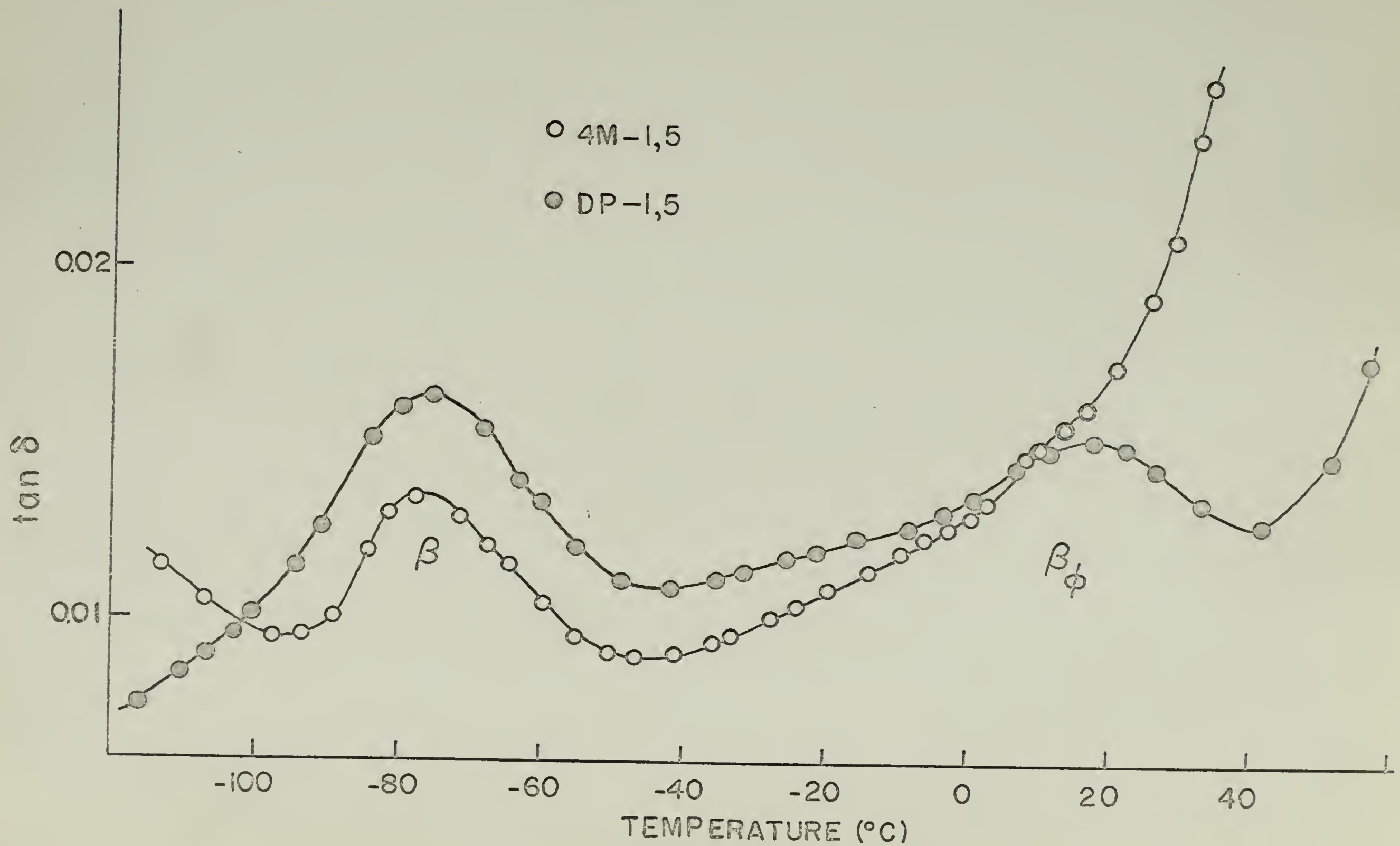

Figure 25

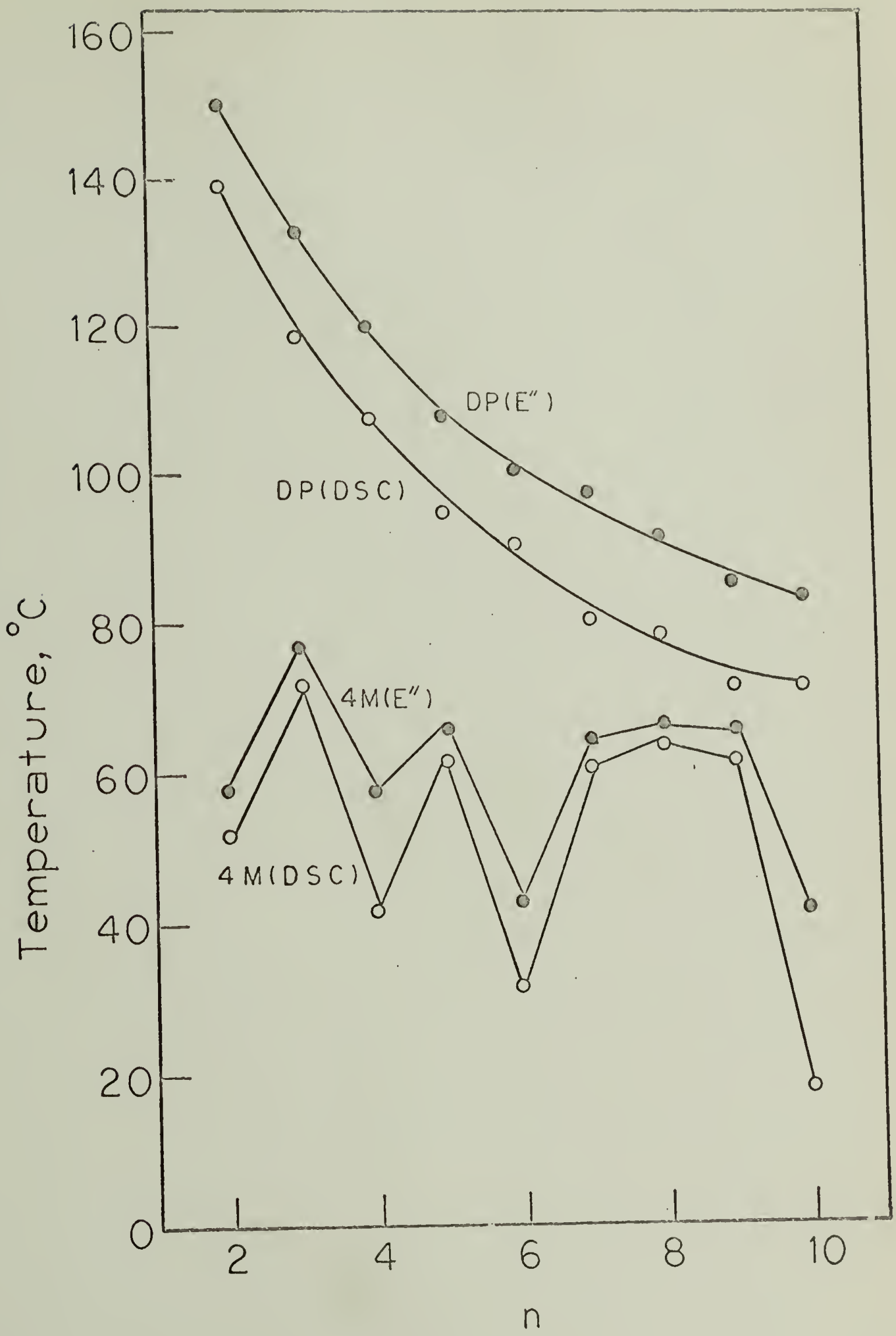
160
140
120
100
80
60
40
20
0
Temperature, °C
DP(E")
DP(DSC)
4M(E")
4M(DSC)
2
4
6
8
10
n

Figure 26

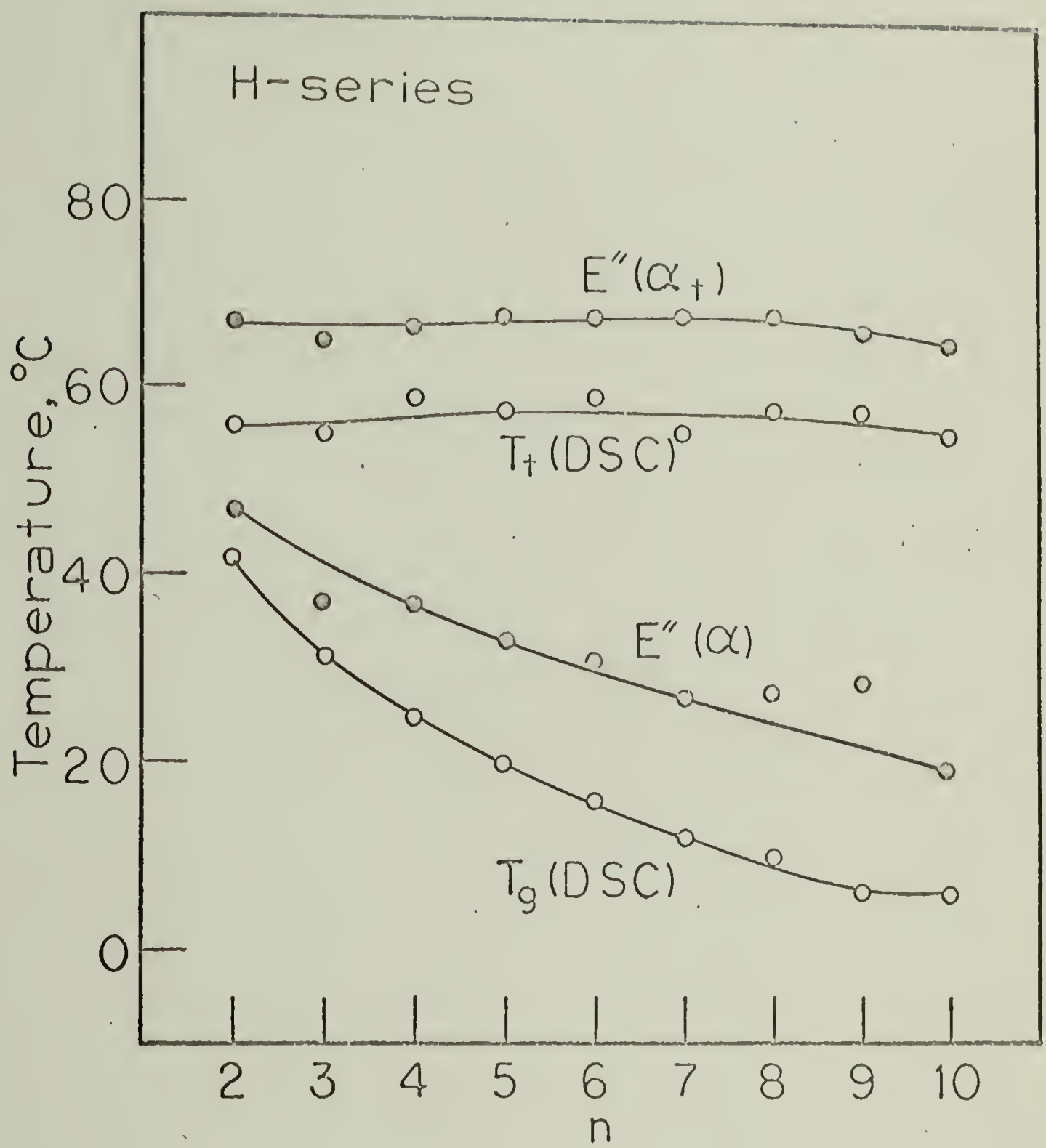
H-series
80
60
40
20
0
Temperature, °C
E″(α_t)
T_t (DSC)°
E″ (α)
T_g (DSC)
2
3
4
5
6
7
8
9
10
n

Figure 27

H-1.2 DSC

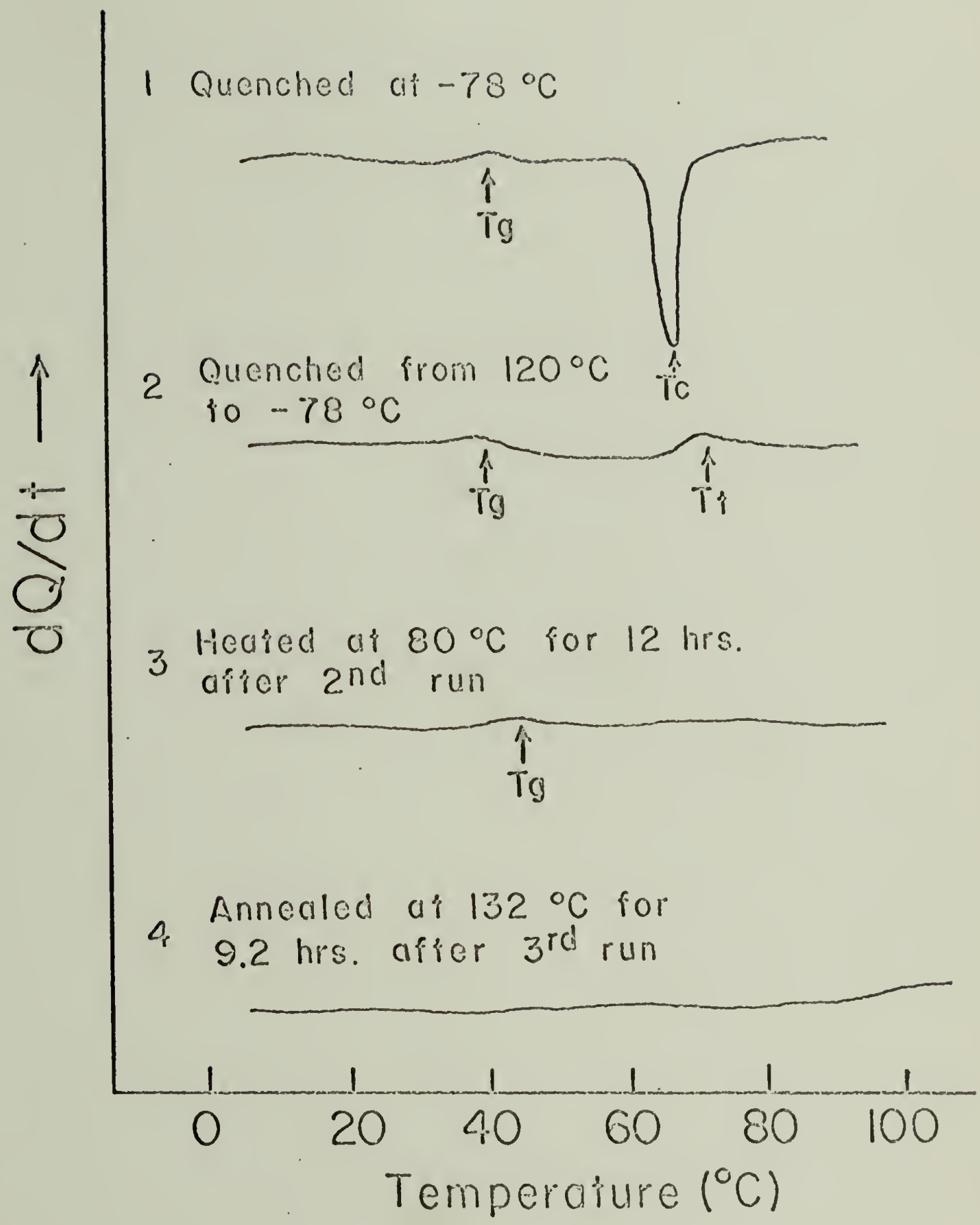

Figure 28

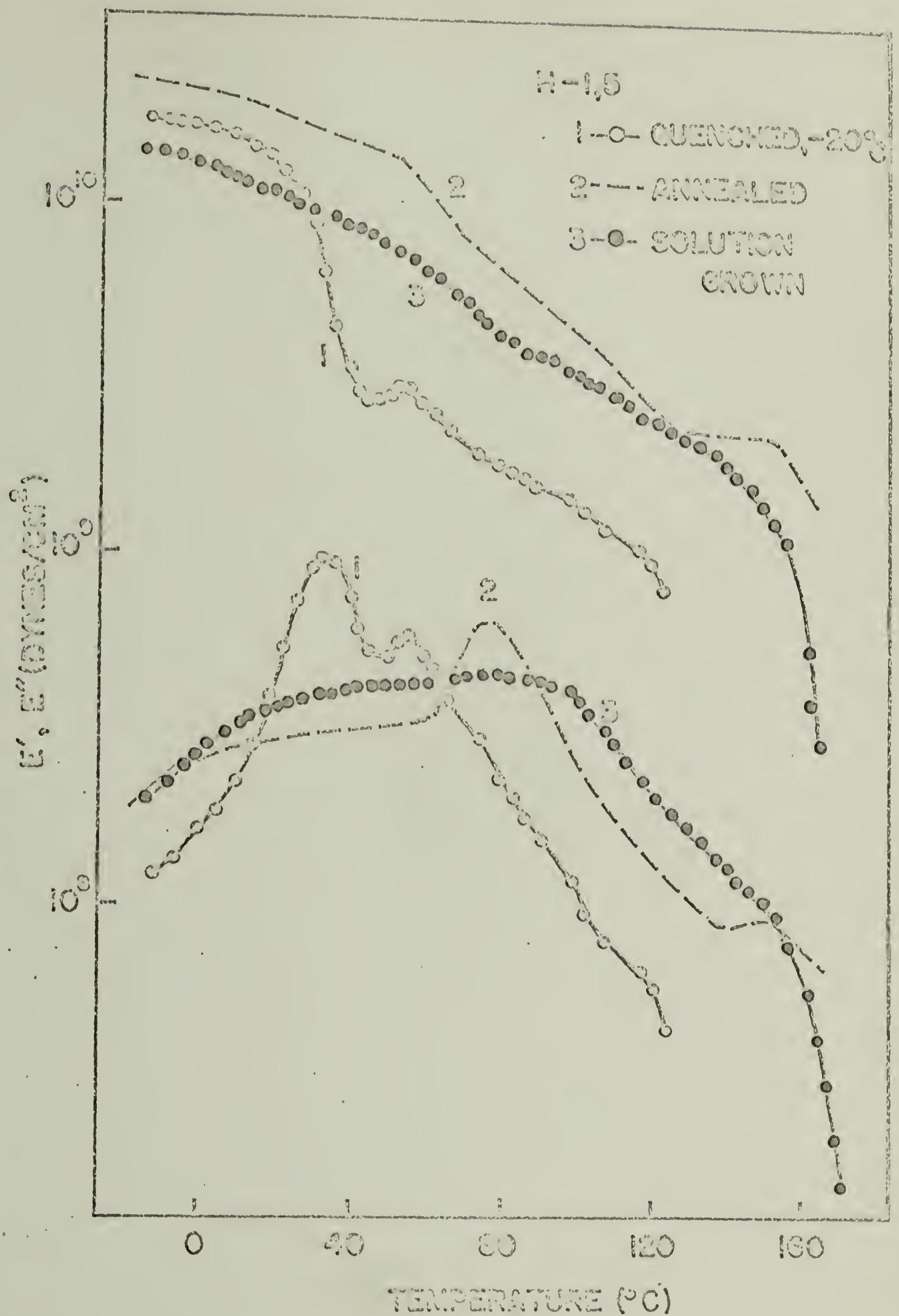
H=1.5
1-O- QUENCHED,-20°C
2-— - ANNEALED
3-O- SOLUTION GROWN
10^{10}
10^{9}
10^{8}
E', E'' (DYNES/CM²)
0
40
80
120
160
TEMPERATURE (°C)

Figure 29

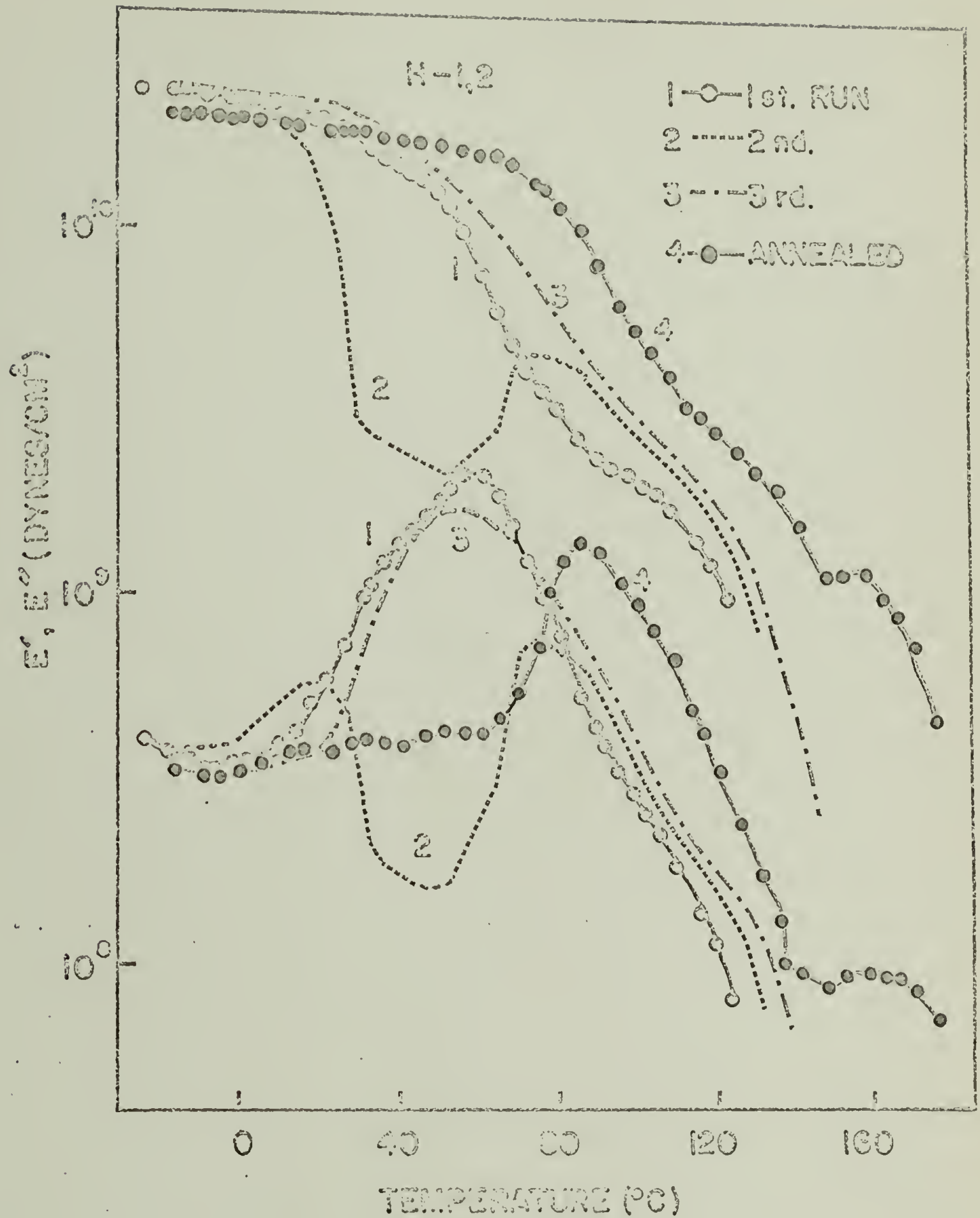
H-1,2
1—O—1st. RUN
2 ------2nd.
3 -·-·-3rd.
4-O—ANNEALED
10^0
10^0
10^0
E_J (DYNES/CM²)
0
40
80
120
160
TEMPERATURE (°C)

Figure 30

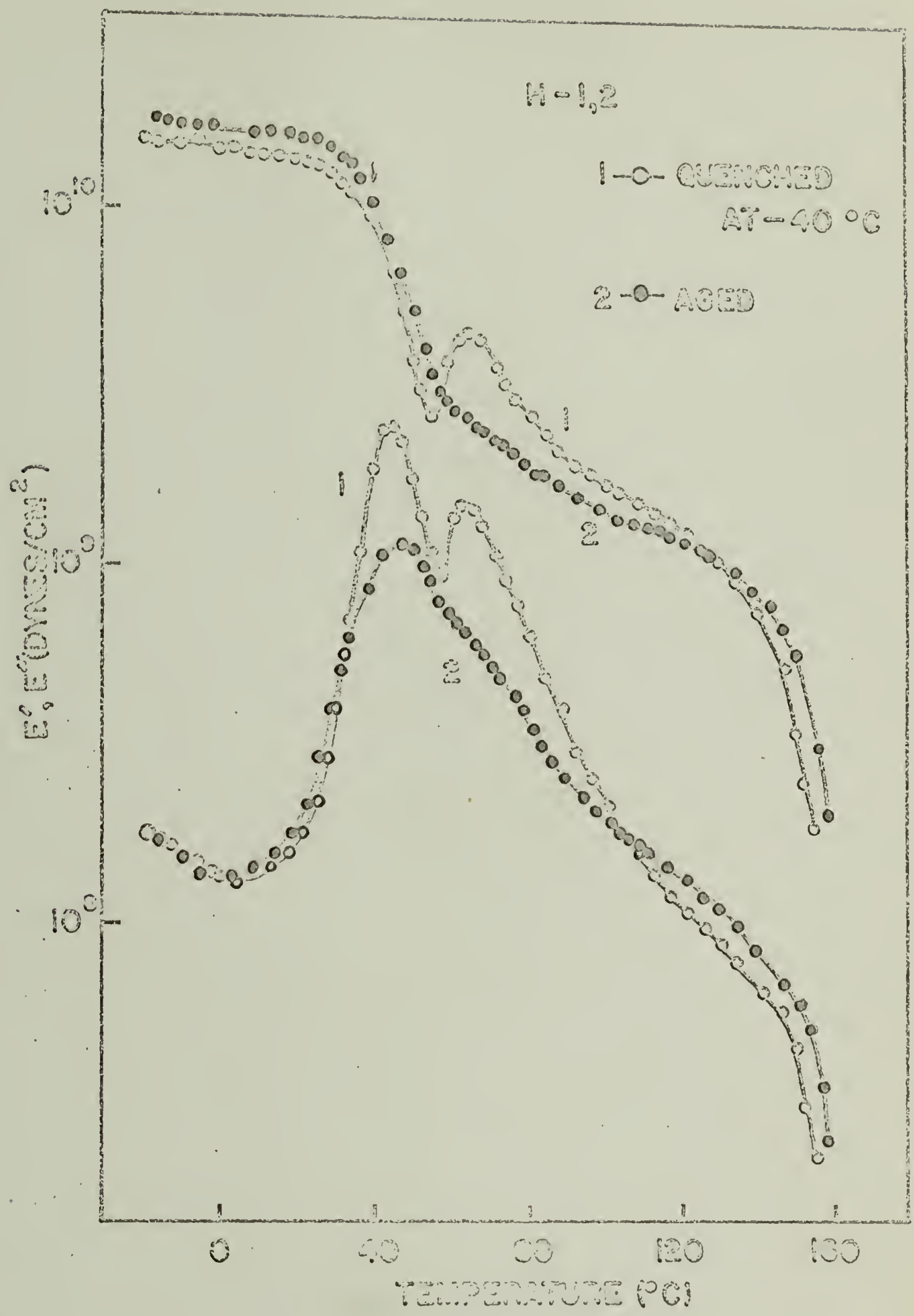
H-1,2
1-O- QUENCHED
AT-40 °C
2-O- AGED
10^{10}
10^{9}
10^{8}
E' (DYNES/CM^2)
0
40
80
120
160
TEMPERATURE (°C)

Figure 31

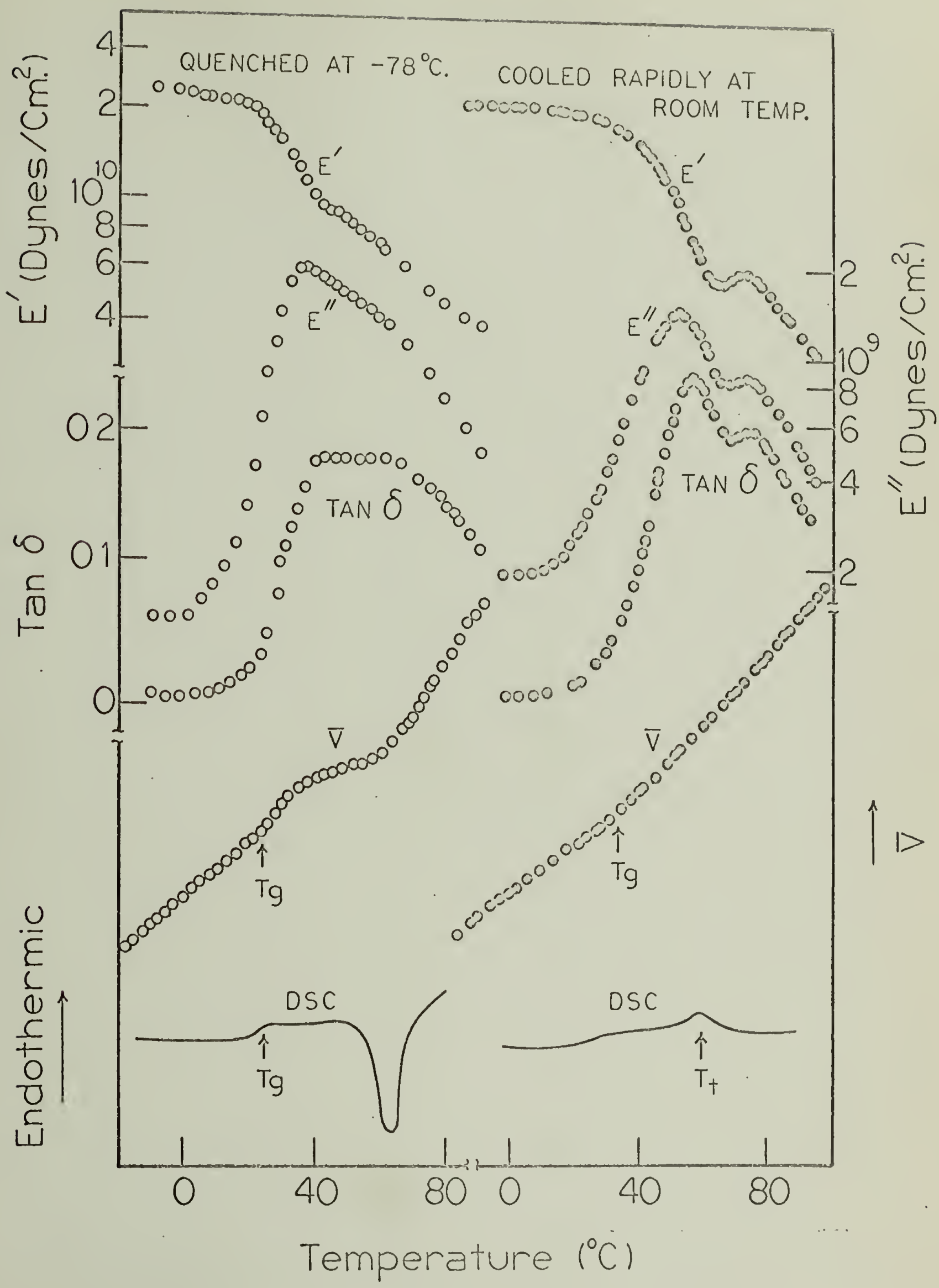
QUENCHED AT -78°C.
COOLED RAPIDLY AT ROOM TEMP.
E′ (Dynes/Cm.²)
E″ (Dynes/Cm.²)
Tan δ
E′
E″
TAN δ
V̄
Tg
DSC
Tg
Tf
Endothermic
0
40
80
Temperature (°C)

Figure 32

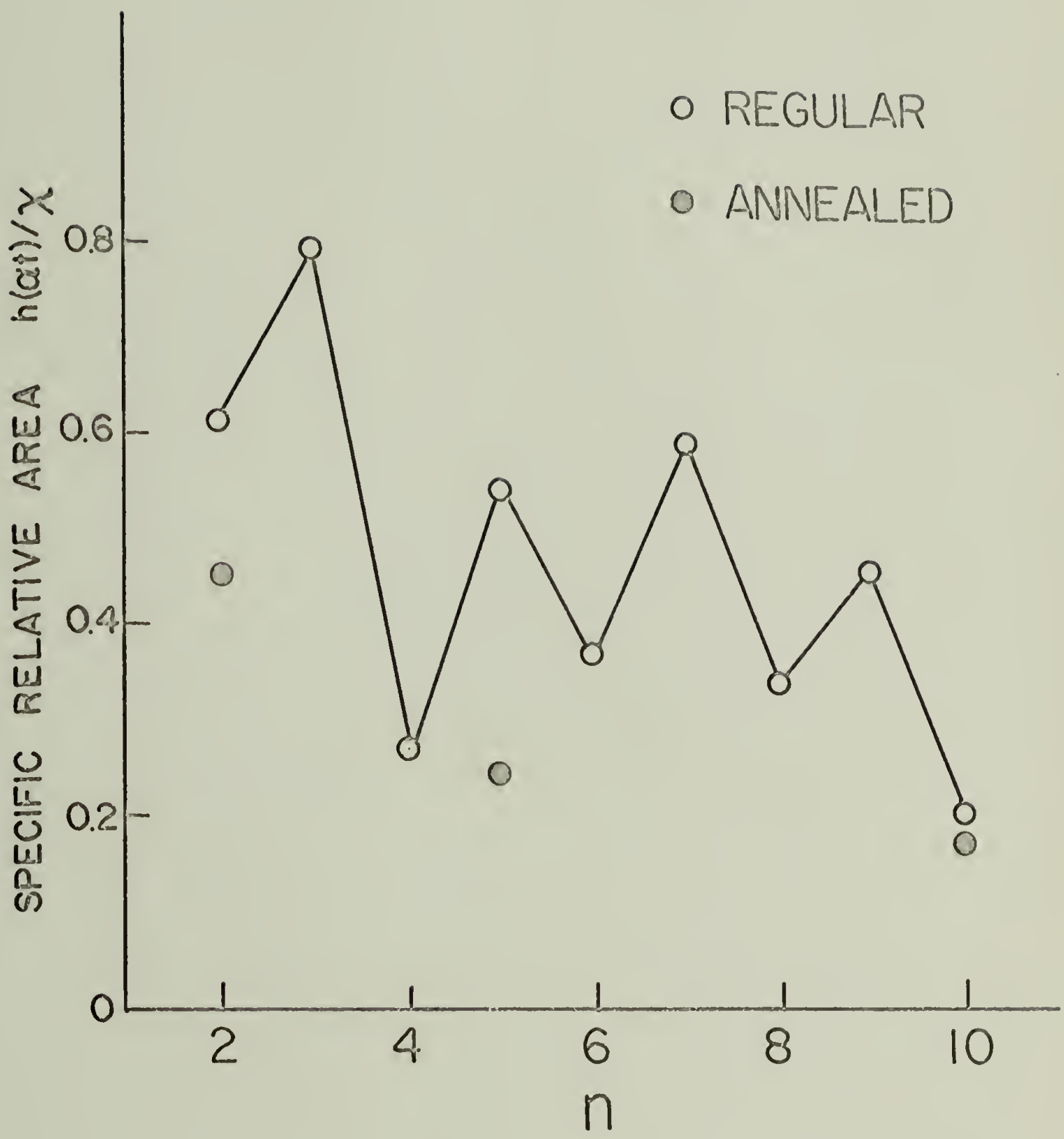
REGULAR
ANNEALED
SPECIFIC RELATIVE AREA h(αt)/χ
0.8
0.6
0.4
0.2
0
2
4
6
8
10
n

Figure 33

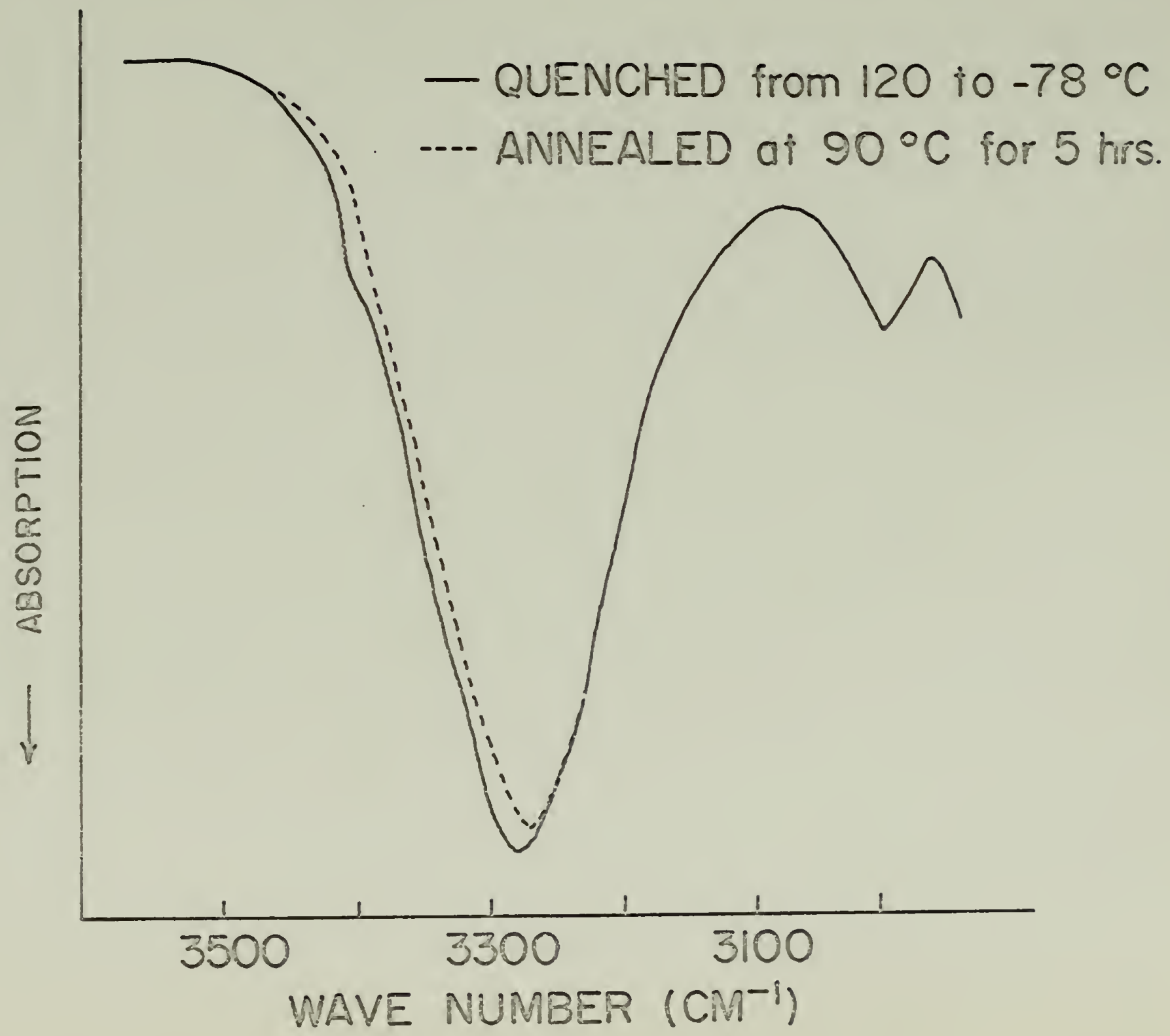
— QUENCHED from 120 to -78 °C
---- ANNEALED at 90 °C for 5 hrs.
ABSORPTION
3500
3300
3100
WAVE NUMBER (CM⁻¹)

Figure 34

THEORETICAL
EXPERIMENTAL
FIBER PERIOD (Å)
50
40
30
20
10
2
3
4
5
6
7
8
9
10
n

Figure 35

H-1.2

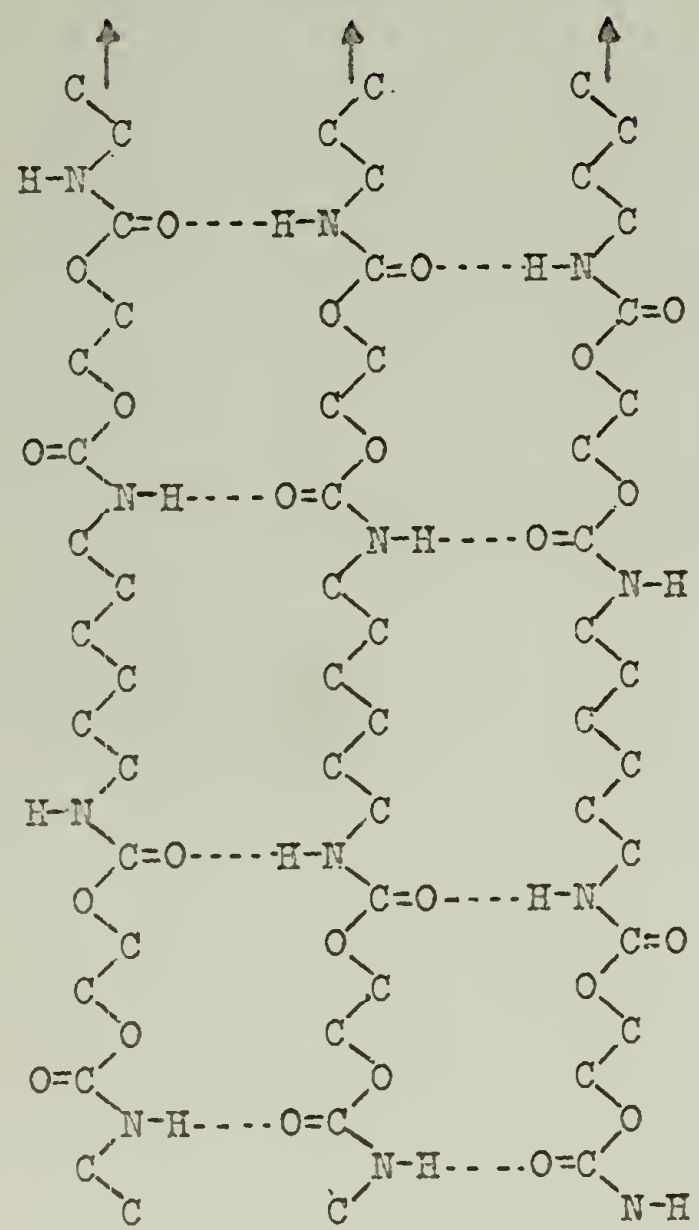

H-1.4

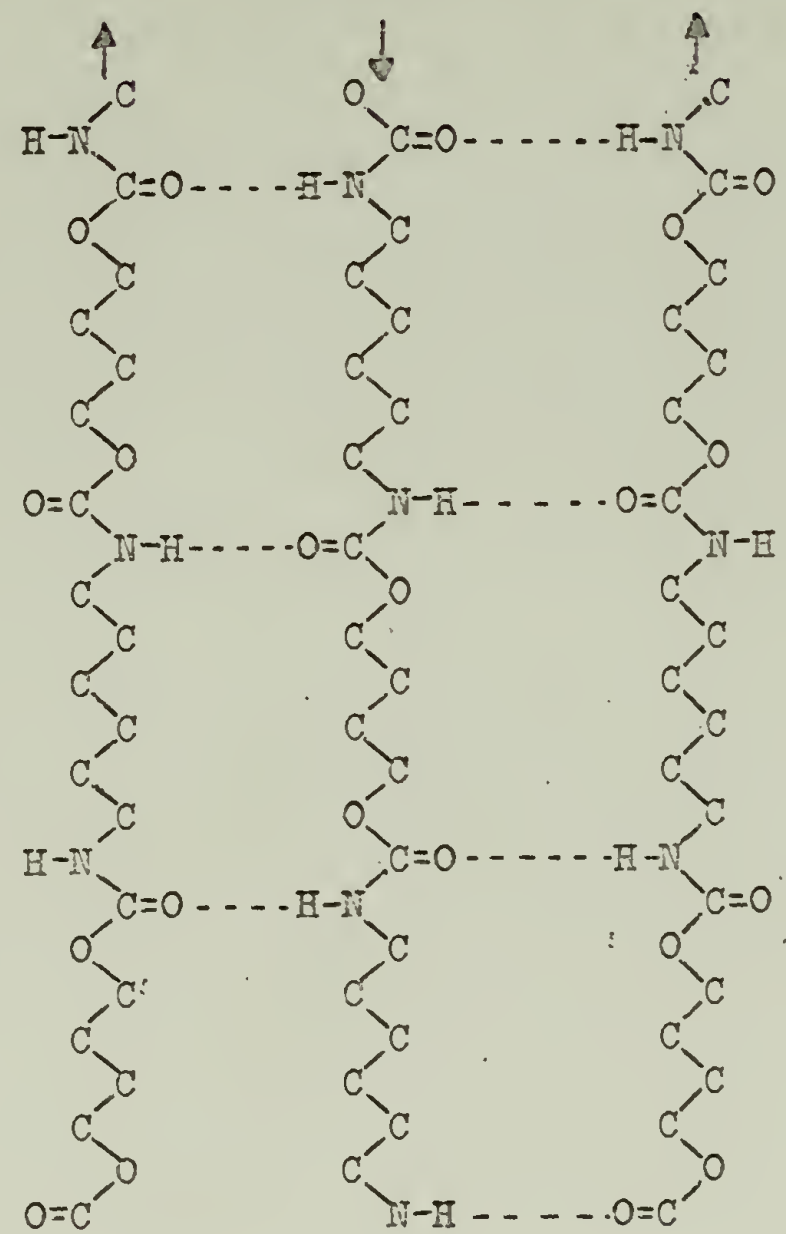

H-1.3

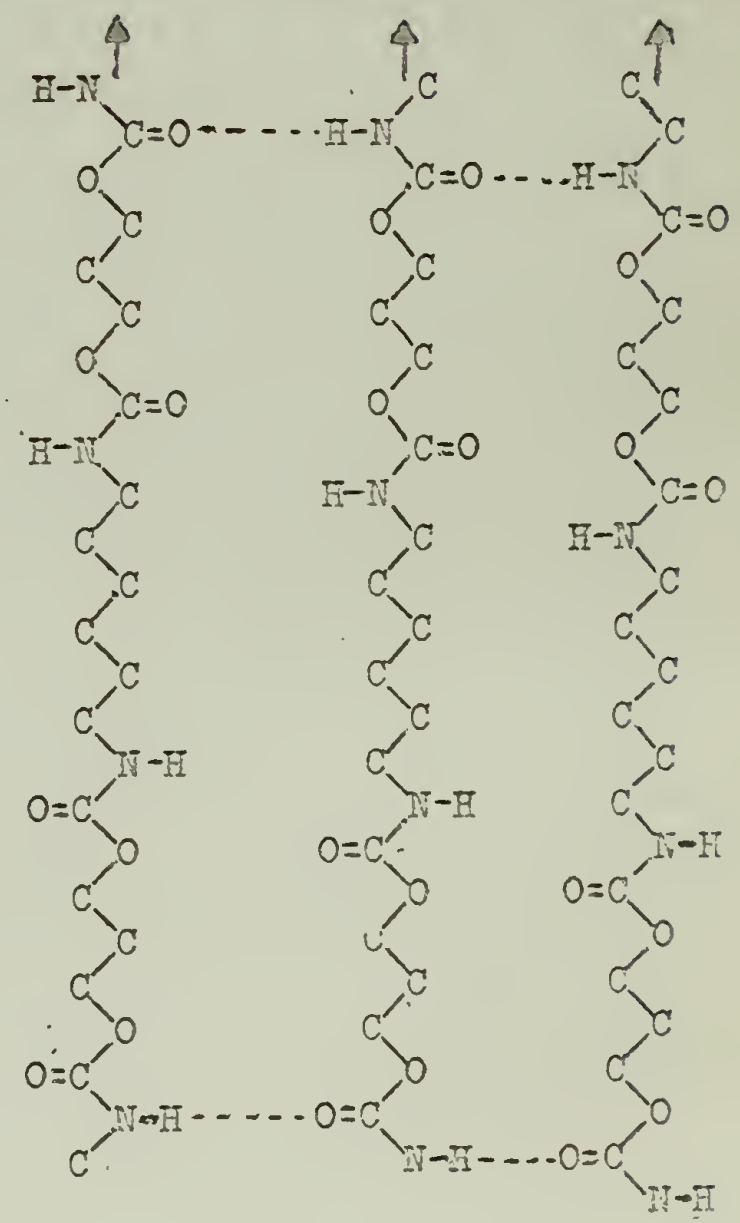

	α	β	γ
	antiparallel	paralell	parallel
n even	not perfect	perfect	perfect
1,4 1,10	perfect	perfect	perfect
n, odd	not perfect	not perfect	perfect

Figure 36

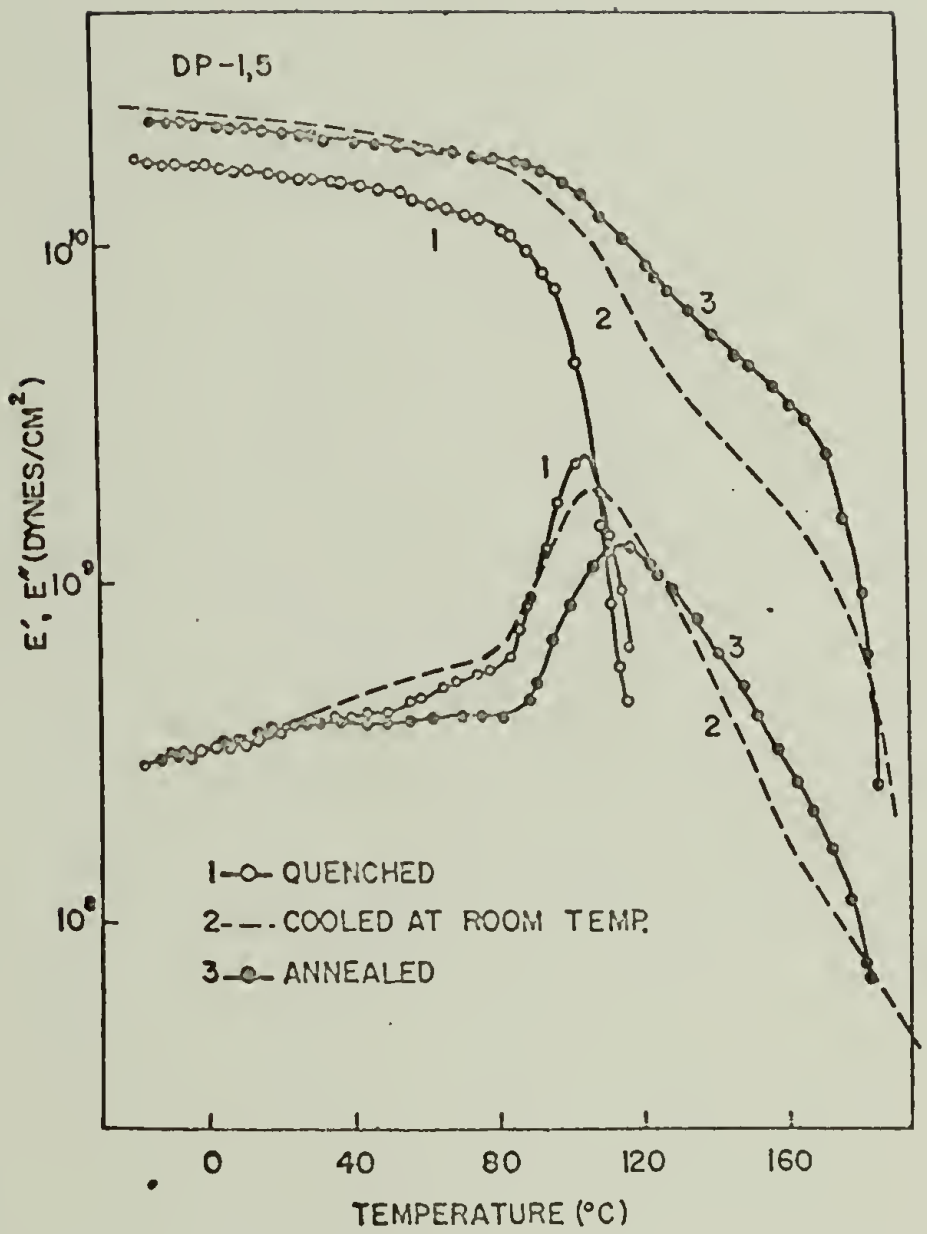
DP-1,5
E', E'' (DYNES/CM²)
10¹⁰
10⁹
10⁸
1
2
3
1
3
2
1—o— QUENCHED
2- — - COOLED AT ROOM TEMP.
3—o— ANNEALED
0
40
80
120
160
TEMPERATURE (°C)

Figure 37

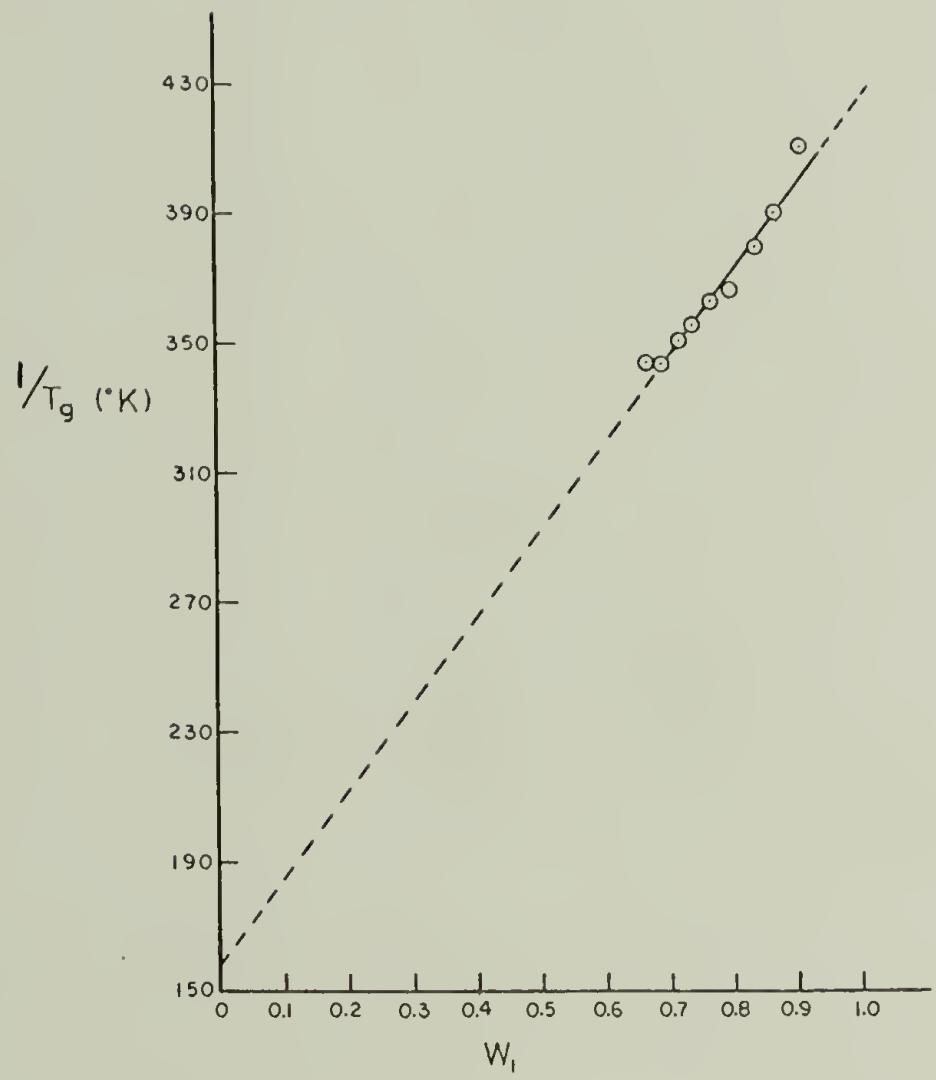
430
390
350
310
270
230
190
150
1/Tg (°K)
0
0.1
0.2
0.3
0.4
0.5
0.6
0.7
0.8
0.9
1.0
W1

Figure 38

H-1,2

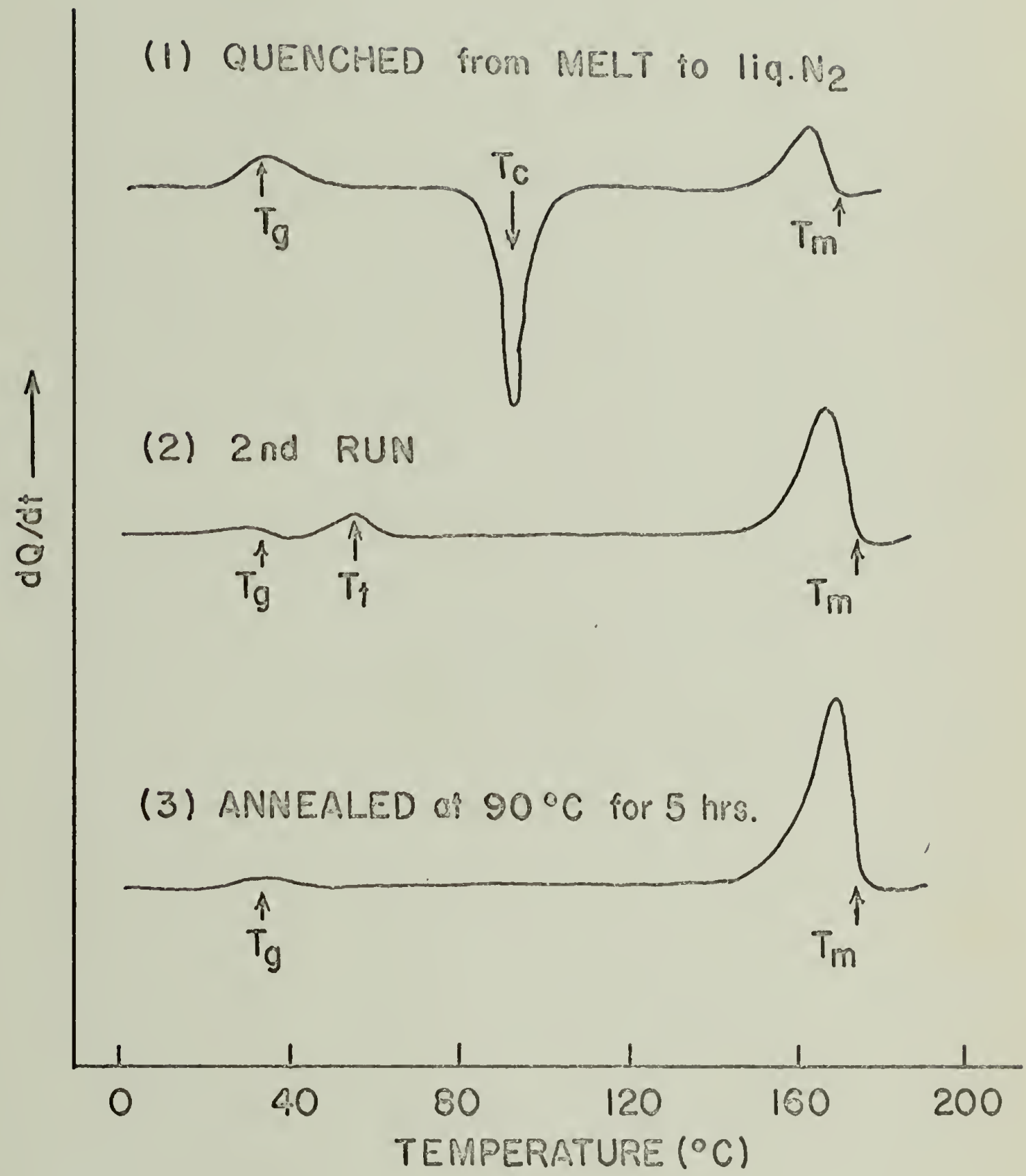

Figure 39

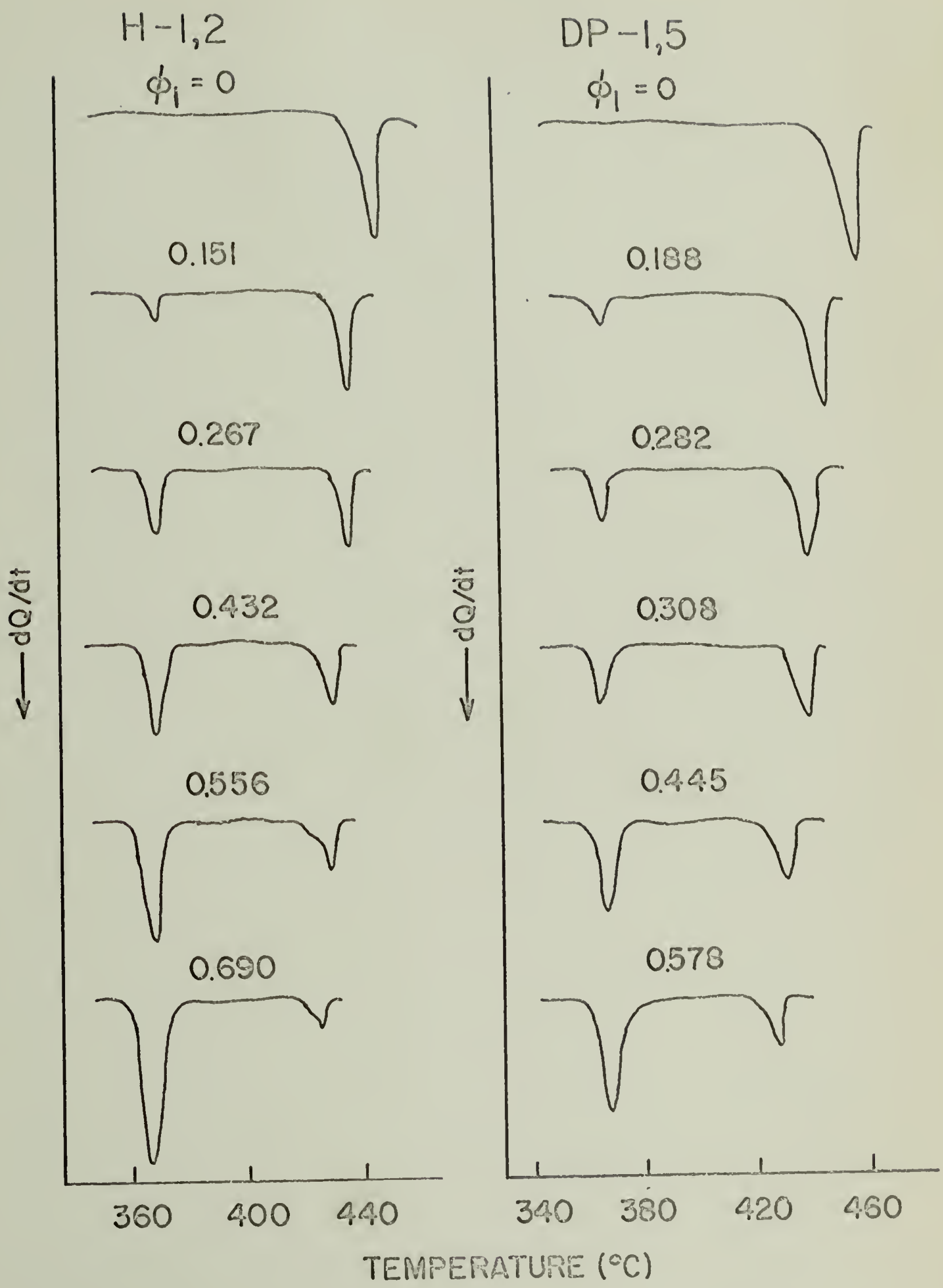
H-1,2
$\phi_1 = 0$
0.151
0.267
0.432
0.556
0.690
dQ/dt
360
400
440
DP-1,5
$\phi_1 = 0$
0.188
0.282
0.308
0.445
0.578
dQ/dt
340
380
420
460
TEMPERATURE (°C)

Figure 40

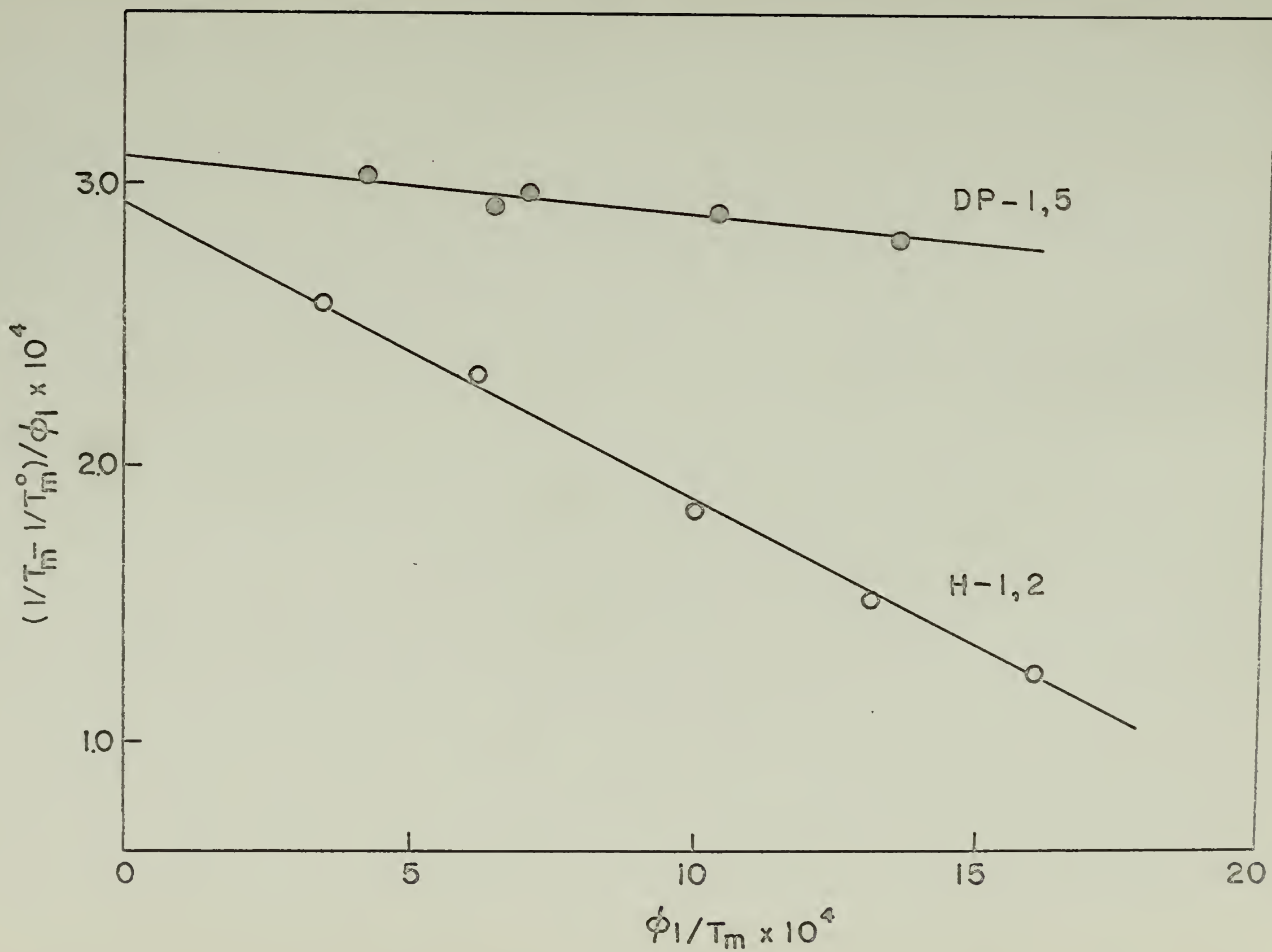
3.0
2.0
1.0
0
5
10
15
20
DP-1,5
H-1,2
$(1/T_m - 1/T_m^\circ)/\phi_1 \times 10^4$
$\phi_1/T_m \times 10^4$

Figure 41

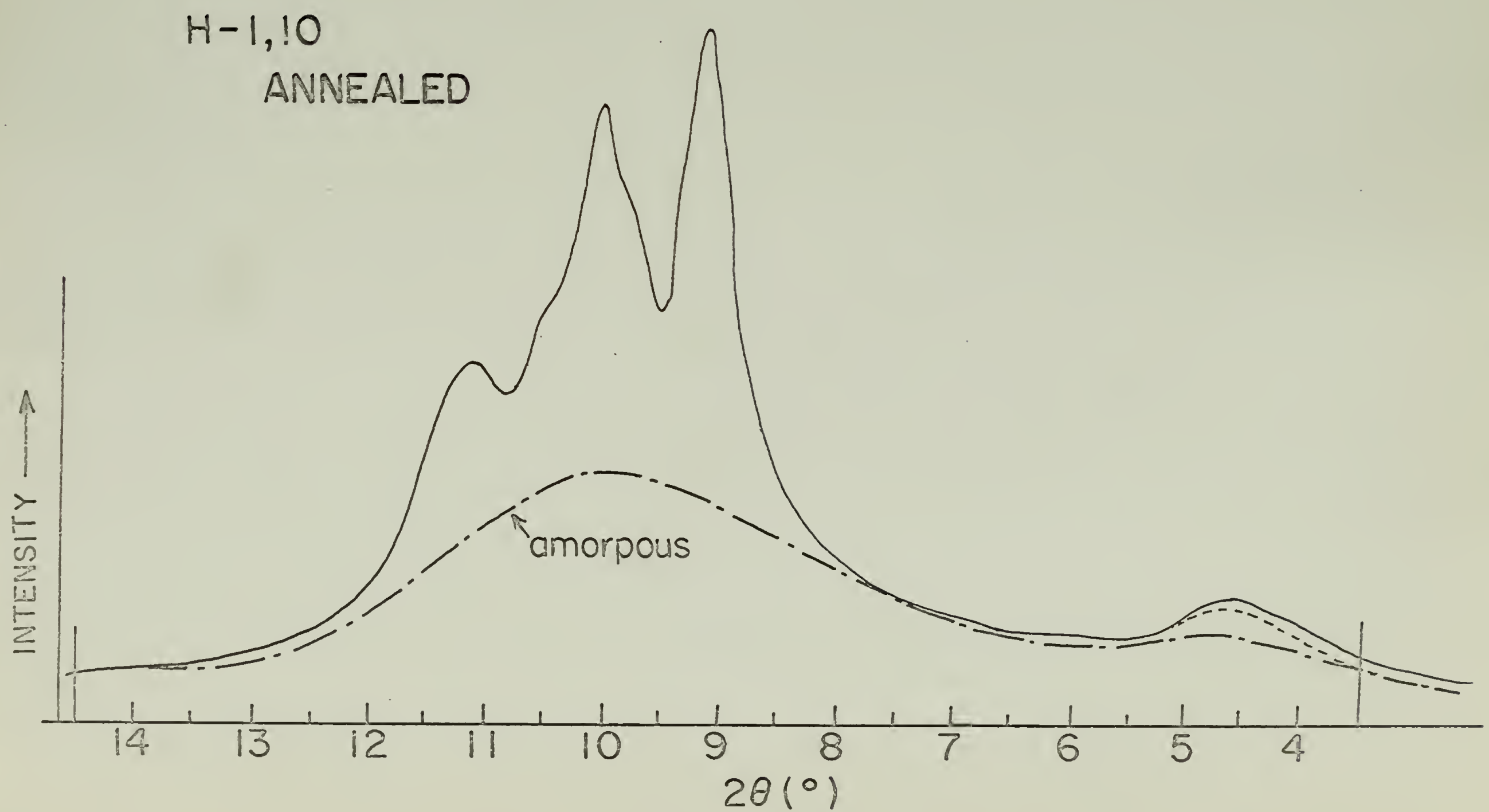

Figure 42

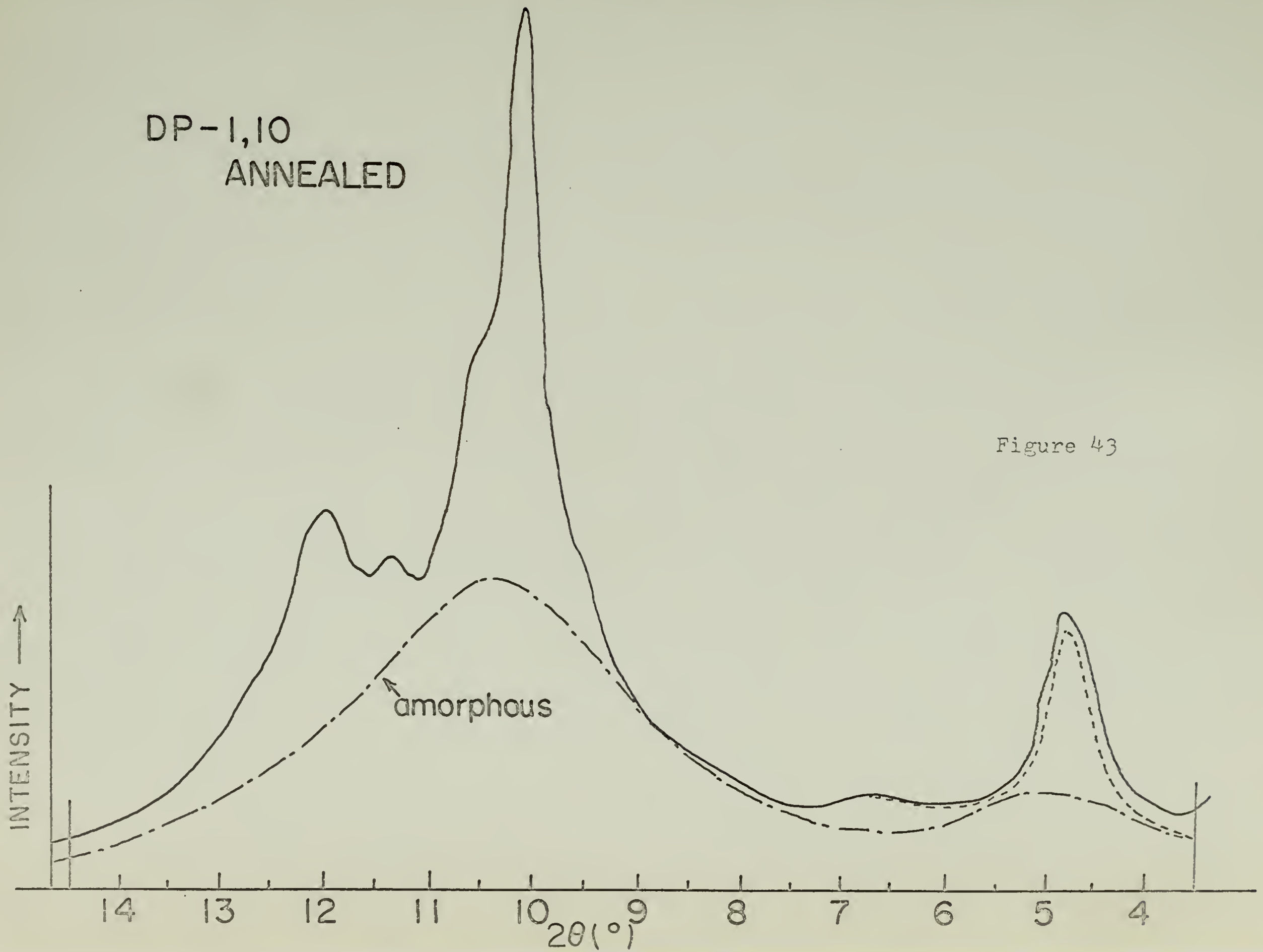

Figure 43

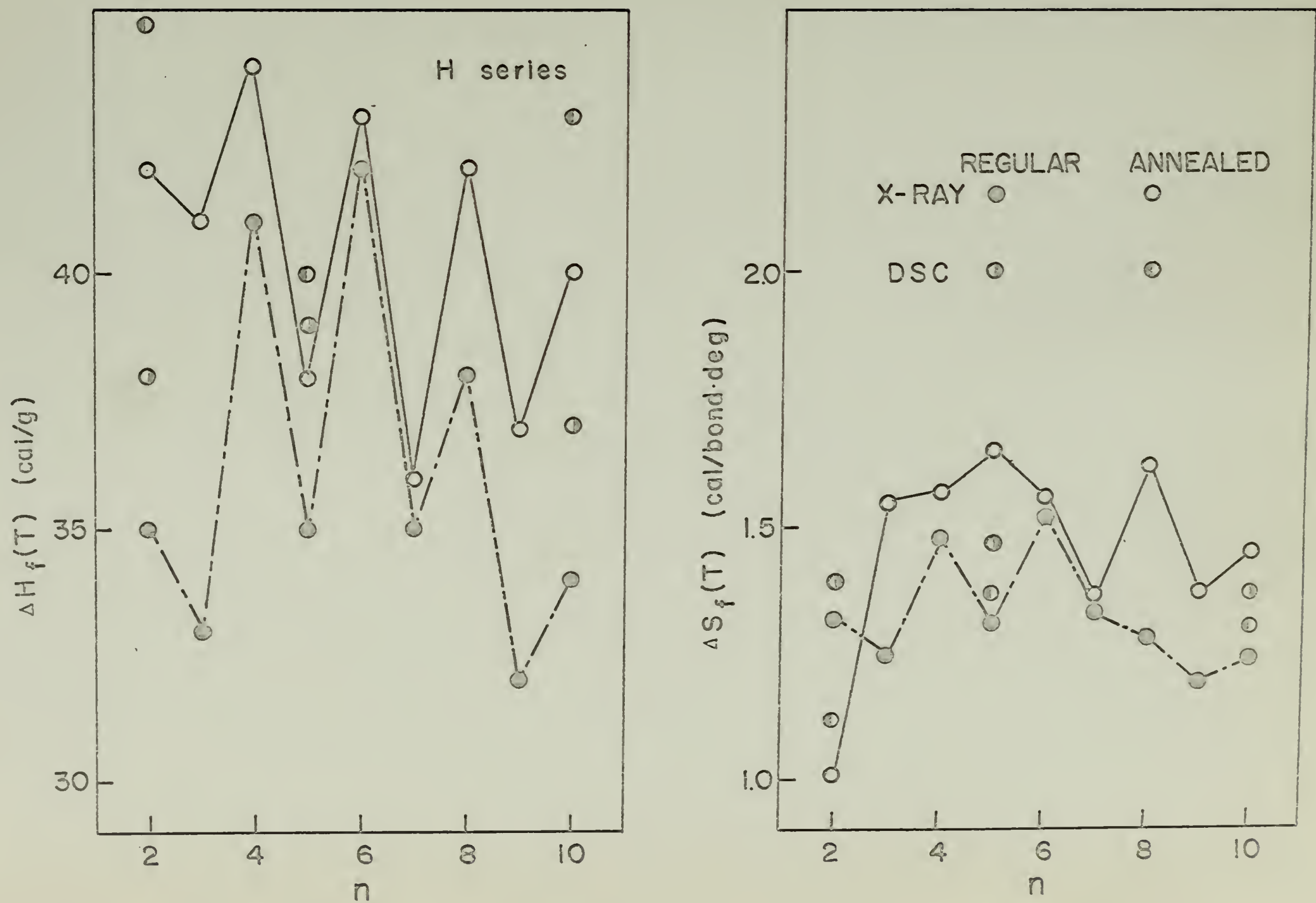
H series
40
35
30
$\Delta H_f(T)$ (cal/g)
2
4
6
8
10
n
REGULAR
ANNEALED
X-RAY
DSC
2.0
1.5
1.0
$\Delta S_f(T)$ (cal/bond·deg)
2
4
6
8
10
n

Figure 44

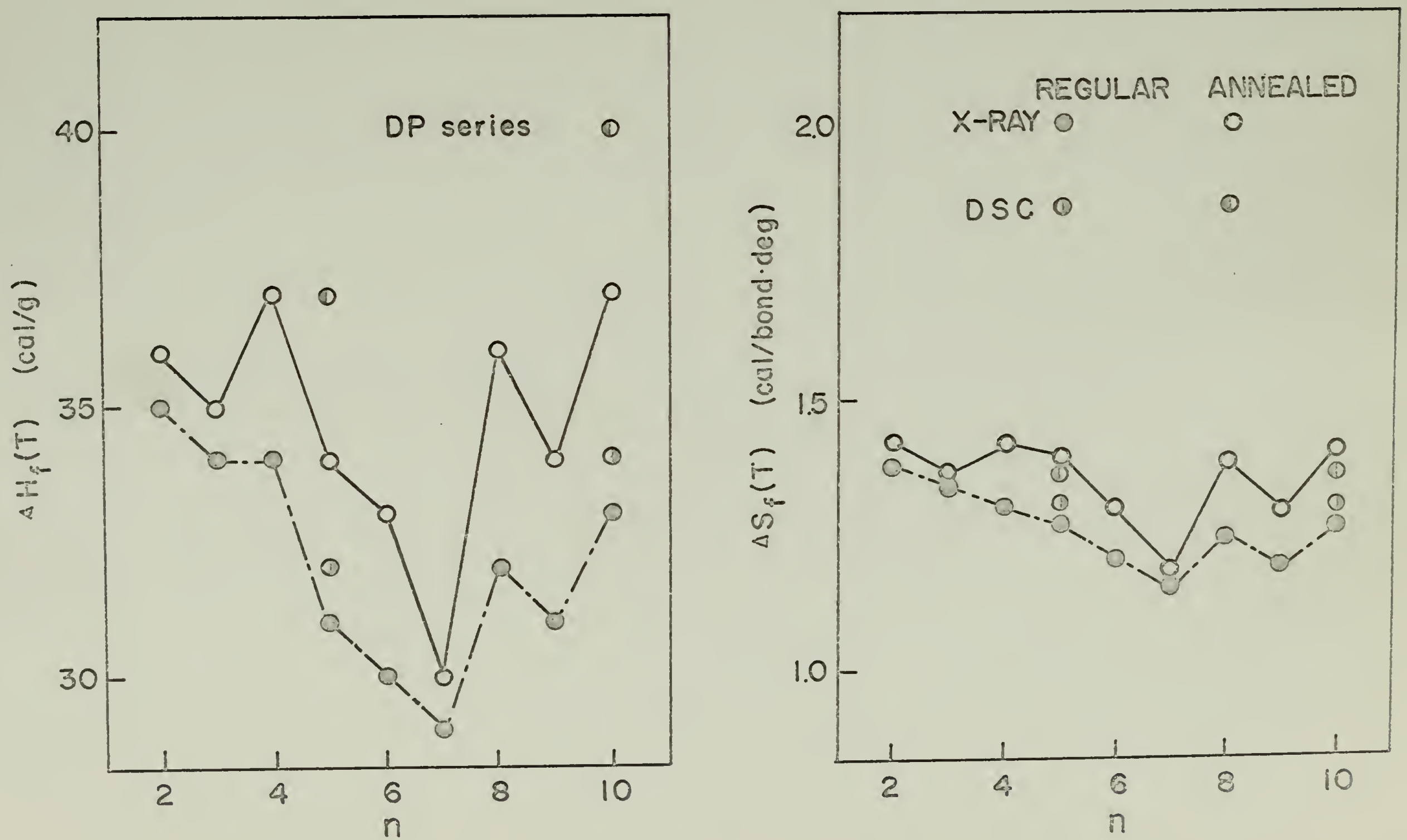
DP series
40
35
30
$\Delta H_f(T)$ (cal/g)
2
4
6
8
10
n
REGULAR
ANNEALED
X-RAY
DSC
2.0
1.5
1.0
$\Delta S_f(T)$ (cal/bond·deg)
2
4
6
8
10
n

Figure 45

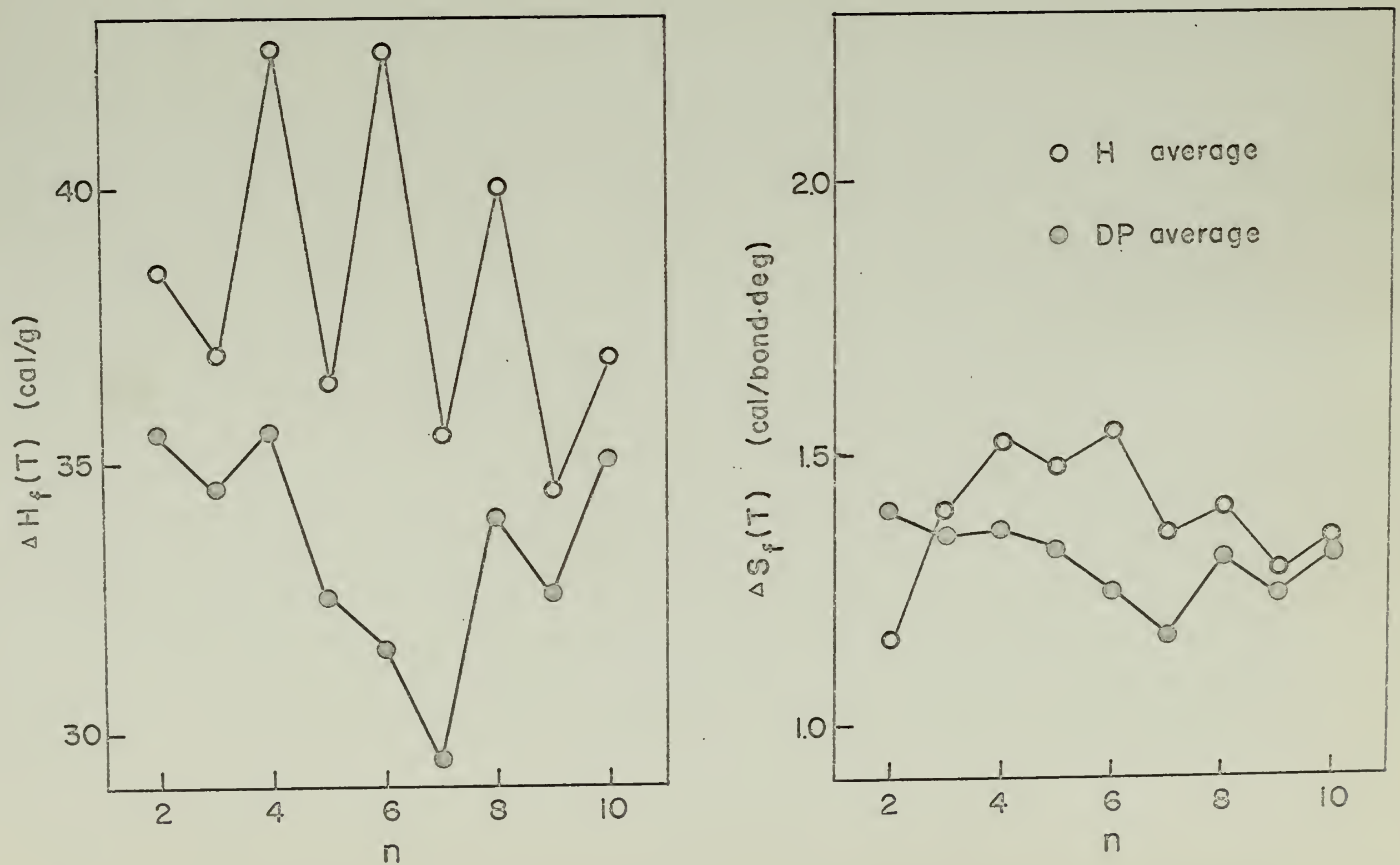
40
35
30
$\Delta H_f(T)$ (cal/g)
2
4
6
8
10
n
2.0
1.5
1.0
$\Delta S_f(T)$ (cal/bond·deg)
H average
DP average
2
4
6
8
10
n

Figure 46

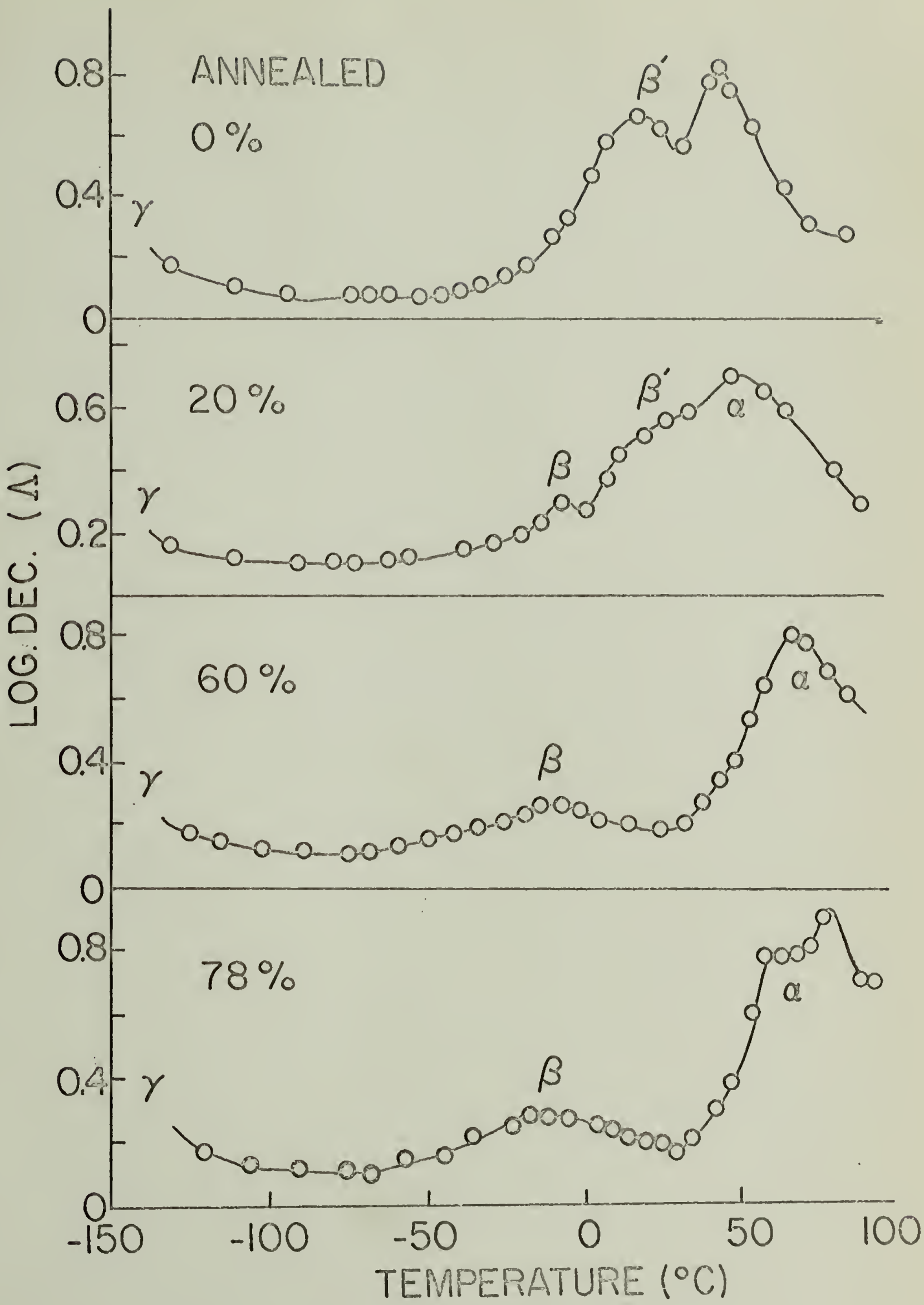
ANNEALED
0 %
20 %
60 %
78 %
LOG. DEC. (Λ)
TEMPERATURE (°C)
0.8
0.4
0
0.6
0.2
-150
-100
-50
0
50
100
γ
β
β'
α

Figure 47

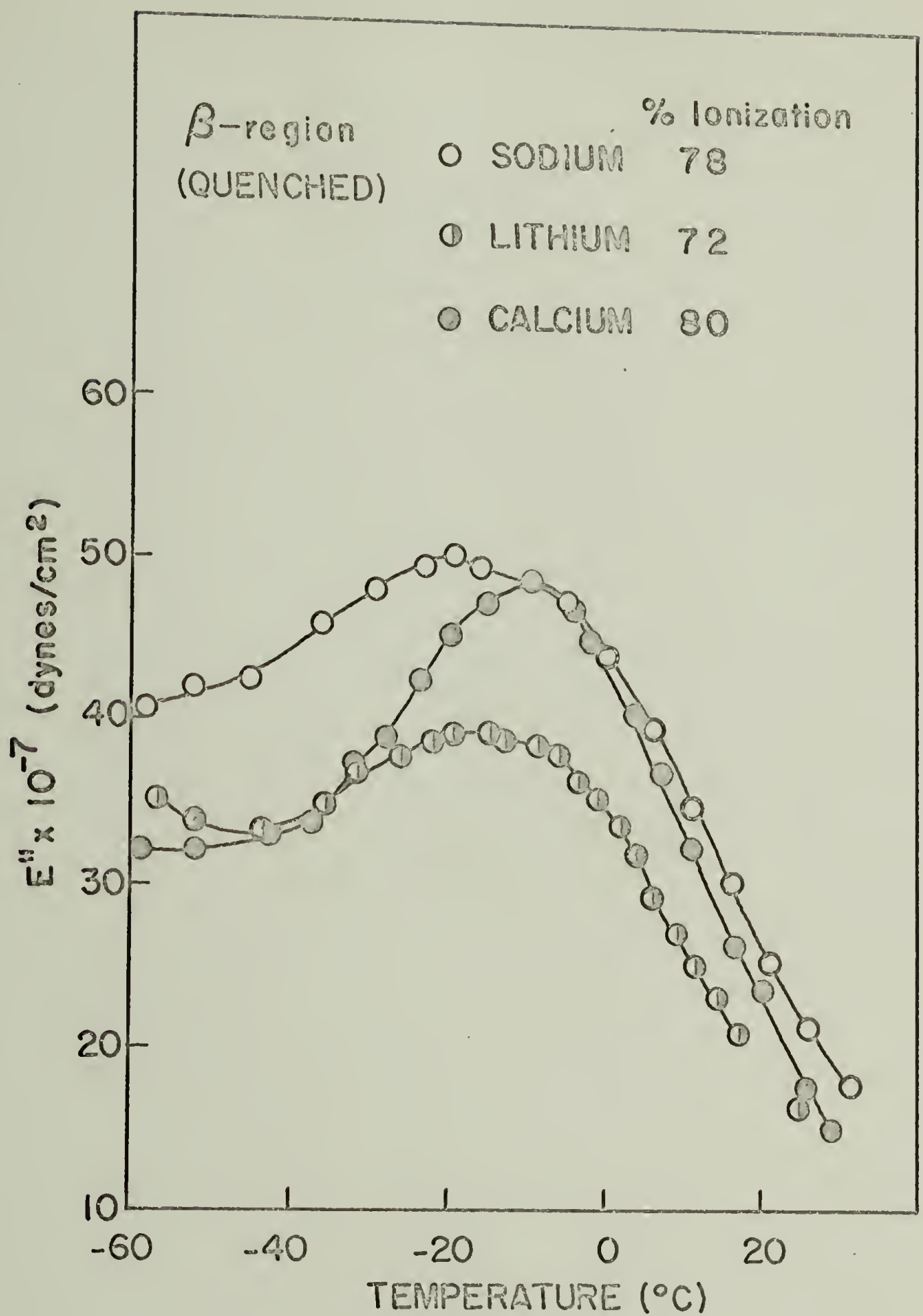
β-region
(QUENCHED)
% Ionization
SODIUM 78
LITHIUM 72
CALCIUM 80
E'' x 10^-7 (dynes/cm^2)
60
50
40
30
20
10
-60
-40
-20
0
20
TEMPERATURE (°C)

Figure 48

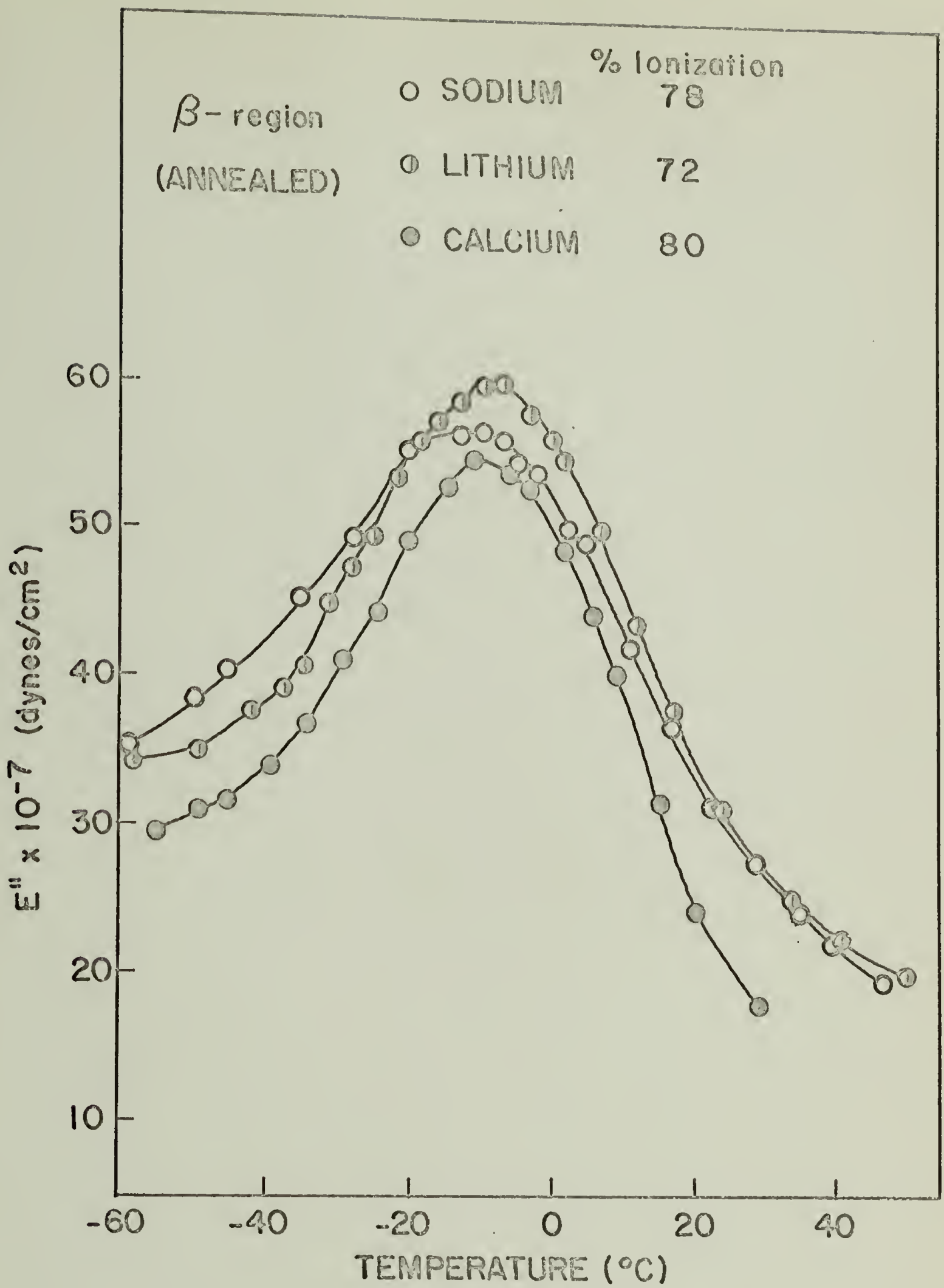
β- region
(ANNEALED)
% Ionization
SODIUM 78
LITHIUM 72
CALCIUM 80
60
50
40
30
20
10
E'' x 10^-7 (dynes/cm^2)
-60
-40
-20
0
20
40
TEMPERATURE (°C)

Figure 49

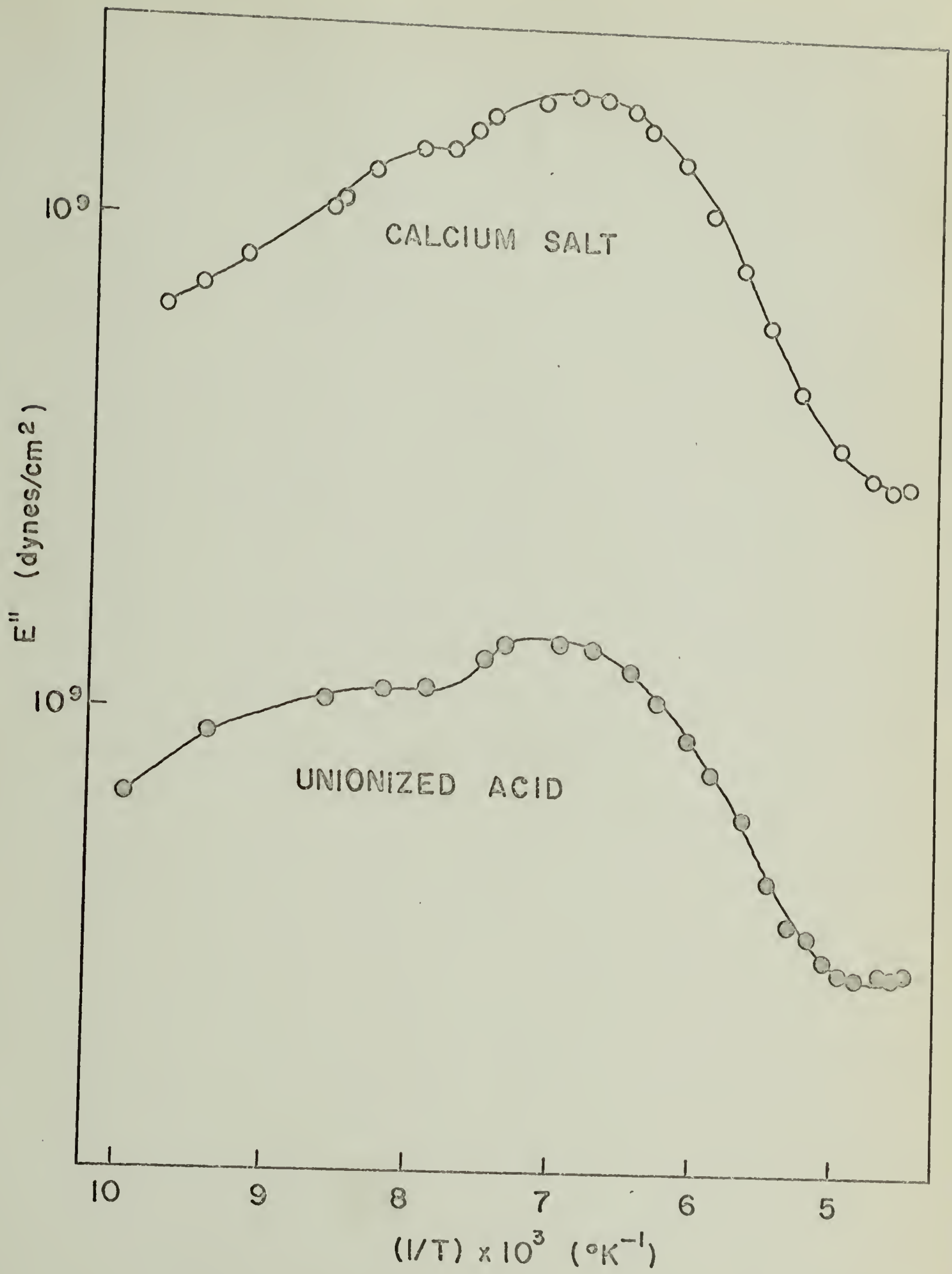
CALCIUM SALT
UNIONIZED ACID
10^9
10^9
E'' (dynes/cm^2)
10
9
8
7
6
5
(1/T) x 10^3 (°K^{-1})

Figure 50

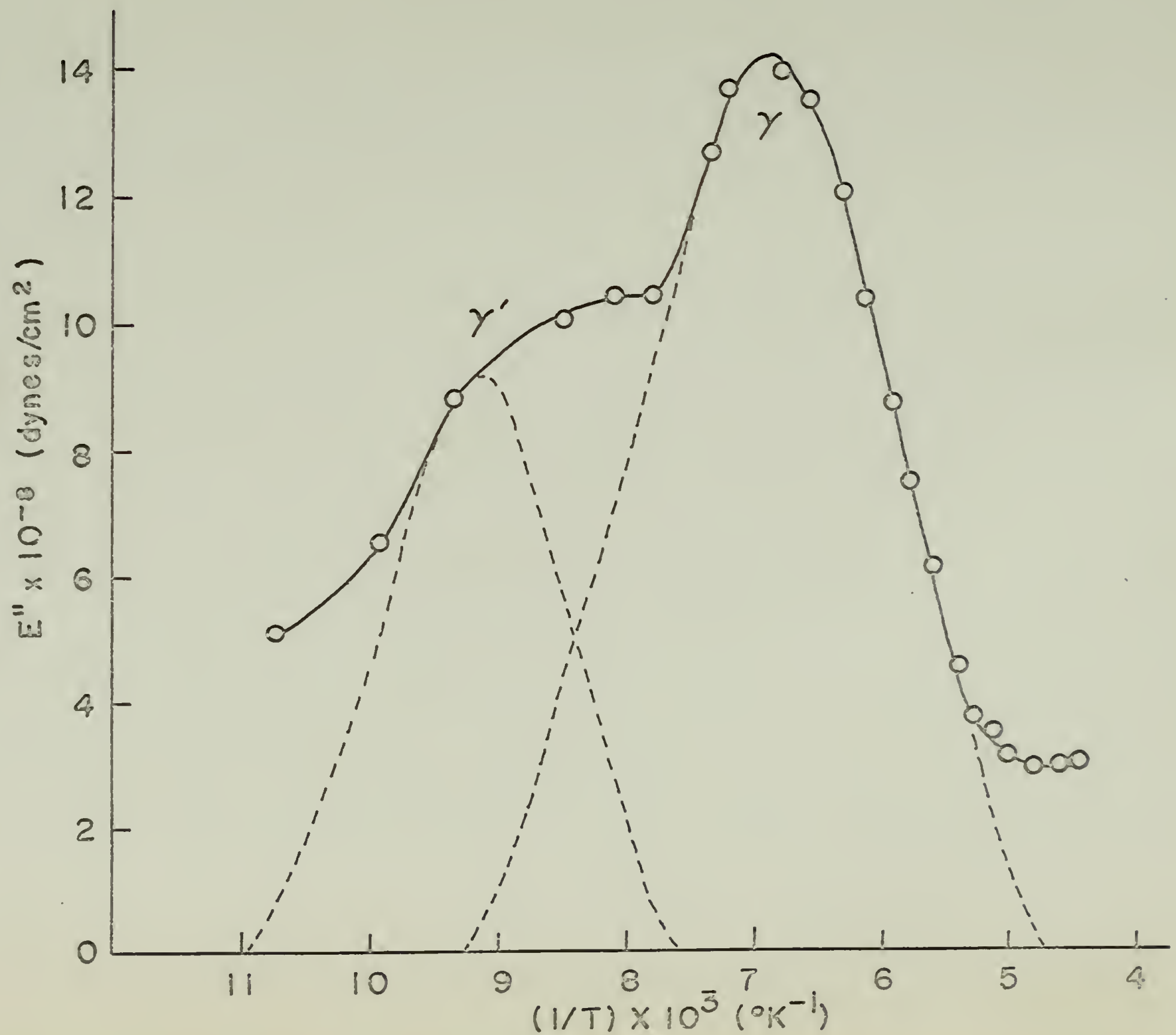

Figure 51

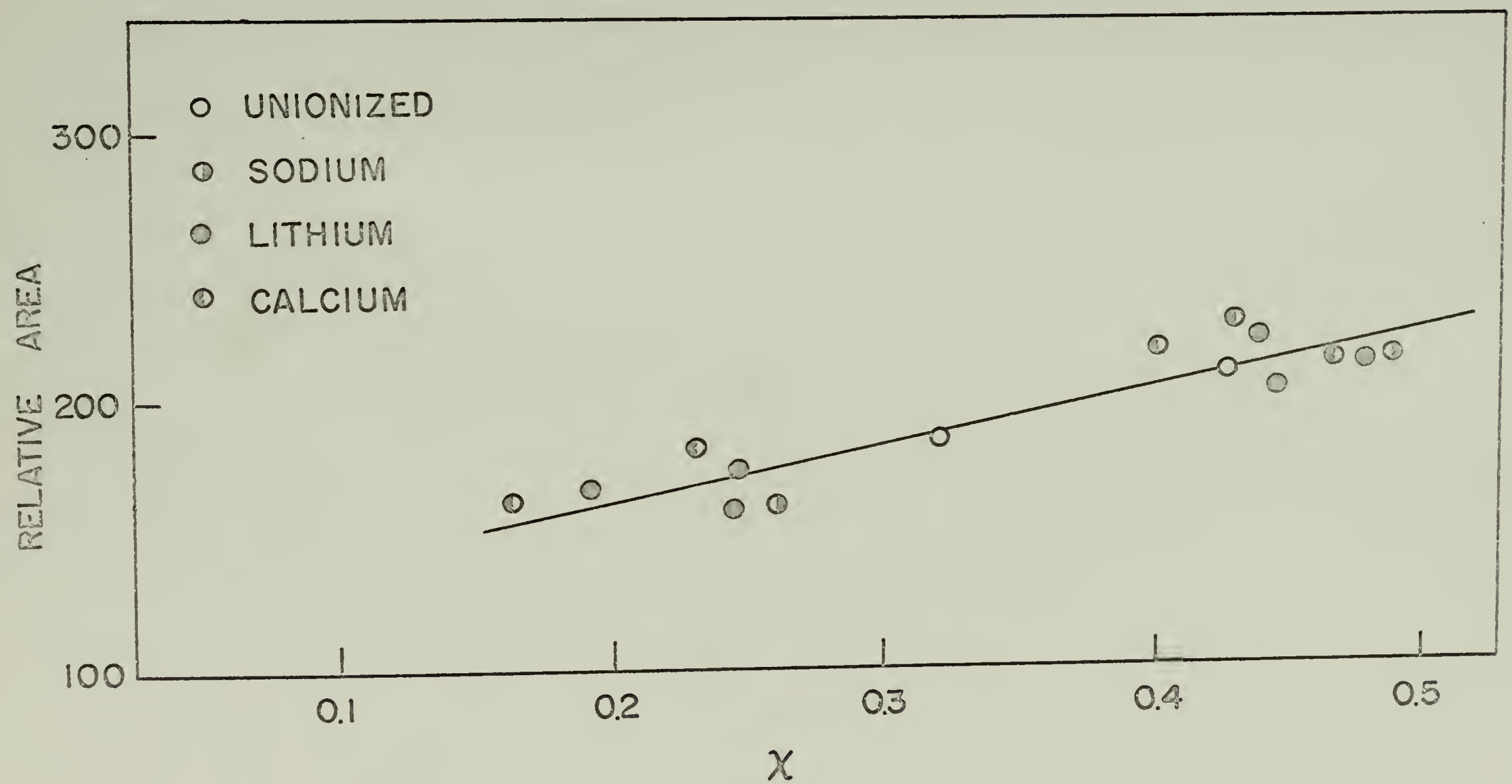
UNIONIZED
SODIUM
LITHIUM
CALCIUM
RELATIVE AREA
300
200
100
0.1
0.2
0.3
0.4
0.5
X

Figure 52

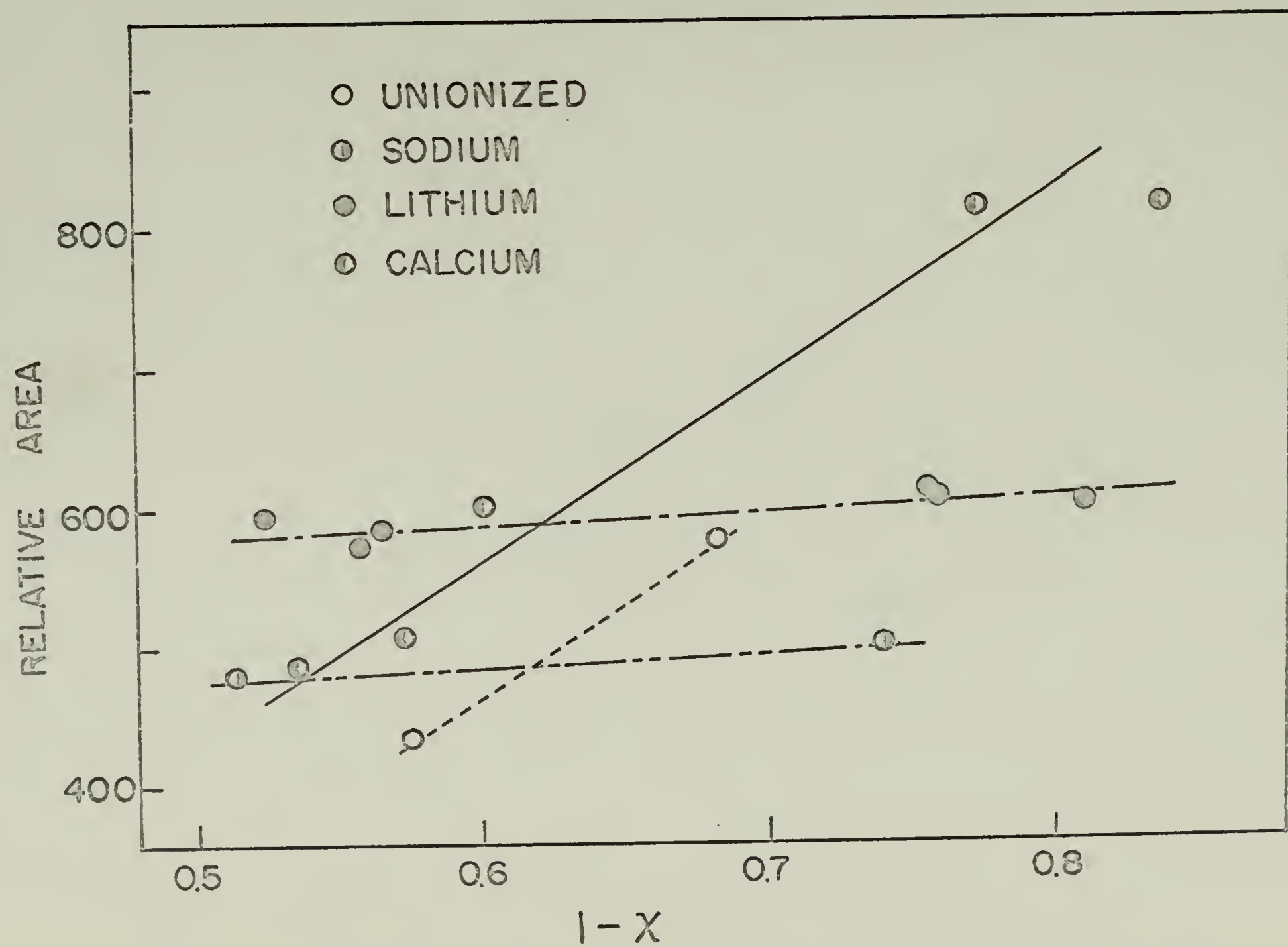
UNIONIZED
SODIUM
LITHIUM
CALCIUM
800
600
400
RELATIVE AREA
0.5
0.6
0.7
0.8
1 - X

Figure 53

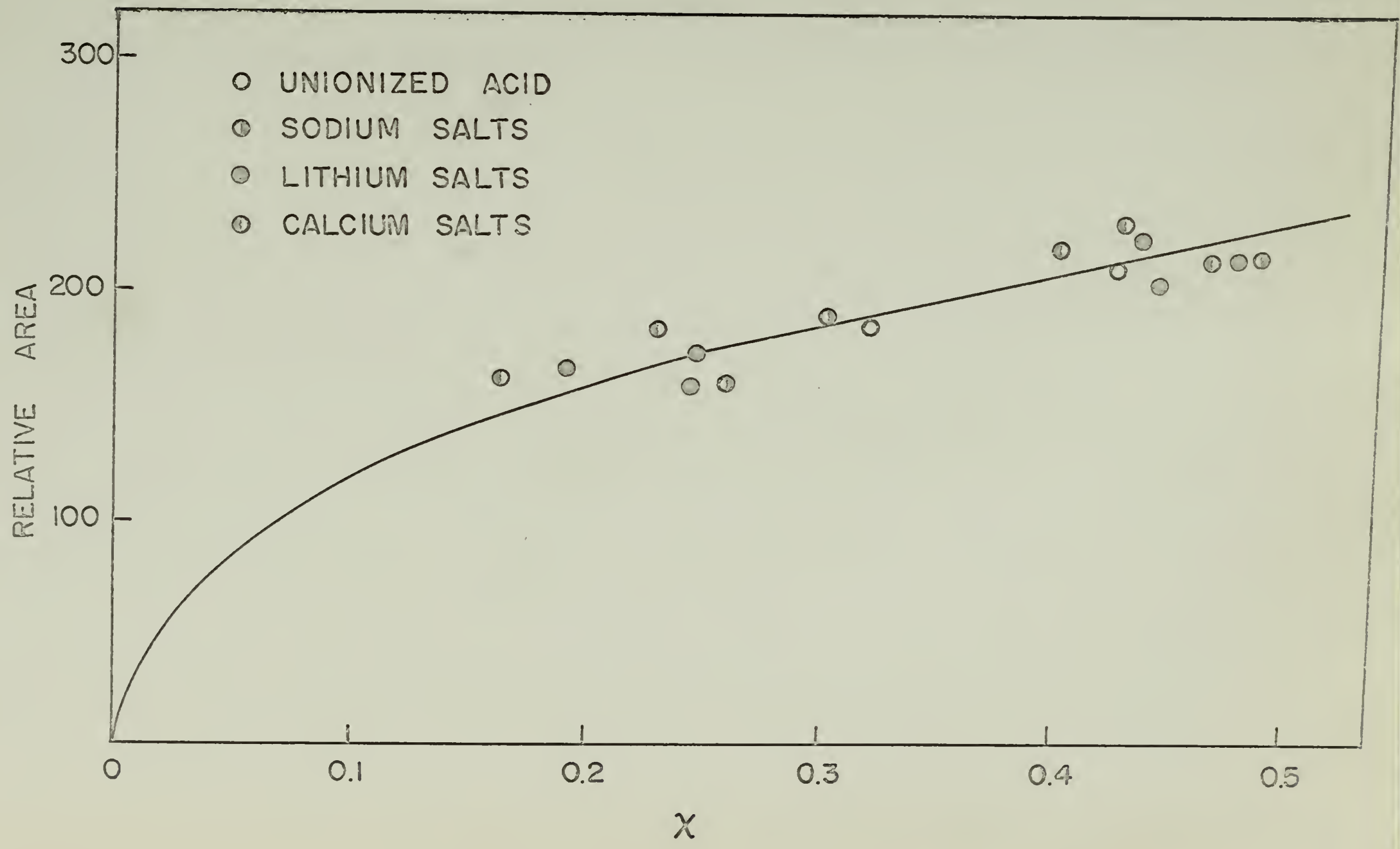
UNIONIZED ACID
SODIUM SALTS
LITHIUM SALTS
CALCIUM SALTS
RELATIVE AREA
300
200
100
0
0.1
0.2
0.3
0.4
0.5
X

Figure 54

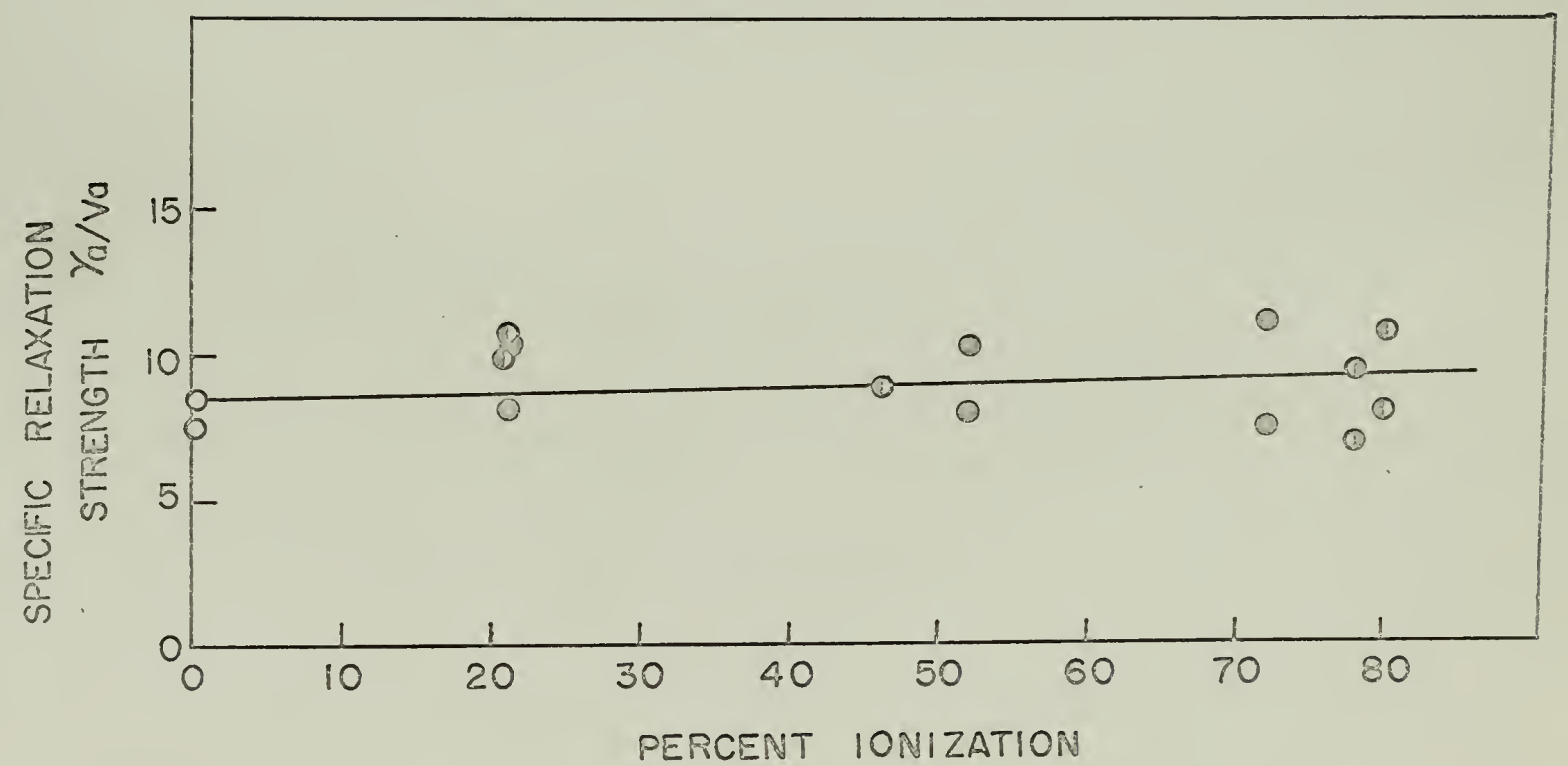
SPECIFIC RELAXATION STRENGTH χ_a/V_a
15
10
5
0
0
10
20
30
40
50
60
70
80
PERCENT IONIZATION

Figure 55